MNDO STUDY OF SOME CAGE MOLECULES

by

Wing-kwong Ip (葉永光)

A thesis submitted in partial fulfilment of the requirement for the degree of Master of Philosophy in the Chinese University of Hong Kong

1983

Thesis Committee :

Dr. W.K. Li, Chairman

Dr. S.P. So

Prof. T.C.W. Mak

Prof. D.N. Hendrickson

CONTENTS

LIST OF FIGURES AND TABLES

ABSTRACT

This work is concerned with the application of the MNDO procedure to some novel inorganic compounds containing boron, nitrogen or sulfur atoms. The thesis consists of the following five parts :

The first part is the dimerization of borane. Three pathways have been studied by imposing different symmetry restrictions, namely, C_{2h} symmetry, least-motion and with no symmetry at all. The last one is found to be the most facile one with low activation energy which is only 2.7 kcal/mol. Moreover, C_s symmetry is assumed automatically for this pathway. It is noted that the dimerization of borane proceeds with high proficiency without severe steric requirements.

The second part is a study of the fluxional behavior of closo-boranes for the series $B_nH_n^{2-}$, n = 5 to 8. For $B_5H_5^{2-}$, it experiences cage opening to a more stable structure with a barrier of about 4 kcal/mol. The $B_6H_6^{2-}$ anion does not show any fluxional behavior even though three pathways for intramolecular rearrangements have been studied. Moreover, MNDO results suggest that this anion can have a stable isomer with chair form skeleton

with D_{3d} symmetry. The $B_7H_7^{2-}$ ion, like $B_6H_6^{2-}$, does not have structural nonrigidity. The most probable pathway (C_{2v} transition state) requires some 35 kcal/mol for the rearrangement. The last anion, $B_8H_8^{2-}$, is found to rearrange very easily according to the experimental results. In gas phase, the D_{2d} structure is more stable than the C_{2v} and D_{4d} structures by 1.8 and 20.6 kcal/mol, respectively. Moreover, the last two structures are not local minima.

The third part concerns hexamethylenetetramine(HMT) and its related compounds. The MNDO geometries of the compounds range from satisfactory to excellent when compared to available experimental results. It is found that when a lone pair of HMT is utilized in salt or adduct formation, the C-N(quaternary) bonds and the adjacent C-N bonds become significantly lengthened and shortened, respectively. This is in accord with crystallographic structural data and Gutmann's bond length variation rule.

The fourth part is a study of the adducts $H_3NBH_nF_{3-n}$, n = 0 to 3. It is found that the acidities of the Lewis acids BH_nF_{3-n} decrease as n gets smaller. This indicates BH_3 is the strongest acid while BF_3 is the weakest. Large charge transfers (>0.4e) are observed in forming the adducts. It is noted that all the adducts are formed with low activation energies, about 3 kcal/mol.

The last part is a study of the cyclopentathiazenium cation $S_5N_5^+$. It is a fourteen pi electron system and is thus of planar structure. Previous X-ray crystallography studies have shown the presence of two different structures, heart-shaped and azulene-like. The MNDO heats of formation of these two structures are very nearly the same, namely, 434.3 and 434.7 kcal/mol, respectively. The energy barrier for the interconvertion of the two is low, about 8 kcal/mol, which leads to a conclusion that crystal forces may be responsible for determining which structure is predominant in a given solid. Furthermore, the transition state structure is of D_{5h} symmetry.

PART 1

THE DIMERIZATION OF BORANE

1.1 Introduction

Borane, BH_3, unlike its trisubstituted derivative BF_3, exists in dimeric form. This is probably due to the lack of stablization to the empty p orbital of boron by back donation and to the partial positive charge on the boron atom. The equilibrium between two BH_3 units and the B_2H_6 species turns out to be exceptionally favorable to the dimeric form. The presence of free BH_3 in any measurable concentration in equilibrium with diborane at elevated temperatures has apparently never been detected[1], though the BH_3^+ ion has been detected from low pressure pyrolysis of B_2H_6 by mass spectrometry[2,3].

The sp^2 hybridized BH_3 proceeds to self associate at high efficiency and requires no activation energy and the measurement of the absolute rate has been carried out[2]. The hybridization scheme for B_2H_6 suggested by Hamilton[4,5] is that two sp^2 hybrid orbitals of boron bond to two terminal hydrogens, while the third sp^2 orbital combines with the remaining p orbital to form two equivalent hybrid orbitals directing towards the two bridging hydrogens.

In the present work, three pathways of the dimerization processes are studied using the MNDO method. These are : pathway with C_{2h} symmetry, pathway of least-motion and pathway with no symmetry constraint.

1.2 Method of Calculation

All the calculations in this study make use of the MNDO approximation, which is believed to be superior to other semi-empirical methods in most aspects. The disadvantages and strong points of this approximation have been discussed by Dewar[6].

Fig. 1.1 depicts the three dimerization paths pictorially. In the first path, Fig. 1.1(a), C_{2h} symmetry is retained. Specifically, atoms B_1,B_2,H_3 and H_4 remain co-planar throughout. In the second path, the least motion path shown in Fig. 1.1(b), also has C_{2h} symmetry. However, in this case, atoms B_1,B_2, and H_3,...,H_6 remain co-planar throughout. In the last path, no symmetry restraint is imposed.

In all the calculations, the B_1-B_2 distance(denoted as r) is taken as the reaction coordinate. Also, except the symmetry conditions, if any, specified, all other structural parameters were optimized.

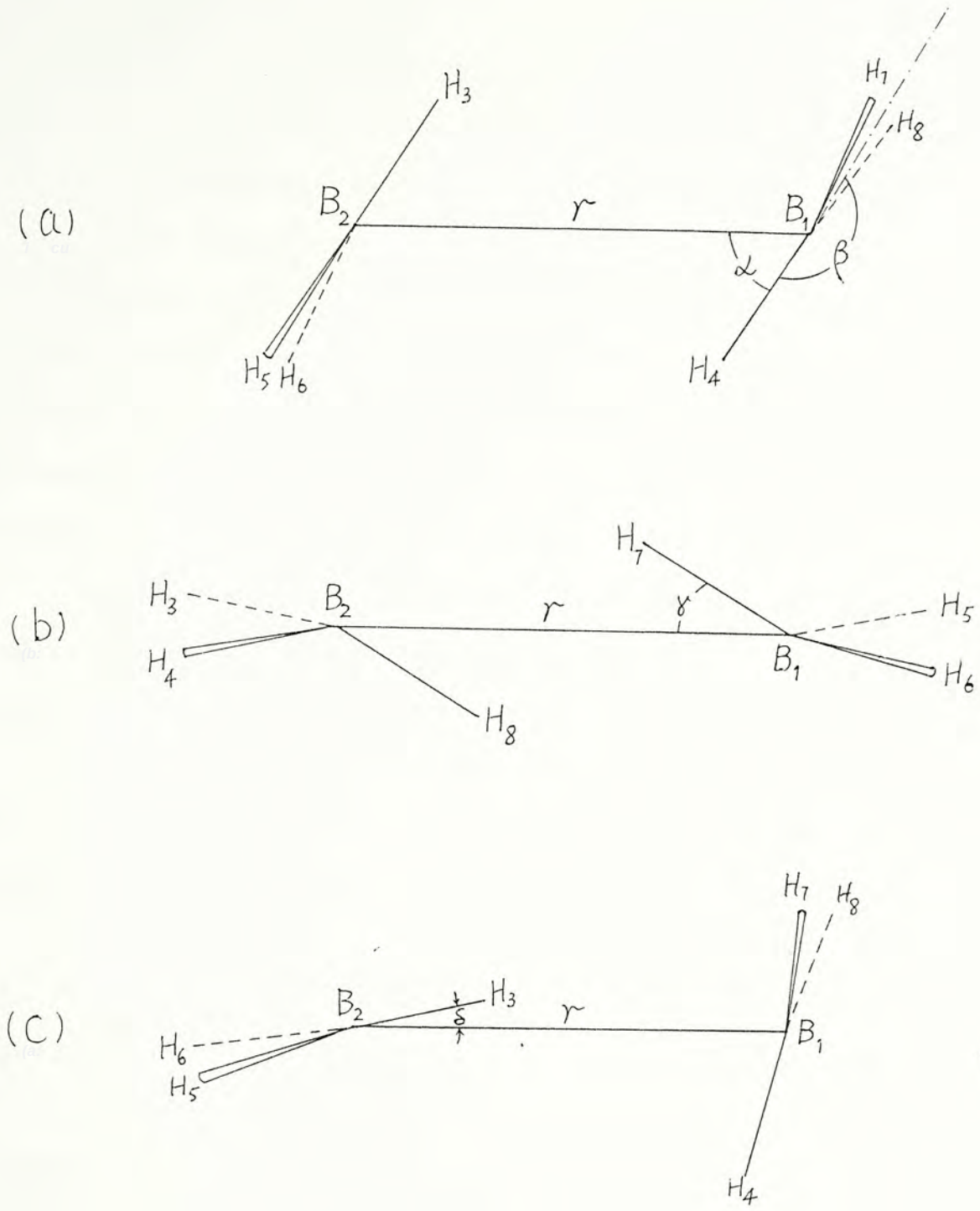

Fig. 1.1 The geometry arrangements and the numbering of atoms for the three dimerization pathways : (a) C_{2h} pathway, (b) least-motion pathway and (c) pathway with no symmetry constraint.

1.3 Results and Discussion

The MNDO structures of BH_3 and B_2H_6 have D_{3h} and D_{2h} symmetries, respectively. The MNDO stuctures of these two species are illustrated in Fig. 1.2, along with the experimental findings[7] for B_2H_6. As can be seen from this figure, the agreement between the MNDO and experimental results are very good. Also, the MNDO results are in good agreements with those of Lipscomb[8], using RH and PRDDO (with extensive configuration interaction) methods.

The MNDO heats of formation of BH_3 and B_2H_6 are 11.7 and -1.8 kcal/mol,respectively, yielding a heat of dimerization of -25.3 kcal/mol. This value deviates somewhat from the experimental results[1,2], about -35 kcal/mol. However, the MNDO result is still better than the PRDDO value of -17 kcal/mol, as calculated by Lipscomb. Finally, it is noted that the empirical fitting process by Wade[9] gives an excellent estimation, -33.8 kcal, for the dimerization energy.

The three dimerization pathways are now discussed in detail.

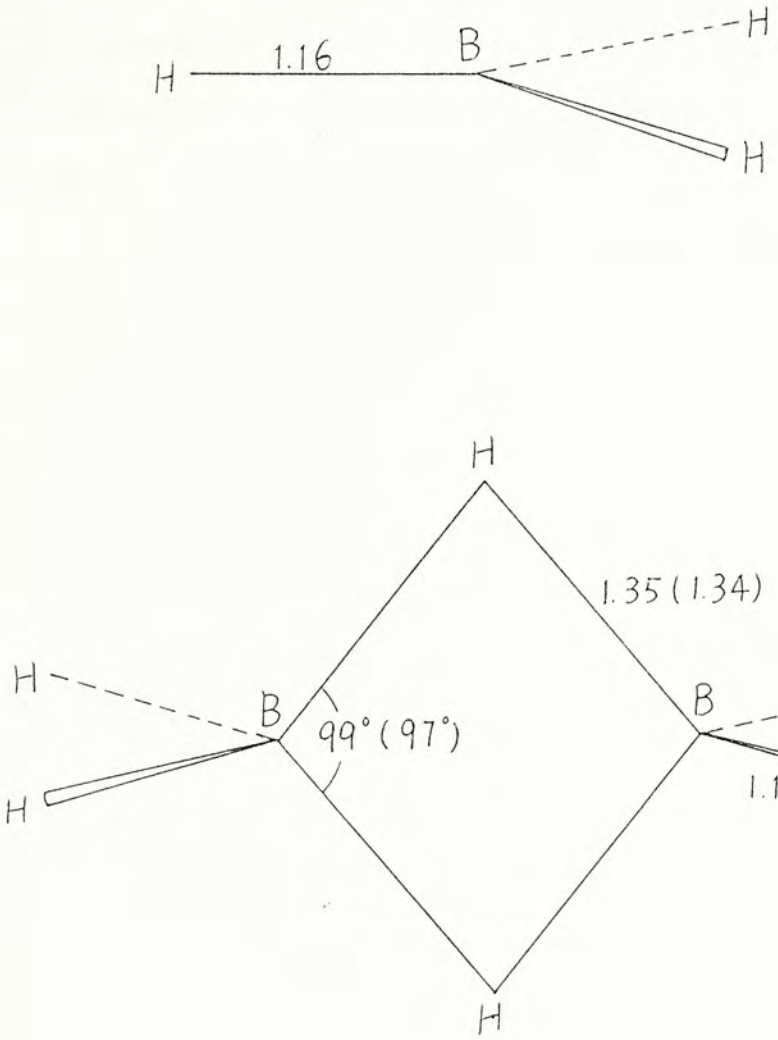

Fig. 1.2 MNDO structures of BH_3(D_{3h} symmetry) and B_2H_6(D_{2h} symmetry). Values in brackets are experimental results. Bond lengths are in Å.

1.3.1 The C_{2h} Pathway

The energy profile of this pathway is shown in Fig. 1.3. From this figure, it can be seen that the activation energy for this pathway is 3.8 kcal/mol, in fair agreement with that obtained by Lipscomb[8], 2.6 kcal/mol.

The course of reaction can be understood by considering the correlation diagram shown in Fig. 1.4 between two BH_3 units and the B_2H_6 species. The six bonding orbitals change their orbital energies accordingly as the two BH_3 units approach each other. The $1a_g$ orbital, which has the lowest energy, is stablized appreciably by a sigma B-B overlap. This is a bonding orbital for the whole skeleton but is mainly localized between the two boron atoms and the two bridging hydrogens. The next low energy orbital, $1b_u$, rises significantly in energy due to the out-of-phase interaction between the boron atoms. This is a bonding orbital for the borons and their terminal hydrogens. The third orbital, $2b_u$, like the $1a_g$ orbital, is responsible for bonding interaction between the borons and the bridging hydrogens. The difference between $1a_g$ and $2b_u$ is that the overlap between the borons is of sigma symmetry in the former and pi symmetry in the latter. Thus, it is not surprising that this orbital gains energy as the two BH_3 units approach each other. Thus, according to these results, it can be seen that the bonds between the borons and the bridging hydrogens

Fig. 1.3 The energy profile of C_{2h} pathway. The activation energy for dimerization is 3.8 kcal/mol.

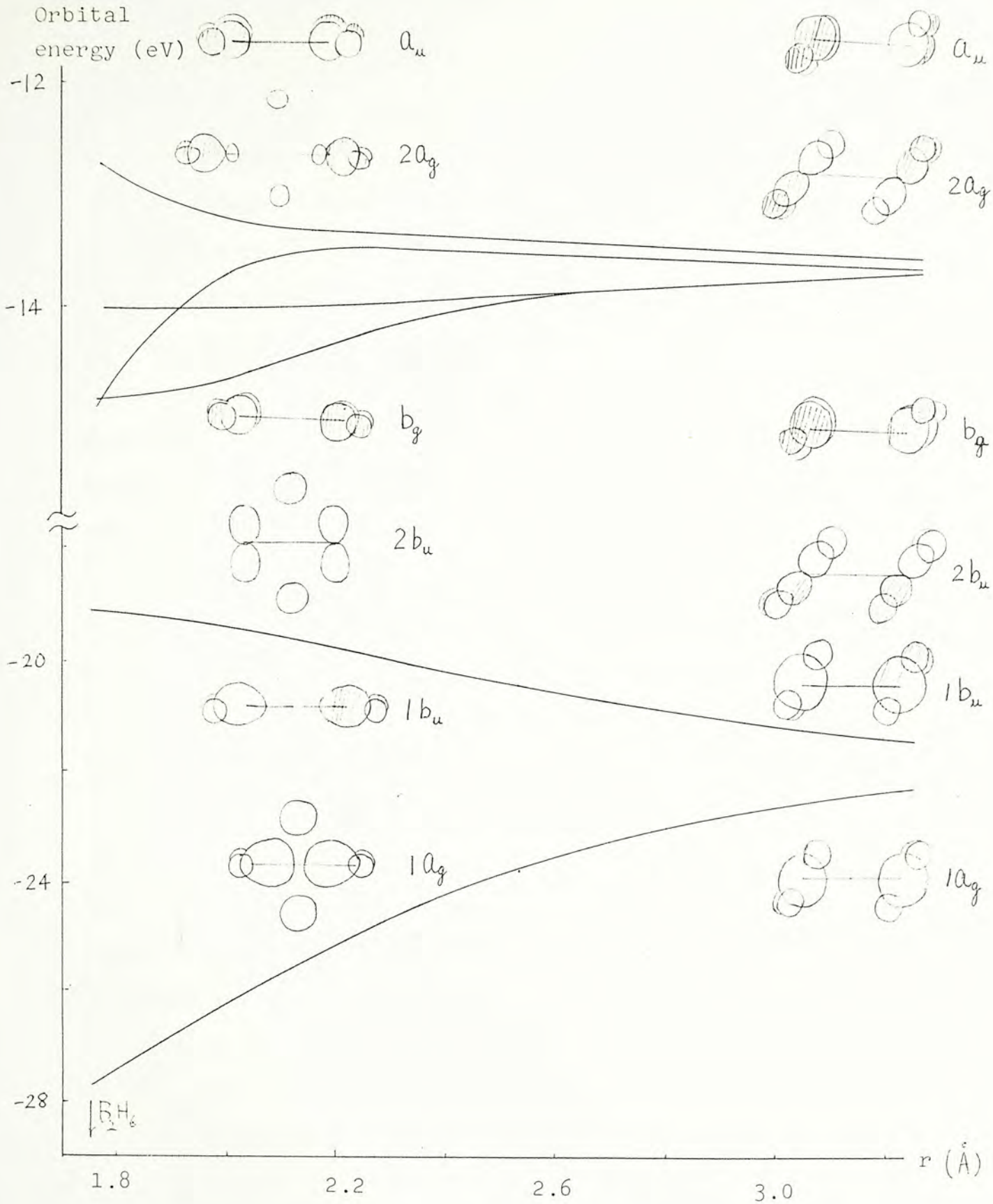

Fig. 1.4 Correlation diagram between two BH_3 units and B_2H_6 for the C_{2h} pathway.

are fairly strong. The fourth orbital, b_g, is higher in energy than $2b_u$ by a very minute amount. It bonds the terminal hydrogens to the borons and the overlap between the two borons is of pi symmetry. The last two orbitals are bonding orbitals mainly for terminal hydrogens to the boron atoms, with the HOMO being anti-bonding between the borons. As a consequence, if B_2H_6 is ionized to $B_2H_6^+$, the bonding between borons and their terminal hydrogens will be weakened, while the boron-boron bond and those between the borons and the bridging hydrogens will be strengthened.

Returning to Fig. 1.3, in the region $r > 2.78\mathring{A}$, energy rises smoothly to reach the transition state, the geometry of which is shown in Fig. 1.5. At the transition state, the interaction between the two BH_3 units is still relatively weak since the shortest distance between the two units is $2.31\mathring{A}$, which is the separation of H_3 and B_1. The small rise in energy at the transition state may be due to the core-core repulsion between the two boron atoms. Also, the charge distribution remains almost unaltered when the transition state is reached. Fig. 1.6 shows how the atomic charges change during dimerization. The bending of each BH_3 unit, defined by the bending angle β, is of interest. The change of this angle throughout the path is shown in Fig. 1.7.

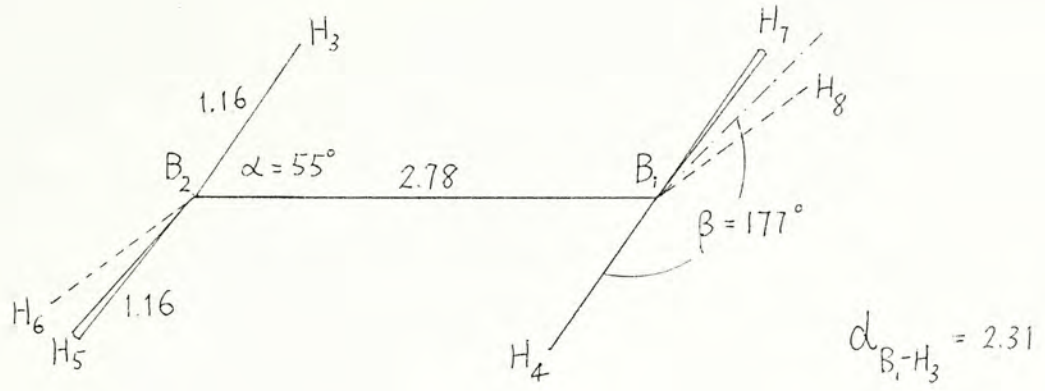

Pathway with C_{2h} symmetry

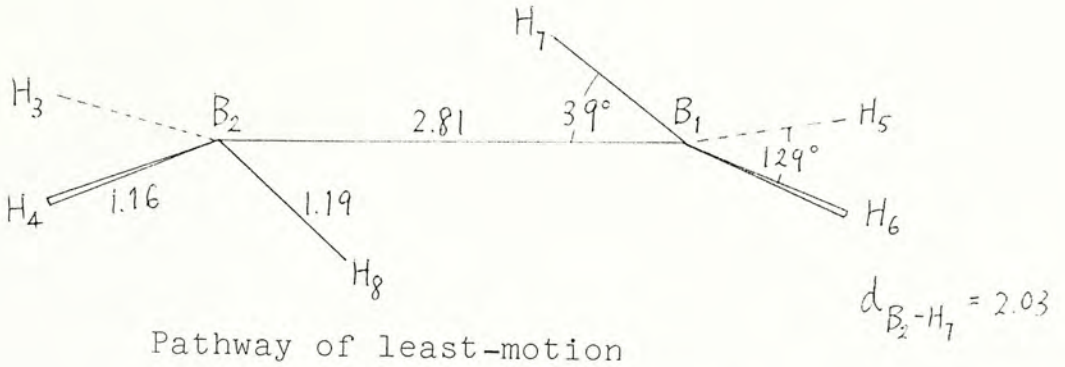

Pathway of least-motion

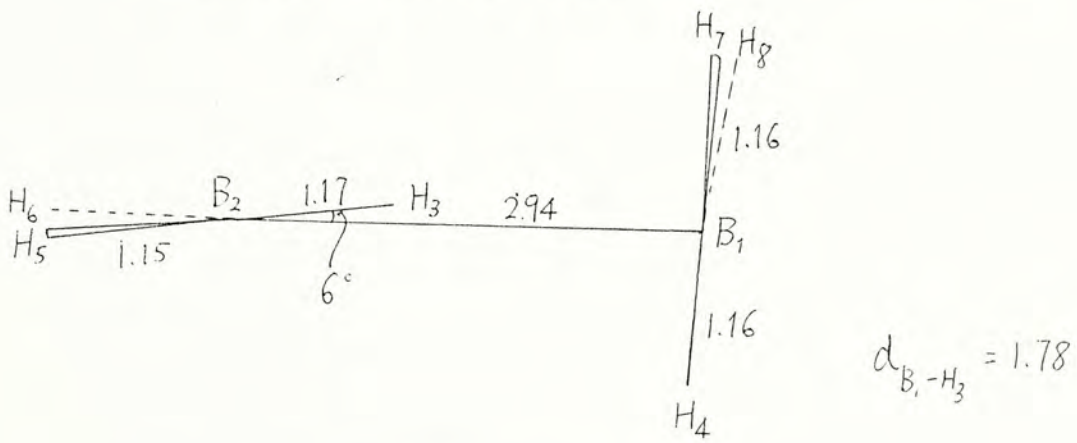

Pathway with no symmetry constraint

Fig. 1.5 Transition state geometries for the three dimerization pathways of borane. Bond lengths are in angstrons.

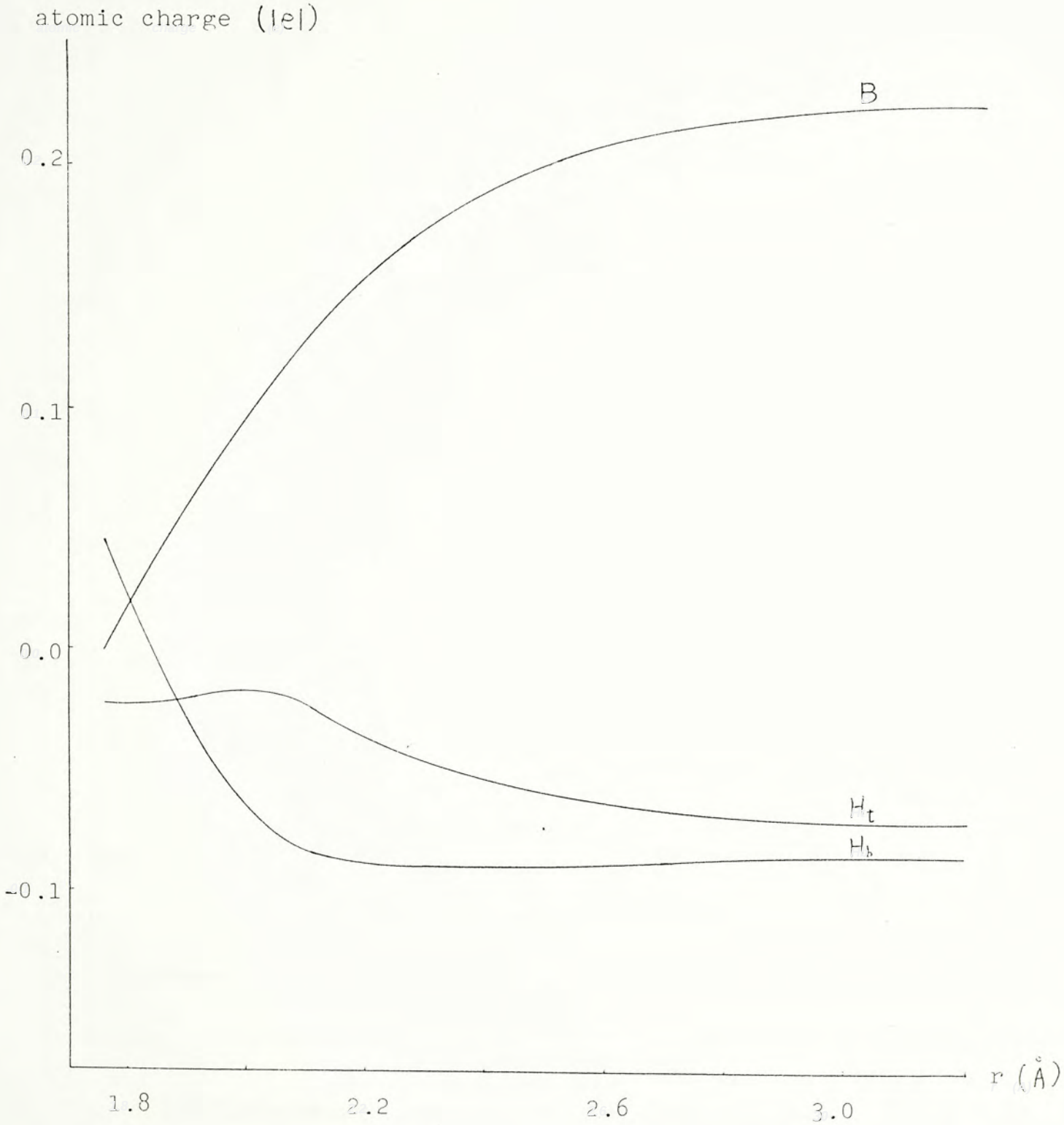

Fig. 1.6 The atomic charge distribution along the C_{2h} reaction pathway.

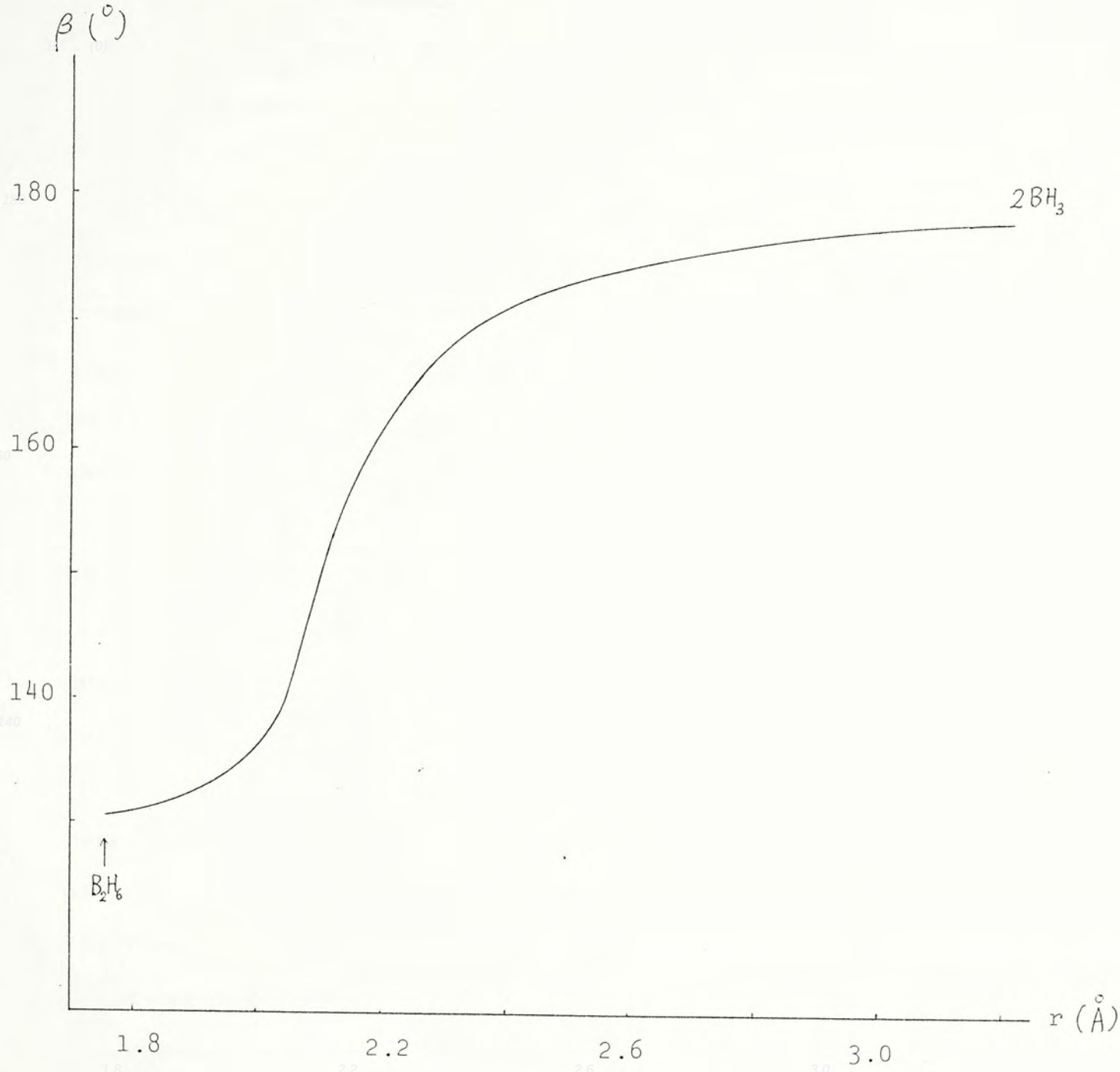

Fig. 1.7 The change of bending angle β along the C_{2h} reaction pathway.

At the transition state, β is 177°, almost equal to that of the planar BH_3 unit. The bond H_4-B_1, which will become part of a three center bond with B_2, remains practically unchanged. The angle α fluctuates in the range of 54-62° before the transition state is reached. At the initial stage of dimerization, an increase in α is expected since there is non-bonding repulsion between H_3 and H_4. As the two BH_3 units approach each other, a decrease in α results. This is due to the interaction between the hydrogens H_3 and H_4 with the empty p orbitals.

After the transition state, to $r \sim 2.1\text{Å}$, the bond order of H_4-B_1 decreases and that of H_4-B_2 increases. This indicates the formation of the three-center bonds. It is noted that the sum of these two bond orders remains constant throughout the reaction path. However, the bond order between the borons increases markedly after the transition state is reached. Hence, according to these results, the stability of B_2H_6 over two BH_3 units is not due to the formation of the three center banana bonds. Rather, it is due to the boron-boron interaction. This can also be seen from the correlation diagram of Fig. 1.4.

Examining Fig. 1.6, it can be seen that after the transition state ($r = 2.78\text{Å}$), there is a steady flow of electron toward the borons. In the range of $2.1\text{Å} < r$ and $r < 2.78\text{Å}$, the sources of the electron are the terminal

hydrogens. For the range of $r < 2.1\text{Å}$, the bridging hydrogens become the electron source, as the three-center bonds start to form.

The formation of the three-center bonds is also evident when the changing pattern of the bending angle β is examined. In the range $2.0\text{Å} < r < 2.2\text{Å}$, there is a dramatic decrease in β, indicating that the three-center bonds are being formed. Also in this range, angle α decreases steadily to a minimum of 43.4° at $r = 2.0\text{Å}$. At this point, the two bridging hydrogens are practically midway between the borons. When diborane is finally formed at $r = 1.75\text{Å}$, α increases back to 49.5°.

Roughly, this dimerization process can be classified into two stages. The first stage is concerned with the increase of boron-boron interaction. The second stage is the formation of B--H-B three-center bonds. The first stage starts at $r = 2.78\text{Å}$ and is almost finished at $r = 2.1\text{Å}$. The second stage does not become important until r reaches 2.1Å.

1.3.2 The Least-Motion Pathway

The energy profile of this pathway, as shown in Fig. 1.8, as expected, gives a high energy barrier for dimerization. The activation energy determined is 31.5 kcal/mol. Such a large activation energy is due to the confinement of the four terminal hydrogens and the borons to stay co-planar. On the other hand,quite accidentially, the transition state of this path has a boron-boron separation of 2.81Å, nearly the same as that for the C_{2h} path. The transition state geometry is shown in Fig. 1.5. Fig. 1.9 shows the redistribution of the atomic charges along the reaction path.

For the region $r > 2.81$Å, the approaching of the hydrogens H_7 and H_8 makes the energy rise smoothly and enormously to reach the transition state. To release the repulsion between them, H_7 and H_8 come out of the plane, thus bending the BH_3 units. The angle χ which indicates the degree of non-planarity of the BH_3 units increases correspondingly to a value of 39.4° at the transition state. Also, at this point, the attraction interaction between the BH_3 units is relatively weak, because atoms H_7 and B_2 are still 2.03Å apart. In other words, no significant three-center bond has been formed at this stage.

Examining Fig. 1.9 , in this region, it is seen that there is an electron flow from the terminal hydrogens, through their respective borons, to the bridging hydrogens.

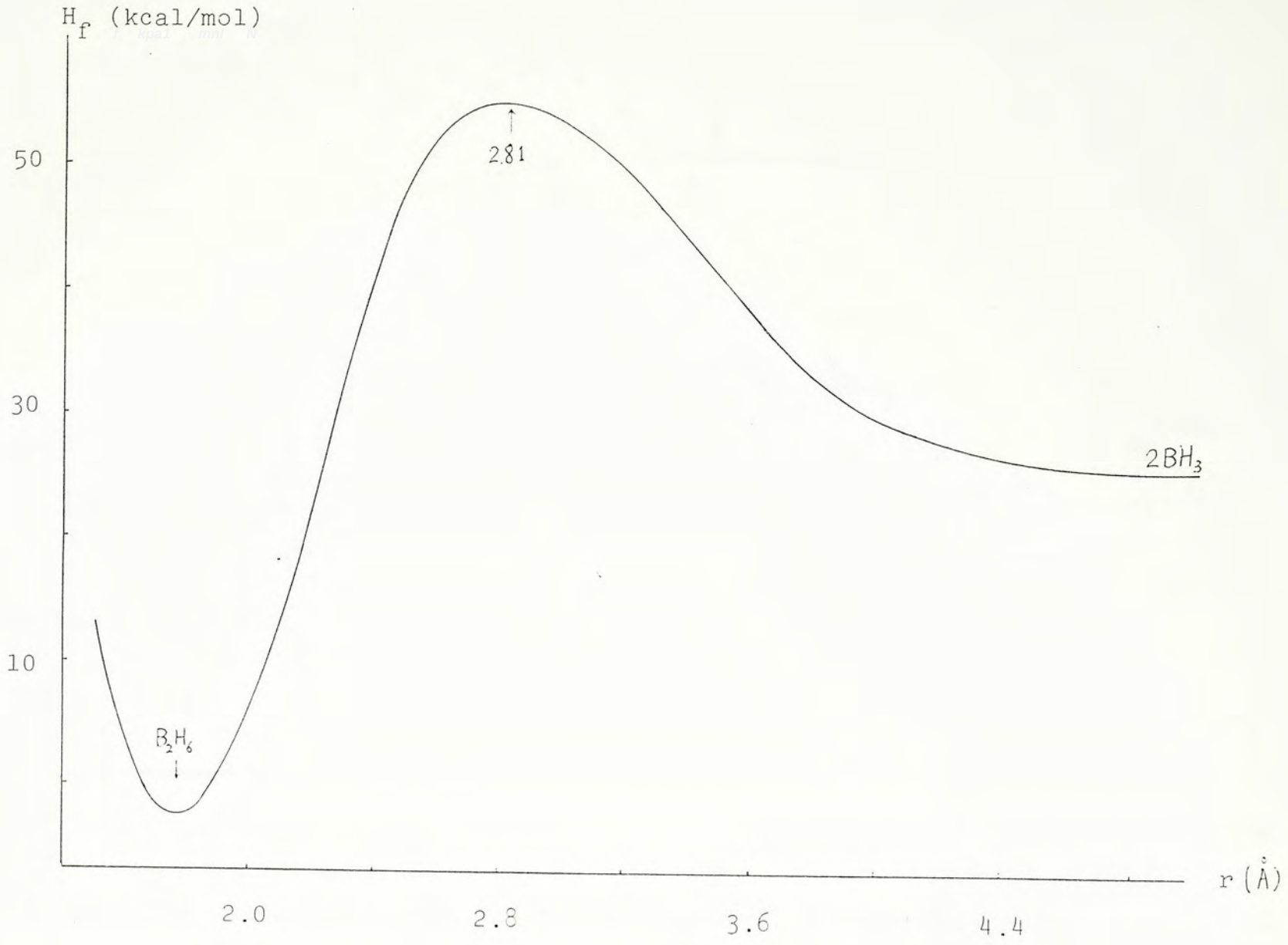

Fig. 1.8 The energy profile for the dimerization of BH_3 by the least-motion pathway. The activation energy is 31.5 kcal/mol.

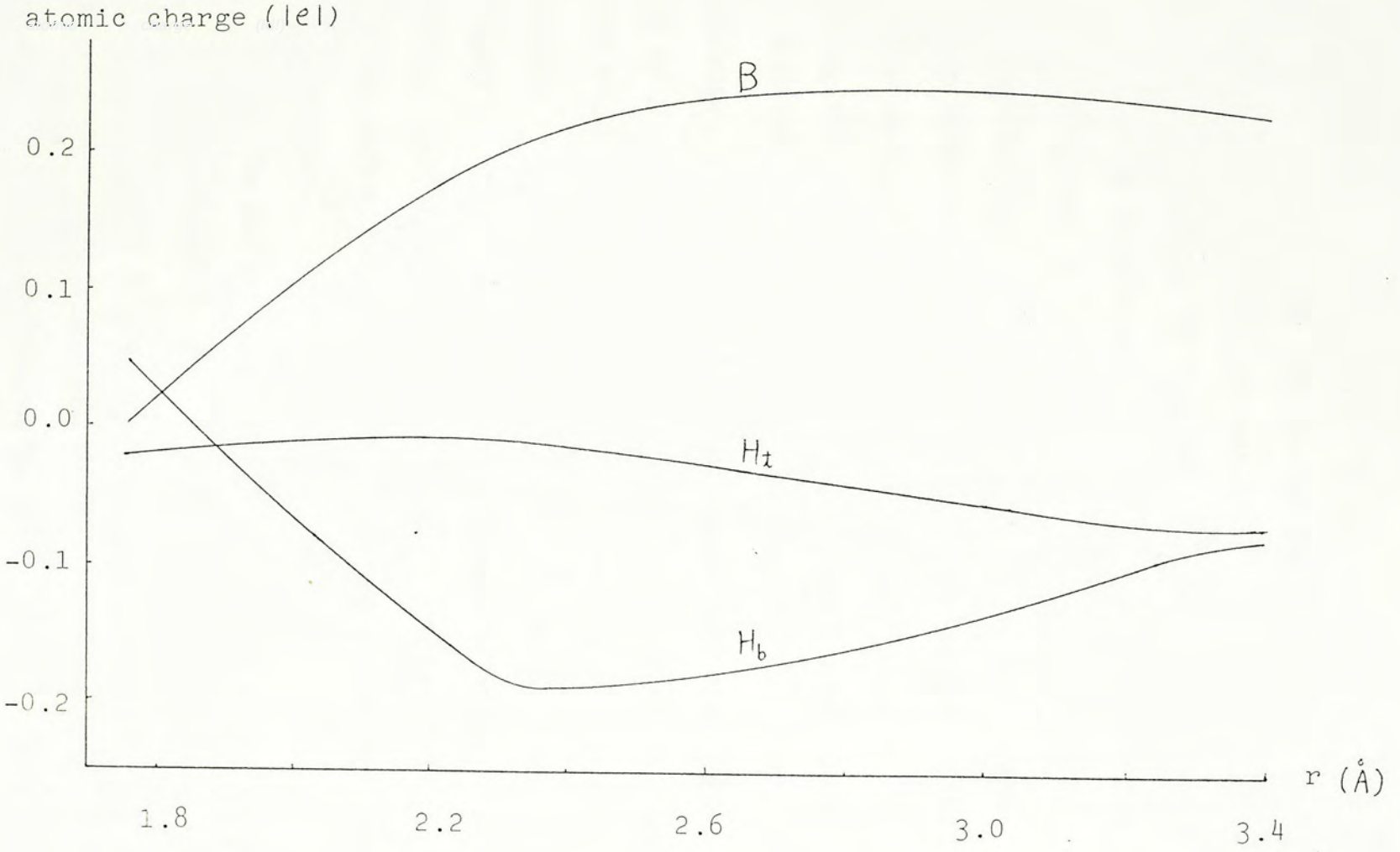

Fig. 1.9 The charge distribution of the least-motion pathway.

In the region 2.30Å < r < 2.81Å, the energy drops rapidly as a consequence of the formation of the three-center bonds and the concommitant increase of boron-boron interaction. In the initial stage of the region, the bending angle γ still increases a little bit then it falls to 36.9° at r = 2.3Å.

The increase in γ shows that the repulsion of the two hydrogens, H_7 and H_8, is still significant. At r = 2.30Å, these hydrogens have shifted to the center position, i.e., three center bonds have been formed. It is noted that, in this path, the three-center bonds are formed at an earlier stage, r = 2.30Å, than in the previous path, r = 2.10Å. This is because, as the terminal hydrogens and the borons are kept to be co-planar throughout this path, earlier formation of the three-center bonds would release the " bending strain " around the borons. From Fig. 1.10, it is seen that, in this region, charges flow from the terminal hydrogens to the borons and the bridging hydrogens. This again is indicative of the formation of the three-center bonds and boron-boron interaction.

In the region of r < 2.30Å, energy drops to a minimum of -1.8 kcal/mol to form diborane. The bending angle γ increases to 49.5° for diborane as the borons approach each other. Also, the charges on the terminal hydrogens are practically unchanged in this region, but there is a steady flow of charge from the bridging hydrogens to the borons. This electron flow serves to strengthen the formation of the three-center bonds.

1.3.3 The Pathway with No Symmetry Constraint

The energy profile of this pathway is shown in Fig. 1.11. In this figure, the transition state cannot be found readily due to the flat energy maximum. Thus, a two-dimensional energy contour map (Fig. 1.11) is constructed to locate the transition state. As expected, the region around the transition state shows very little variation in energy. Hence the location of the transition state is far from obvious and the one we have determined must be viewed with caution. The transition state geometry is shown in Fig. 1.5.

For the region $r > 3.20\text{Å}$, energy rises from 23.5 kcal/mol to 26.1 kcal/mol, which is very close to the transition state energy, namely, 26.2 kcal/mol. In this region, the angle δ (see Fig. 1.1c) remains close to 0°, i.e., the bond B_2-H_3 is pointing directly to the empty p orbital of B_1. At $r = 3.20\text{Å}$, the interaction between B_1 and H_3 is still rather weak for their separation is 2.04Å. Electron flow from B_2 to B_1 through H_3 is observable, though the amount, about 0.02e, is small. Charges on other atoms remain unchanged. Fig. 1.12 shows the redistribution of charges on every atom along the path.

As r continues to shorten, energy remains practically unchanged till $r = 2.70\text{Å}$. At this point, the energy is equal to that at $r = 3.20\text{Å}$, but is 0.1 kcal/mol lower than the transition state energy, as shown by Fig. 1.10. From

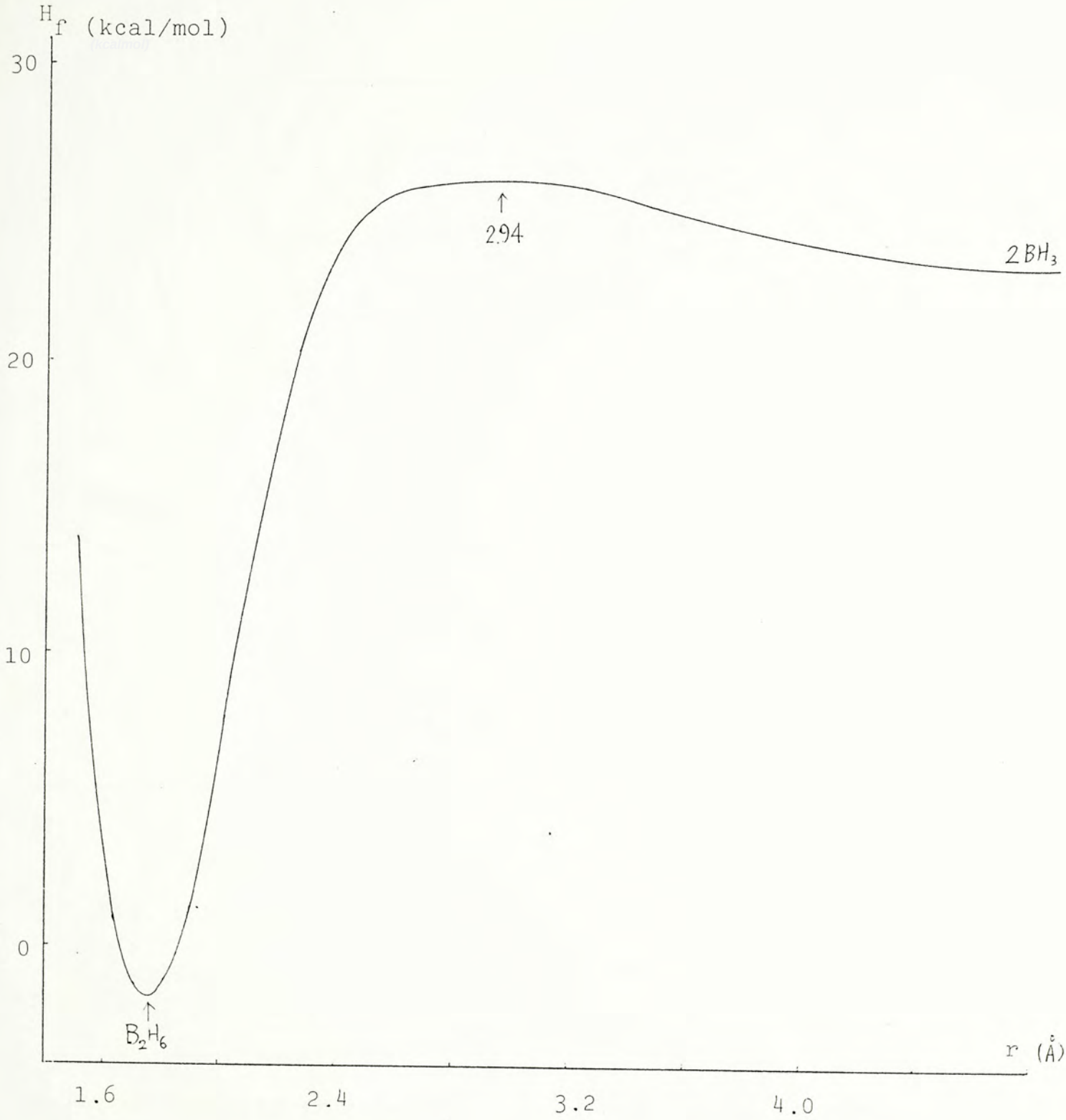

Fig. 1.10 The energy profile of the pathway without symmetry constraint. The activation energy is 2.7 kcal/mol.

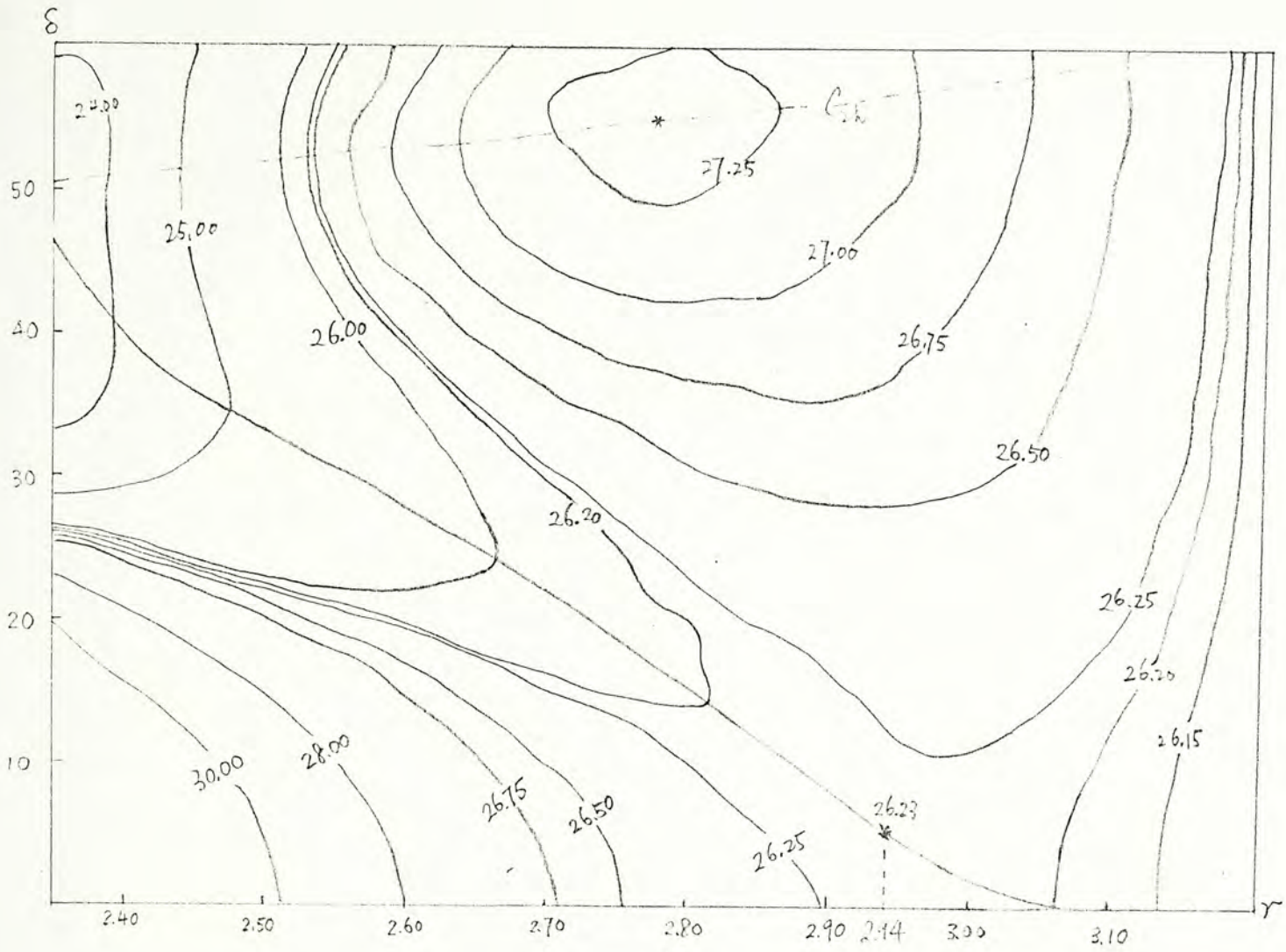

Fig. 1.11 Energy (kcal/mol) contour map for the pathway without symmetry constraint. Ordinate is the value of δ (^{o}) and the abscissa is the B-B separation(Å). The transition state is shown by an asterisk. In addition, the C_{2h} pathway is also shown for reference.

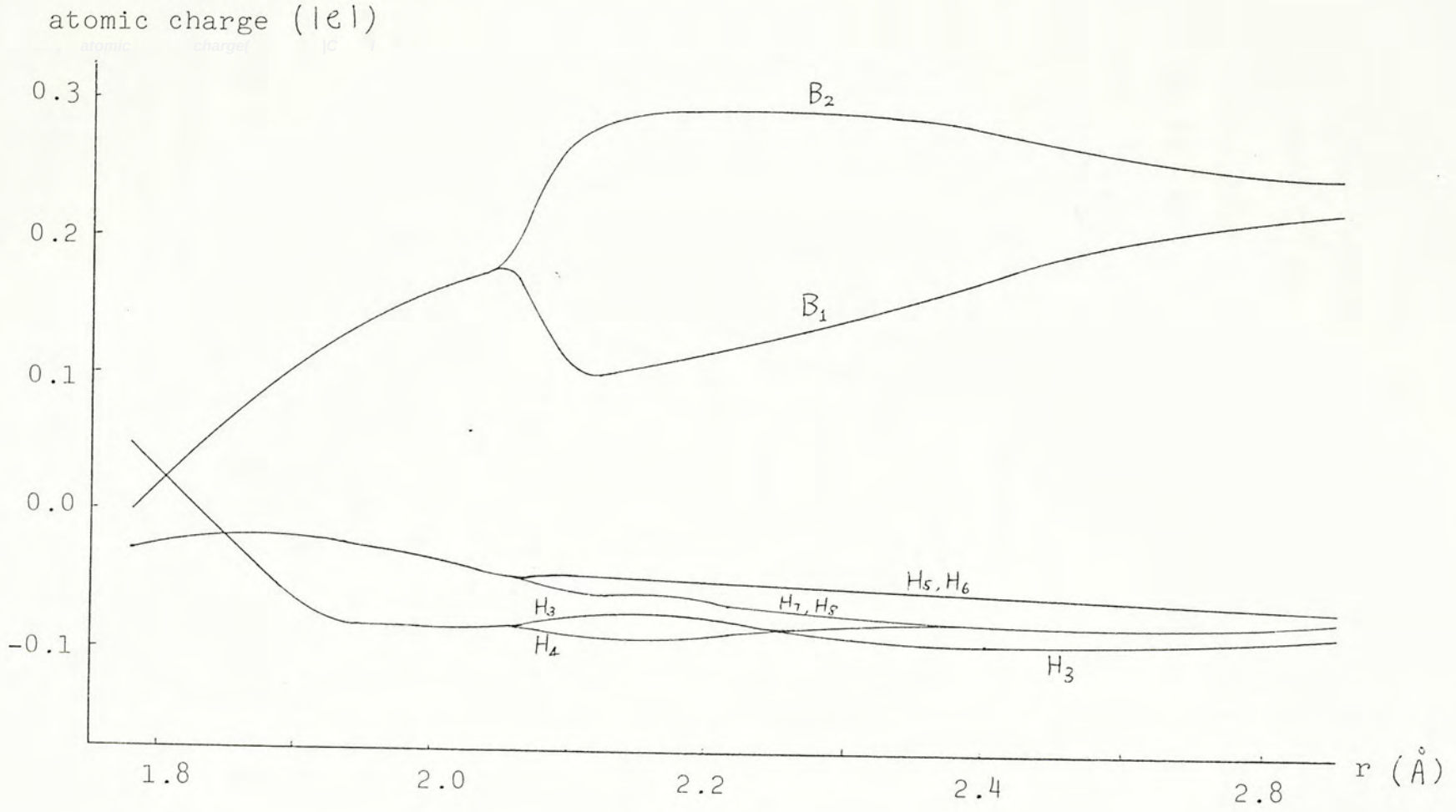

Fig. 1.12 Atomic charge densities along the C_s reaction pathway.

Fig. 1.11, it is seen that, even though the energy change in this region is exceptionally small, the angle δ increases rapidly from about 0° to 22.6°. The bond order between H_3 and B_1 increases by a small amount, but the electron flow from B_2 to B_1 is large, while the charges on all the hydrogens are nearly unchanged.

For the region $2.31\text{Å} < r < 2.70\text{Å}$, energy is on the decrease. The angle δ increases dramatically to 49.3° while the angle H_4-B_1-B_2 decreases to the same value. The B_1-H_3 separation increases to a maximum of 1.79Å, as a consequence of the increase in δ. Charge continues to flow from B_2 to B_1 until the two charges become equal. Needless to say, the flow back of charge is through H_4. It is noted that so far the change of charge densities on all the hydrogens are negligible.

For the region of $r < 2.31\text{Å}$, the path is the same as the C_{2h} path discussed previously. Again, at $r = 2.0\text{Å}$, the bridging hydrogens become equidistant between the two borons and act as electron sources for the formation of the three-center bonds. Energy drops to a minimum at $r = 1.75\text{Å}$ for diborane. It is noted that even no symmetry condition is imposed, the reaction path assumes C_s symmetry throughout.

1.4 Conclusion

As a consequence of the involvement of an empty valence orbital in the reaction, the dimerization of borane has a transition state with a large boron-boron separation. Another consequence is the low energy barrier for the reaction. Among the paths studied, the path having the lowest barrier is that with C_s symmetry. The activation energy for this path is 2.7 kcal/mol. For this path, it is rather difficult to locate the transition state since large rearrangement of atoms brings about a small variation in energy, i.e., the transition state is on a flat surface. Thus it is obvious that the stereo-requirement for the dimerization is not strictly confined and the dimerization can proceed very efficiently.

The C_s path has been suggested by Gimarc[10] and Fehlner[2], but rejected by Lipscomb . According to Lipscomb, the optimal path is the one with C_{2h} symmetry, which yields an activation energy of 2.6 kcal/mol. This value is almost identical to the one, 2.7 kcal/mol, obtained for our C_s path. Also, when CI is included in his SCF calculation, the transition state occurs at a boron-boron separation of 3.0Å, in fair agreement with our result.

REFERENCES

1. L.H. Long, Progr. in Inorg. Chem., 15, 1(1972)
2. G.W. Mappes, S.A. Fridmann and T.P. Fehlner, J. Phys. Chem., 74, 3307(1970)
3. T.P. Fehlner and S.A. Fridmann, Inorg. Chem., 9, 2288(1970)
4. W.C. Hamilton, Proc. Roy. Soc.(London), A235, 395(1956)
5. W.C. Hamilton, J. Chem. Phys., 29, 460(1958)
6. M.J.S. Dewar and M.L. McKee, J. Amer. Chem. Soc., 99, 5231(1977)
7. D.S. Jones and W.N. Lipscomb, Acta. Cryst., A26, 1961(1970)
8. D.A. Dixon, I.M. Pepperberg, and W.N. Lipscomb, J. Amer. Chem. Soc., 96, 1325(1974)
9. C.E. Housecroft, R. Snaith and K. Wade, Inorg. Nucl. Chem. Letter, 15, 343(1979)
10. B.M. Gimarc, J. Amer. Chem. Soc., 95, 1417(1973)

PART 2

FLUXIONAL BEHAVIOR OF SOME CLOSO-BORANES

2.1 Introduction

The closo-borane series, with a general formula $B_nH_n^{2-}$ for n = 6 to 12, is of much chemical interest because of their cage geometries and their considerable stability. Numerous theoretical studies have been carried out for these species. For example, their bonding schemes have been studied by Lipscomb[1] and their aromaticity by Aihara[2]. Though calculations concerning the molecular geometries and the related chemical properties are rather thorough, there appears to be a lack of systematic study to investigate the intramolecular rearrangements of closo-boranes. So far, only Muetterties[3,4] has suggested some stylistic pathways for the rearrangements.

In this work, rearrangements with presumed pathways are examined for the series n = 5 to 8 by the MNDO procedure. The unknown $B_5H_5^{2-}$ is also studied in order to find out if it is likely to exist on theoretical grounds.

2.2 $B_5H_5^{2-}$

2.2.1 Introduction

Among the closo-boranes $B_nH_n^{2-}$, n = 5 to 12, only $B_5H_5^{2-}$ has not been found experimentally. However it has been studied in some theoretical calculation assuming D_{3h} symmetry.

Since $B_5H_5^{2-}$ has never been synthesized, it is reasonable to assume that either it is not a stable species or its stability is extremely low. The present study suggests the latter assumption.

In addition to the widely accepted D_{3h} structure[3,4,5], MNDO calculation gives another stable structure having C_2 symmetry. This structure so far has not been proposed in the literature. The MNDO structures of this species with D_{3h} and with C_2 symmetries are shown in Fig. 2.1.

An isomerization pathway has been proposed to connect the two structures. The reaction coordinate is the angle α which has been defined in Fig. 2.1. This angle is the twist angle of B_3 and B_6 about the axis containing B_2 and the dummy atom D_1, or simply, $\alpha = B_3\text{-}B_2\text{-}D_1\text{-}B_6$. Throughout the pathway, C_2 symmetry is assumed, while all other geometrical parameters are optimized.

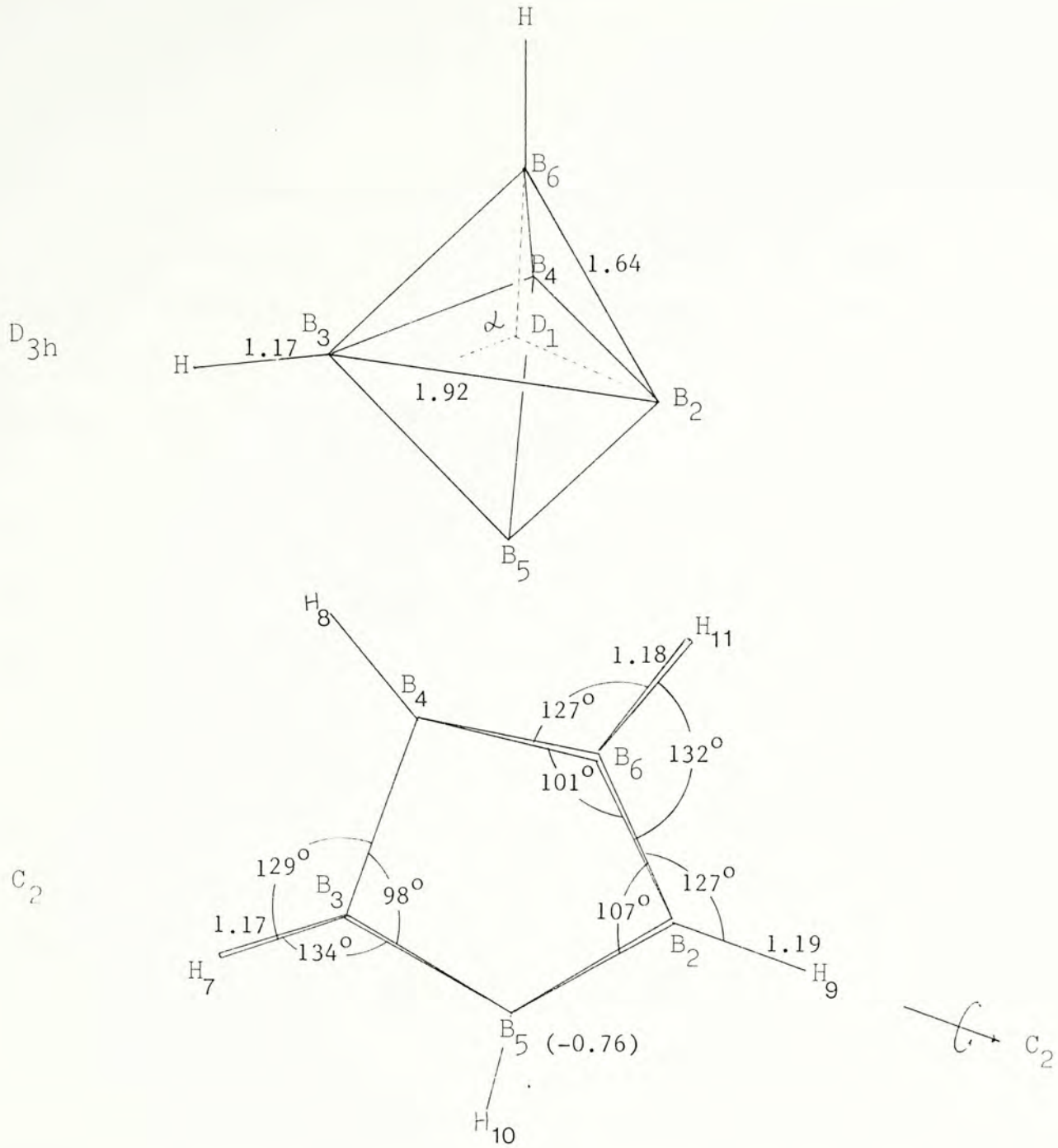

Fig. 2.1 MNDO geometries for the two stable isomers of $B_5H_5^{2-}$. Value in parenthesis indicates the distance of B_5 below the paper. The reaction coordinate α is B_6-D_1-B_2-B_3. All the distances are in Å.

2.2.2 Results and Discussion

The energy profile of the reaction path is shown in Fig. 2.2. The reaction coordinate α ranges from 90° to 180°. The two stable structures are at $\alpha = 90^{\circ}$ for D_{3h} and at $\alpha = 143^{\circ}$ for C_2.

For $90^{\circ} < \alpha < 115^{\circ}$, there is an energy increase of 4.4 kcal/mol to reach the transition state, whose geometry is shown in Fig. 2.3. Evidently, the closo-structure has not been opened at the transition state since the separation between B_4 and B_6 is only 2.03Å. During the opening of the cage, all the specified B-B bonds increase their strengths. It is noted that B_6 does not stay midway between B_2 and B_4. The interaction between B_4 and B_6 is stronger than that between B_2 and B_6. This may be viewed as a compensation for the larger loss of coordination for the borons B_4 and B_6. Fig. 2.4 shows the corresponding charge redistribution during the rearrangement. In this region, charge flows away from B_5 and B_6 due to the breaking of B_3-B_6 and B_4-B_5 bonds. The large flow of charge from the axial borons indicates the breaking of these two bonds. Consequently, charges accumulate on the other three boron atoms, with B_2 gaining more electronic charge than the other two.

In the region $115^{\circ} < \alpha < 143^{\circ}$, energy drops smoothly

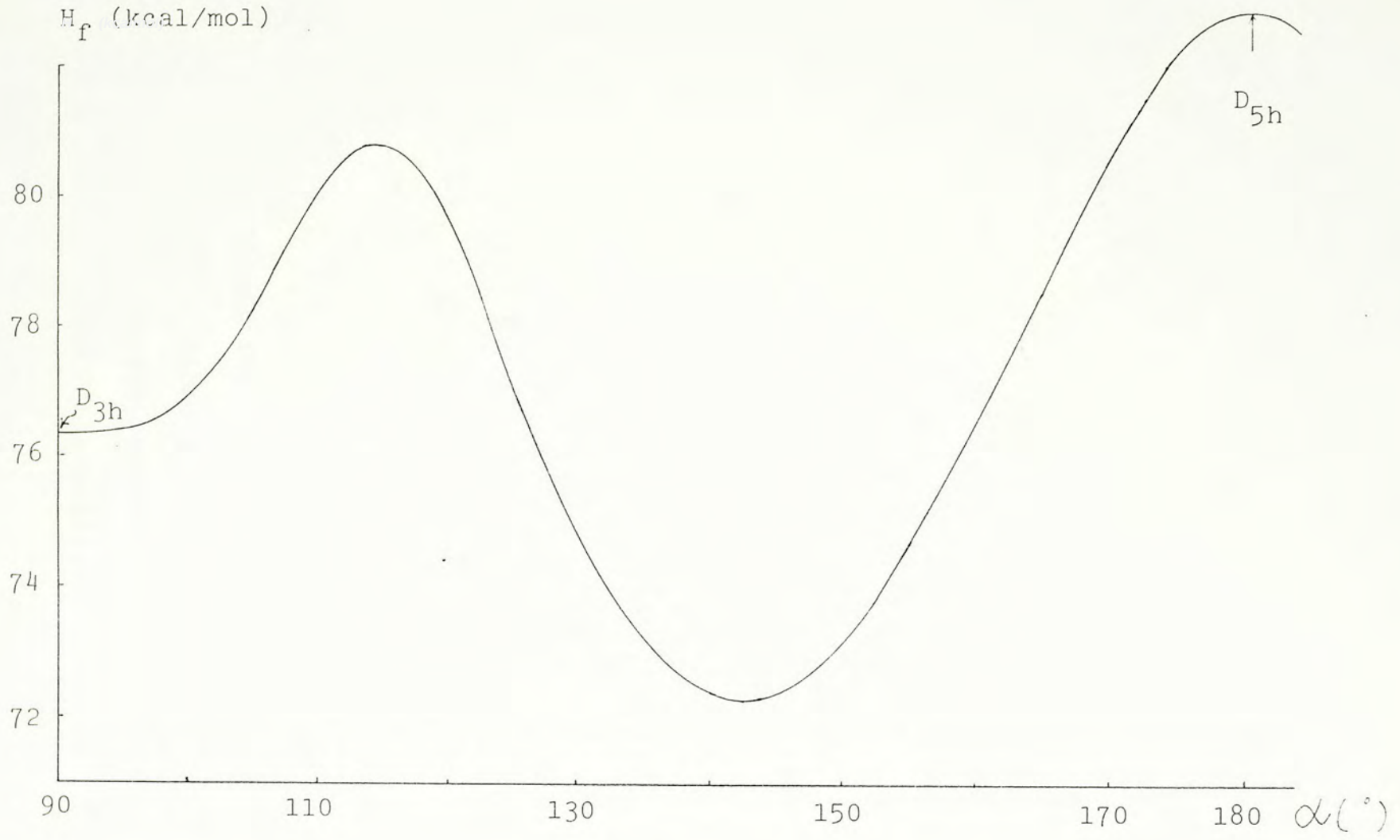

Fig. 2.2 The energy profile for the opening of the D_{3h} cage for the $B_5H_5^{2-}$ anion. Note that, except when $\alpha = 90^{\circ}$ and 180°, the symmetry is C_2 throughout.

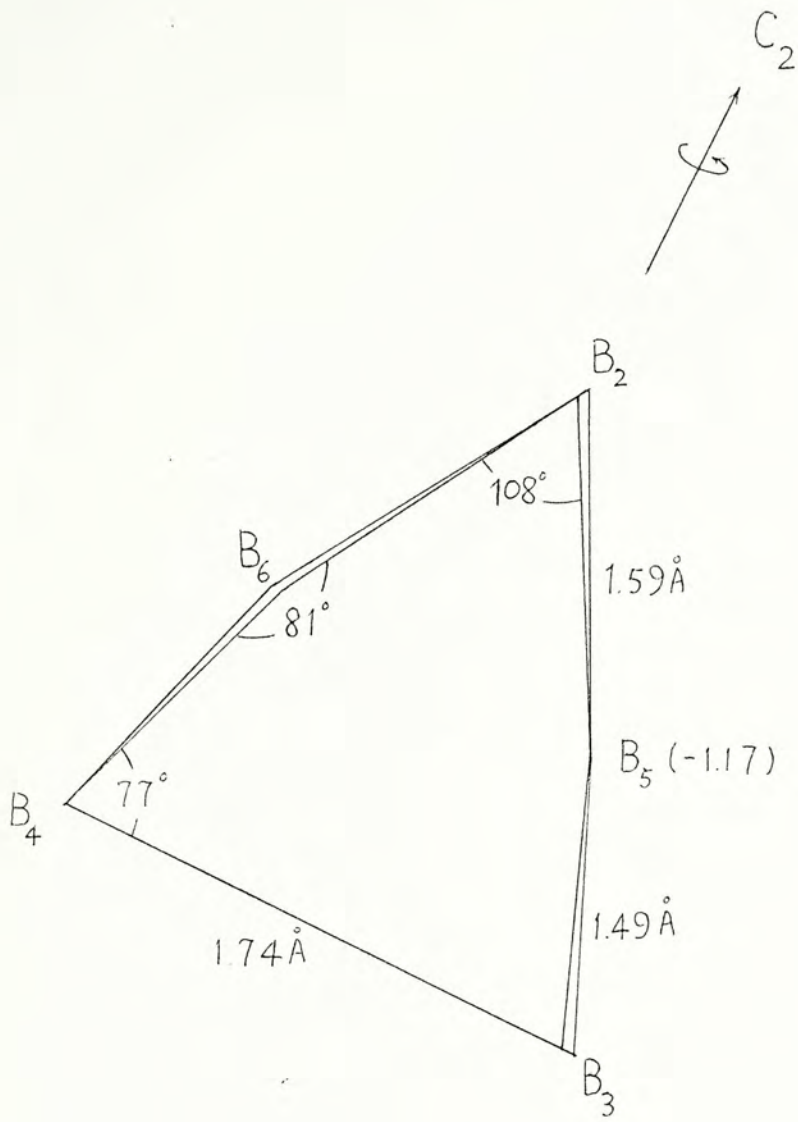

Fig. 2.3 Transition state geometry for the isomerization of $B_5H_5^{2-}$. Atoms B_6 and B_5 are 1.17Å above and below the paper, respectively. Hydrogens have been omitted for simplicity.

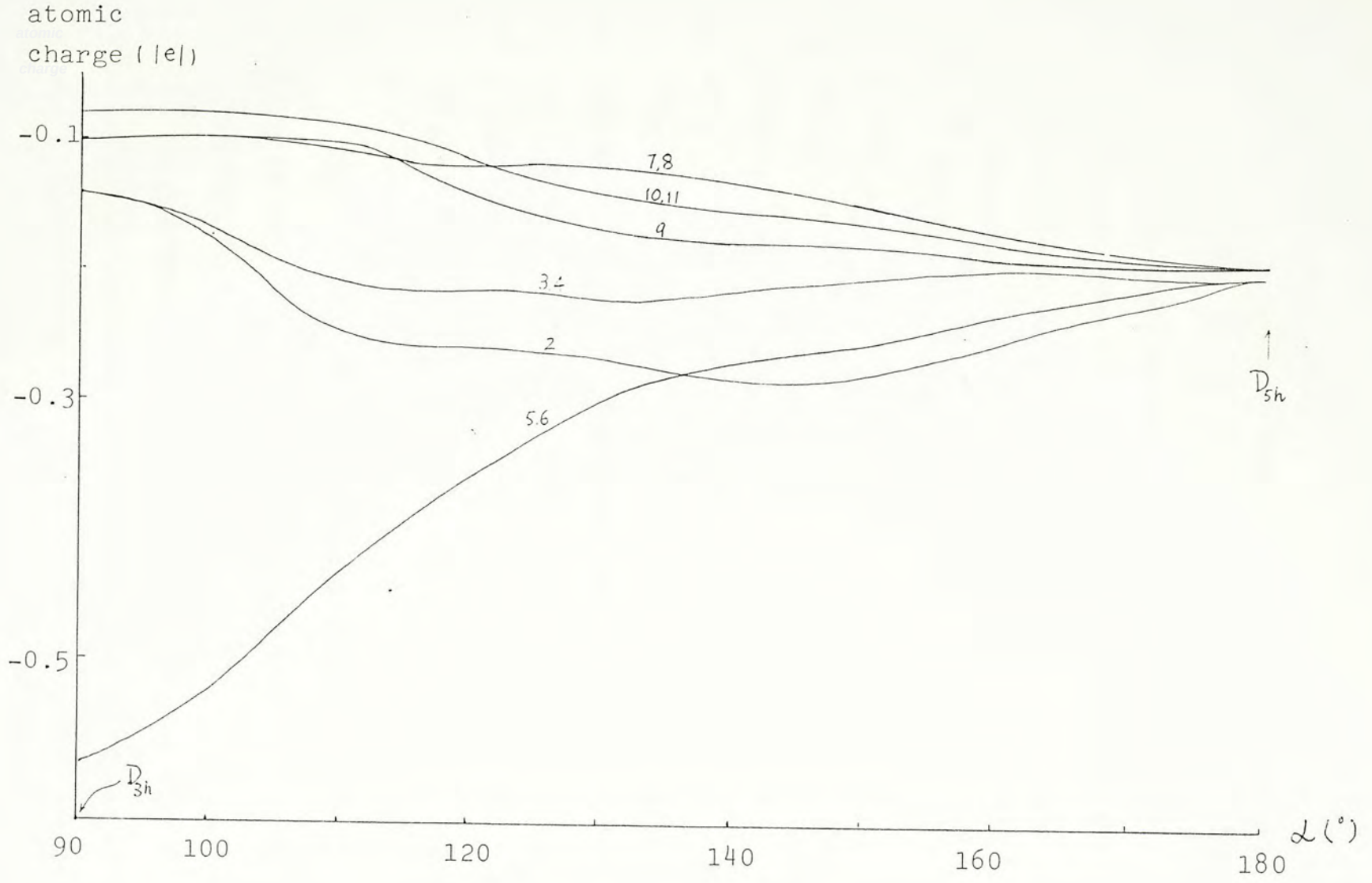

Fig. 2.4 The charge densities on the boron atoms of $B_5H_5^{2-}$ along the reaction path.

to a minimum to yield the C_2 structure. Though the five B-B bonds are nearly of the same length, their bonding interactions are quite different, as indicated by the borons' charges in Fig.2.4. In this region, charges continue to flow away from B_5 and B_6. The main acceptors now are the hydrogens H_9, H_{10} and H_{11}.

For $143^\circ < \alpha < 180^\circ$, the anion continues to open to a flat moiety. The energy rises by 10.5 kcal/mol from 72.3 to 82.8 kcal/mol. The flat structure has D_{5h} symmetry. The B-B bond lengths and the B-H bond lengths are 1.58Å and 1.19Å, respectively. The short B-B bond lengths indicate the presence of multiple bonding. The charges redistribute in this region such that they flow from boron atoms to the hydrogen atoms. The atomic charges accumulated on the hydrogens indicate that the B-H anti-bonding orbital are populated, thus lengthening the B-H bonds to 1.19Å.

The present results suggest that the closo D_{3h} structure is rather unstable; it only requires 4.4 kcal/mol to rearrange to the C_2 structure.

The instability of closo $B_5H_5^{2-}$ may be due to the high charges on the axial borons(0.58e). Hence, delocalization, which is believed to be the main source of stability for the closo structures, is lacking. Viewed another way,

the orientations of the atomic orbitals on the axial and equatorial borons are such that effective overlaps cannot be resulted. However, as pointed out by Dewar[5], the MNDO approximation underestimates the stability of three-center bonds. Hence, the instability of the closo $B_5H_5^{2-}$ species is yet unresolved.

The D_{5h} structure of $B_5H_5^{2-}$ occupies a maximum on the energy profile. Its instability may be due to the combined effects of B-B-B bond strain and the repulsion among the eclipsing hydrogens. Thus, as in the case of cyclopentane, such a structure will undergo out-of-plane bending. Finally, it is mentioned that another route for internal rearrangement for $B_5H_5^{2-}$ has been suggested by Muetterties. The transition state proposed has C_{4v} symmetry. However, according to MNDO calculation, this structure has energy 55.8 kcal/mol higher than that for the D_{3h} structure. Thus, this pathway has not been considered in the present work.

2.3 $B_6H_6^{2-}$

2.3.1 Introduction

Three stable geometries were found for this anion according to the present MNDO results. They are depicted in Fig.2.5, together with their calculated bond lengths and angles. Of the three, the isomer having O_h symmetry is a known entity. According to the MNDO approximation, it is the most stable isomer, with the heat of formation equal to 33.0 kcal/mol. The other two isomers have nearly the same energy, namely, 54.6 and 54.3 kcal/mol for D_{3d} and C_2 structures, respectively. In the following sections, reaction pathways are studied to connect the two isomeric structures of $B_6H_6^{2-}$ to the known structure with O_h symmetry.

2.3.2 Method of Calculation

Three isomerization pathways have been studied. The reaction coordinates of these pathways are shown in Fig. 2.6. Pathway (a) examines the fluxional behavior of the O_h isomer. In this pathway, D_3 summetry is assumed throughout and the transition state has D_{3h} symmetry. The twist angle B_6-D_1-D_2-B_3 is the reaction coordinate.

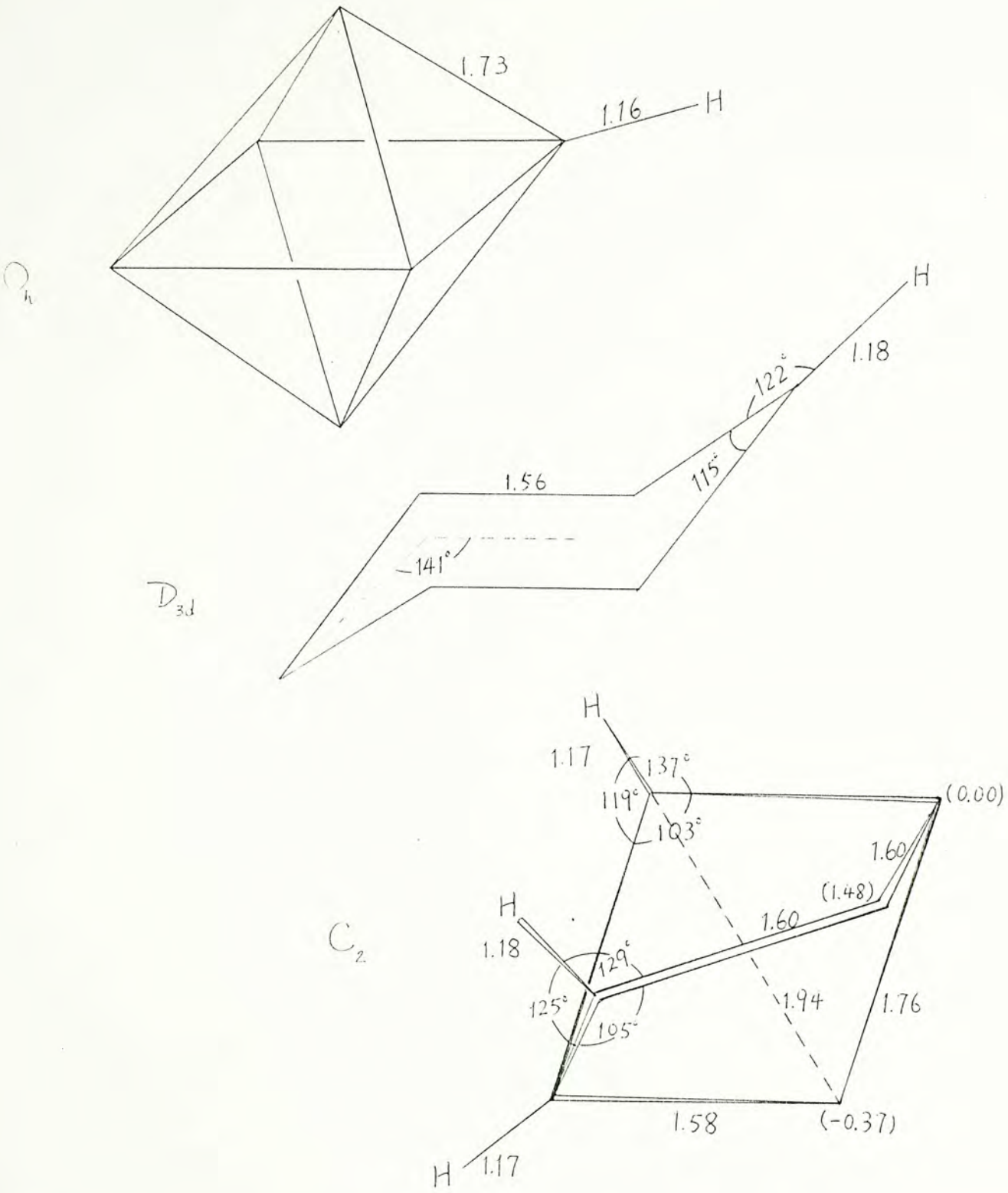

Fig. 2.5 The stable isomers of $B_6H_6^{2-}$. The values in brackets give the distances of the atoms above (>0) or below (<0) the paper. All distances are in Å.

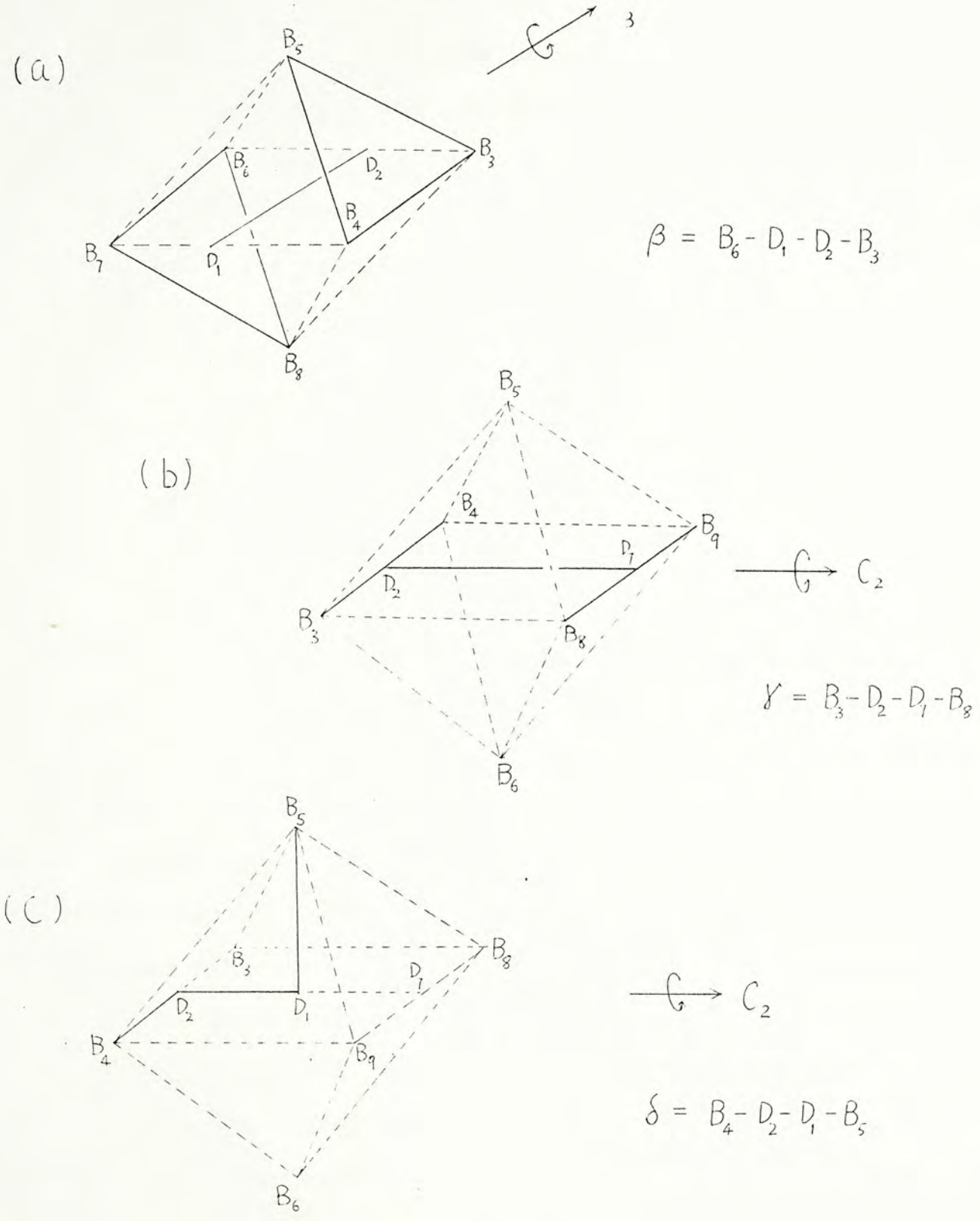

Fig. 2.6 The numbering of atoms for the three isomerization pathways of octahedral $B_6H_6^{2-}$.

Pathway (b) connects the isomers with O_h and D_{3d} symmetries. The reaction coordinate is the twist angle B_3-D_2-D_7-B_8 and C_2 symmetry is assumed throughout.

Pathway (c) connects the isomers with O_h and C_2 symmetries. The reaction coordinate is the twist angle B_4-D_2-D_1-B_5 and C_2 symmetry is assumed throughout.

2.3.3 Results and Discussion

(i) Pathway (a)

This pathway, which is commonly referred to as the Bailar twist[6], assumes D_3 symmetry, i.e., two parallel congruent triangles having their direction vectors coincided, are made to twist. The energy profile along this pathway is shown in Fig. 2.7.

In the region of $60^\circ > \beta > 40^\circ$, the energy of the system remains practically unchanged, although the octahedral structure has been distorted considerably. The enlarging of the two triangles is not considerable, as indicated by the B_3-B_4 interatomic separation which increases from 1.73Å to 1.76Å. The energy gained by bonds such as B_3-B_6 is offset by the energy loss of the partial breaking of the bonds such as B_3-B_8. Also, the interplanar separation remains at roughly 1.42Å. The electronic charges flow away from the boron skeleton to the hydrogens by an amount less than 0.01e per boron atom.

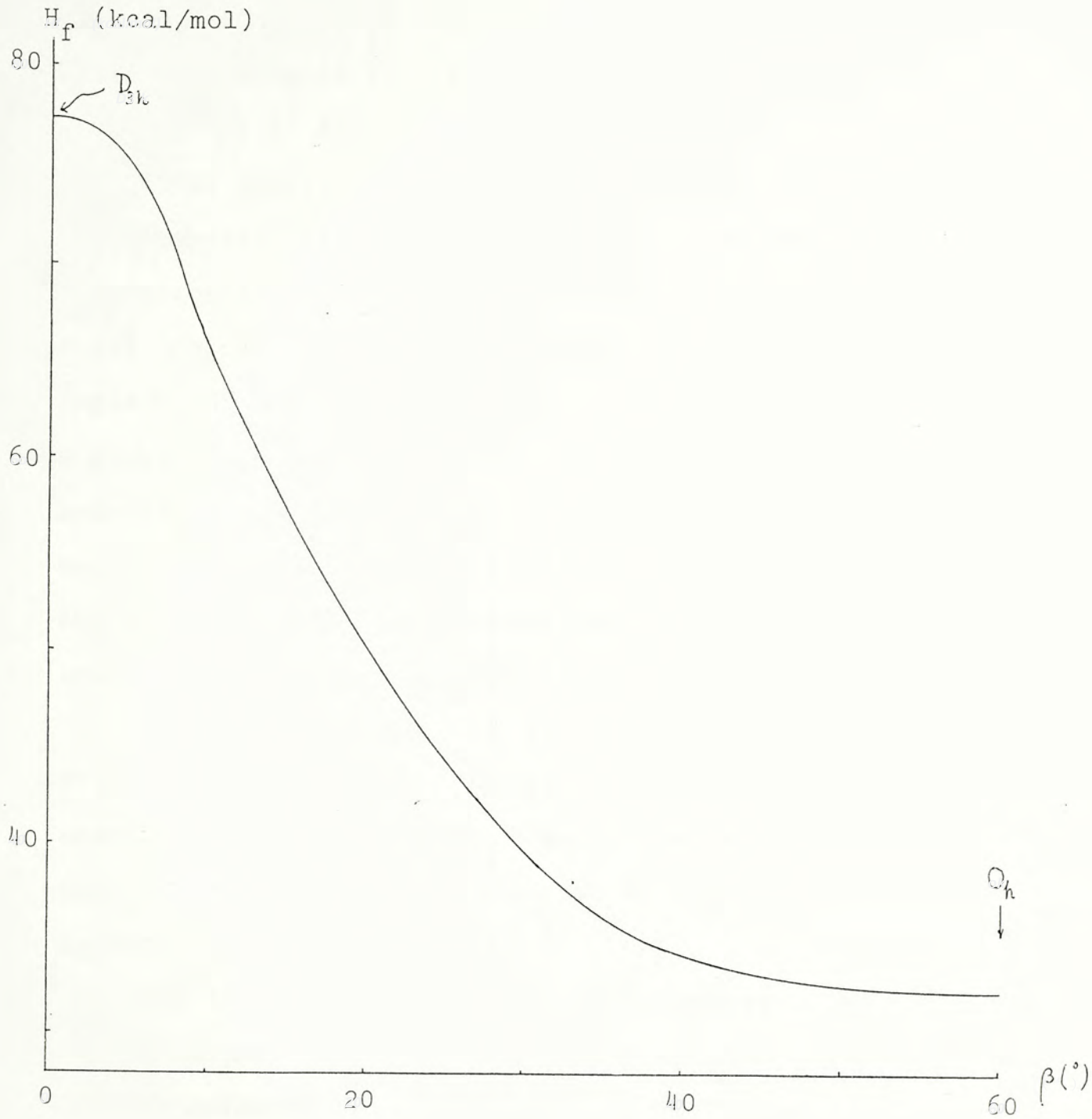

Fig. 2.7 Energy profile of the rearrangement of $B_6H_6^{2-}$ by the D_3 mode (pathway (a)).

In the region $0^{\circ} < \beta < 40^{\circ}$, energy rises sharply to reach the value of 77.2 kcal/mol at the transition state, at which $\beta = 0^{\circ}$ and with D_{3h} symmetry. This yields an activation energy of 44.2 kcal/mol. In this region, the separation between B_3 and B_4 and the interplanar separation increase to reach maximum values of 1.81Å and 1.51Å, respectively. Also, at the transition state, the angle H_9-B_3-B_6 is 127°. A small charge flow (about 0.04e/atom) is observed from the borons to the hydrogens. The B-H bond lengths are gradually lengthened to 1.17Å at the transition state, compared to 1.16Å for the O_h system. This indicates the B-H anti-bonding orbitals have been populated to some extent.

Since the D_{3h} structure is higher in energy by 44.2 kcal/mol than the O_h system and this activation energy is much higher than those for pathways (b) and (c), this route for intramolecular rearrangement is unlikely to occur.

The instability of the D_{3h} structure relative to the O_h structure may be explained by considering their bonding schemes. According to the MNDO results, the inter-boron bond orders for the D_{3h} framework are 1.29 for B_3-B_6 and 0.52 for B_4-B_8 while the bond order for B_3-B_4 is 0.65 in the O_h system. Canonical forms of the D_{3h} structure are shown in Fig. 2.8, along with the topologically allowed structure[1] for the O_h structure.

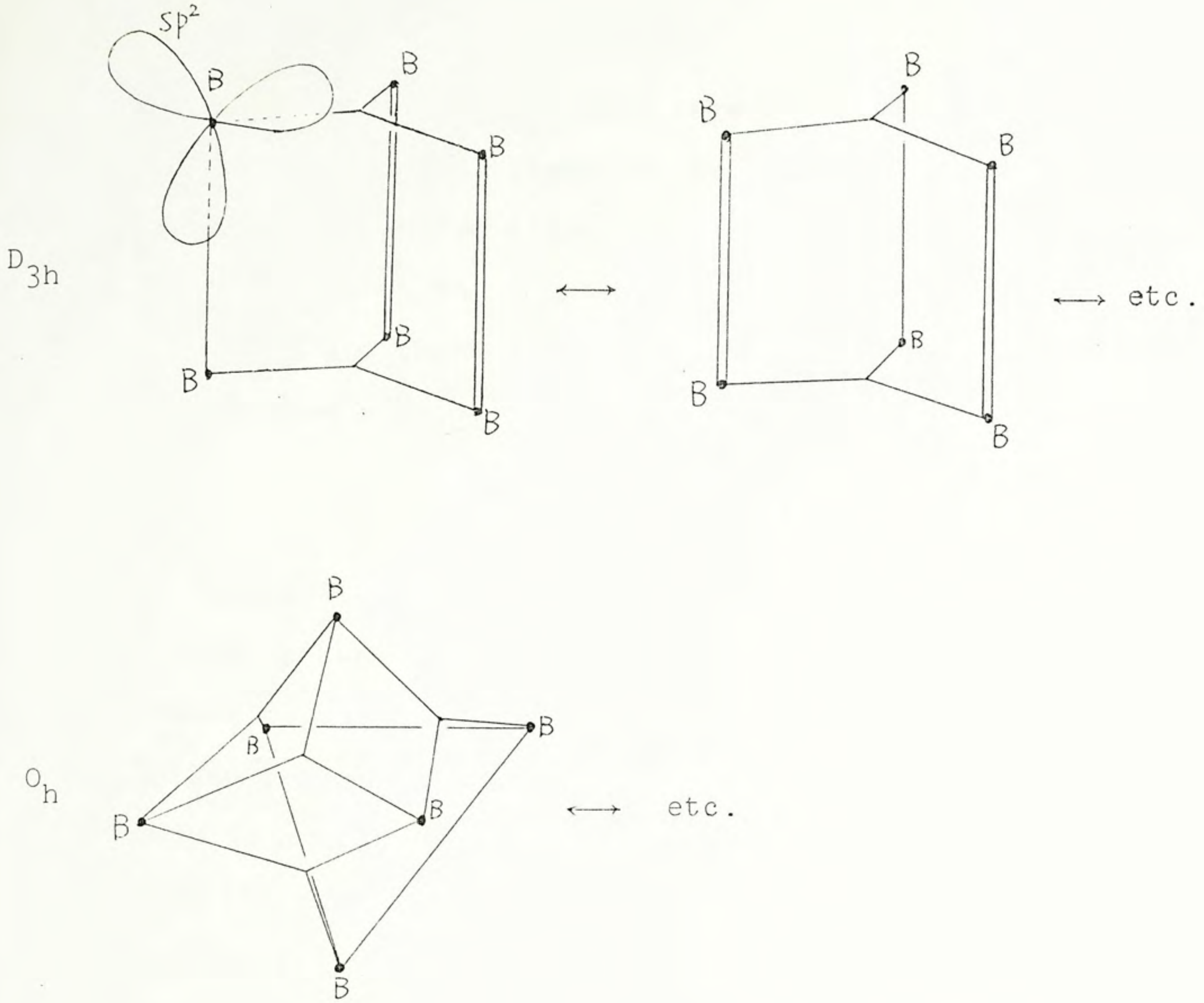

Fig. 2.8 The canonical forms of the D_{3h} and O_h structures of $B_6H_6^{2-}$.

The borons in the D_{3h} structure are assumed to be sp^2 hybridized so that the structure has two three-center bonds, two pi bonds and three sigma bonds for the skeletal bonding. On the other hand, the O_h structure has formally four three-center bonds and three two-center bonds. Thus, the O_h system is more stable.

(ii) Pathway (b)

This pathway is designed to connect the octahedral structure to the cyclohexane-like D_{3d} structure by intramolecular rearrangement. The energy profile of the pathway is shown in Fig. 2.9.

In the region of $0^\circ < \gamma < 90^\circ$, the small increase in energy for the first 20° shows that the closo structure allows slight structural distortions. For the next 70°, energy rises sharply to 67.4 kcal/mol. In this region, it is found that D_{2d} symmetry is preserved; hence the boron atoms B_3, B_4, B_8 and B_9 are equivalent. At $\gamma = 90^\circ$, the bond angle B_4-B_5-B_8 reaches 119° and B_5-B_8-B_9 is 97°. This indicates that B_5 and B_6 have nearly reached their final state as in a D_{3d} structure, while the other four borons are still on the way. The atomic charges on the borons fluctuate in the region of 0.05e, but a trend

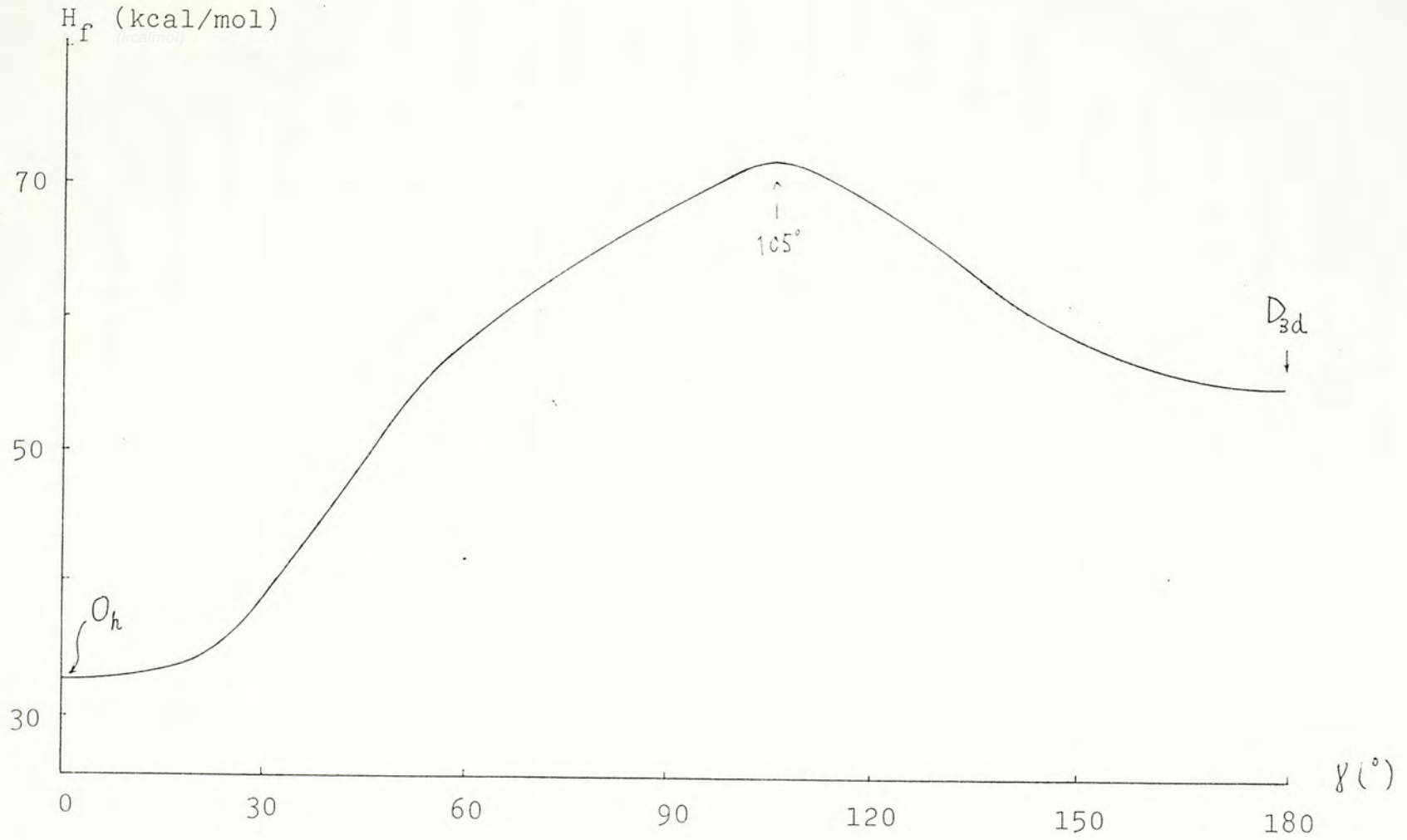

Fig. 2.9 Energy profile for the intramolecular rearrangement of $B_6H_6^{2-}$ between O_h and D_{3d} symmetries.

suggests that charges flow away from the borons. This again indicates the ability of closo structure to accommodate electronic charges. At $\gamma = 90^{\circ}$, B_3 carries a charge of -0.17 and B_5 carries -0.24, compared to their O_h values of -0.28.

In the region of $90^{\circ} < \gamma < 105^{\circ}$, energy rises to the maximum value of 71.1 kcal/mol, yielding an activation energy of 38.1 kcal/mol. The transition state geometry is shown in Fig. 2.10. The geometry in this region has no extra symmetry other than the imposed C_2-axis. In other words, B_8 and B_9 are becoming closer with B_5 and B_6, respectivity. At the transition state, the separation between B_3 and B_5 is 2.31Å, indicating the opening of the cage is practically complete. Considering the charge distribution so far, a total of 0.82 electron flows away from the borons. This may be in part due to the breakdown of the octahedral cage and in part due to the strain of the boron skeleton at the transition state.

In the region of $\gamma > 105^{\circ}$, energy drops steadily to a minimum at $\gamma = 180^{\circ}$ for the D_{3d} structure. As far as this pathway is concerned, the reverse rearrangement to an O_h system requires an activation energy of 16.5 kcal/mol. The B_3-B_6-B_9 bond angle for the D_{3d} structure is 115° with B_3-B_6 separation being 1.56Å. The bond angle of 115°

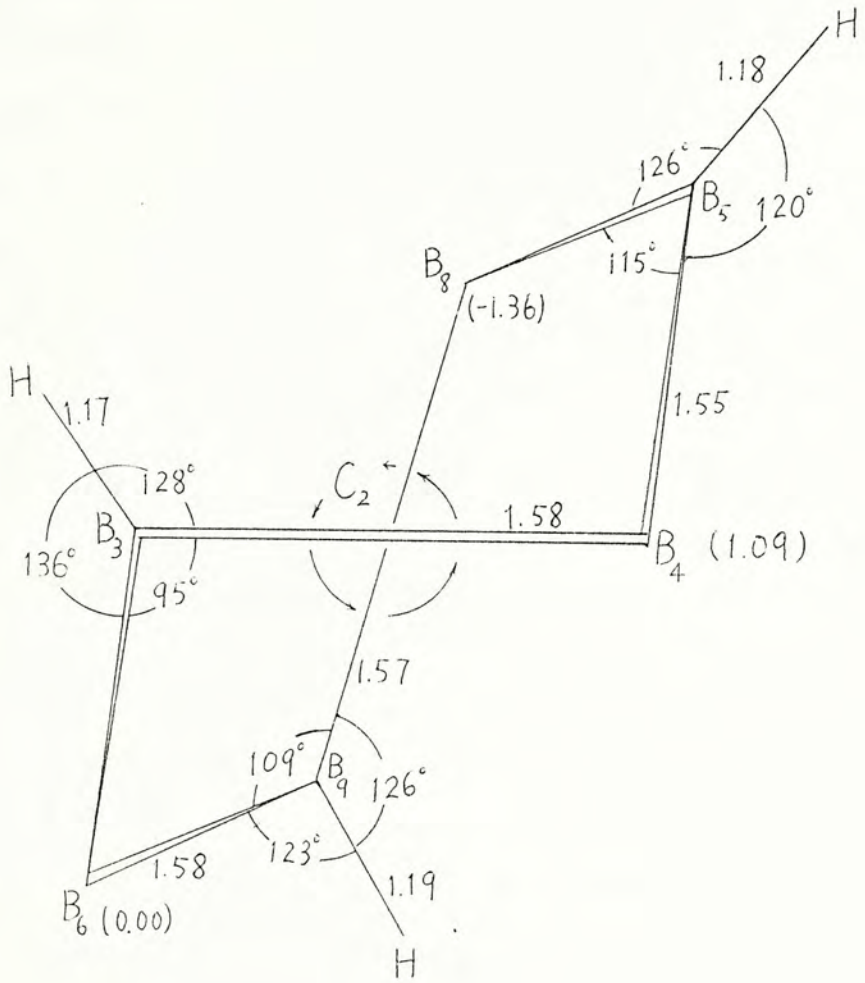

Fig. 2.10 Transition state of the rearrangement pathway (b) of $B_6H_6^{2-}$. Note that the cage is opened and that the separation between B_3 and B_5 is 2.31Å. All distances are in Å.

suggests that the hybridization of each boron is about midway between sp^2 and sp^3.

The rearrangement stops at the D_{3d} structure and does not yield a planar benzene-like structure because, in the latter structure, the negatively charged hydrogens would be in an eclipsed configuration and the pi bonding interactions between the borons are not strong enough to overcome the repulsions between the hydrogens.

Finally, it is remarked that the activation energy of 38.1 kcal/mol for this pathway is still higher than the to-be-discussed pathway(c). Hence this rearrangement pathway is also unlikely to occur.

(iii) Pathway (c)

This pathway connects the O_h and the C_2 bicyclic structures. The fused-ring structure is found to be 21.3 kcal/mol higher in energy than the O_h one.

The energy profile and the charge distribution for this pathway are shown in Figs. 2.11 and 2.12, respectively.

For $70^\circ < \delta < 90^\circ$, it can be seen from Fig. 2.11 that the energy begins to rise sharply at $\delta < 80^\circ$ and reaches a value of 38.4 kcal/mol. The charges on the borons fluctuate in the region of 0.03e, as shown in Fig. 2.12.

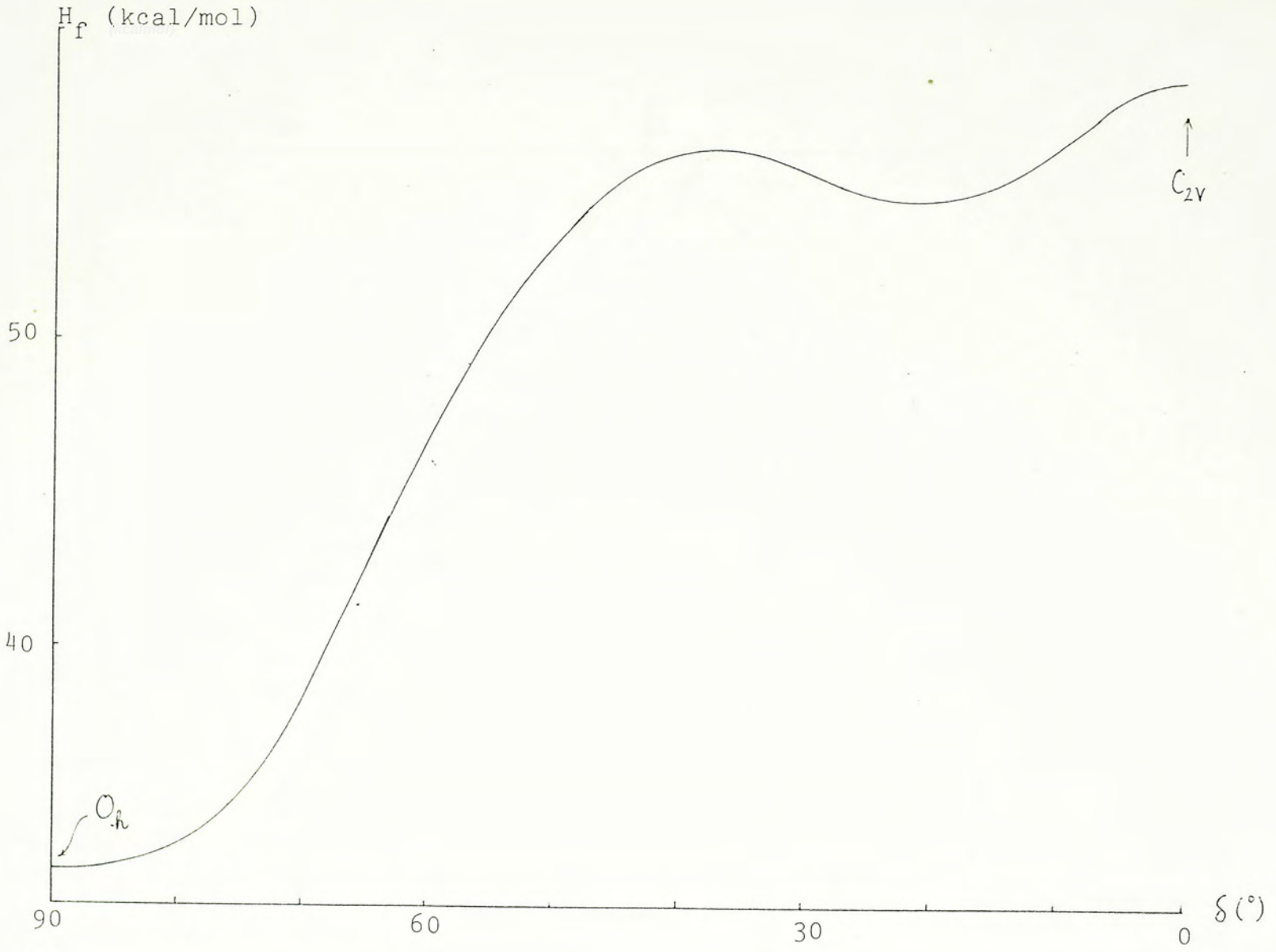

Fig. 2.11 The energy profile for the pathway (c) of the isomerization of $B_6H_6^{2-}$.

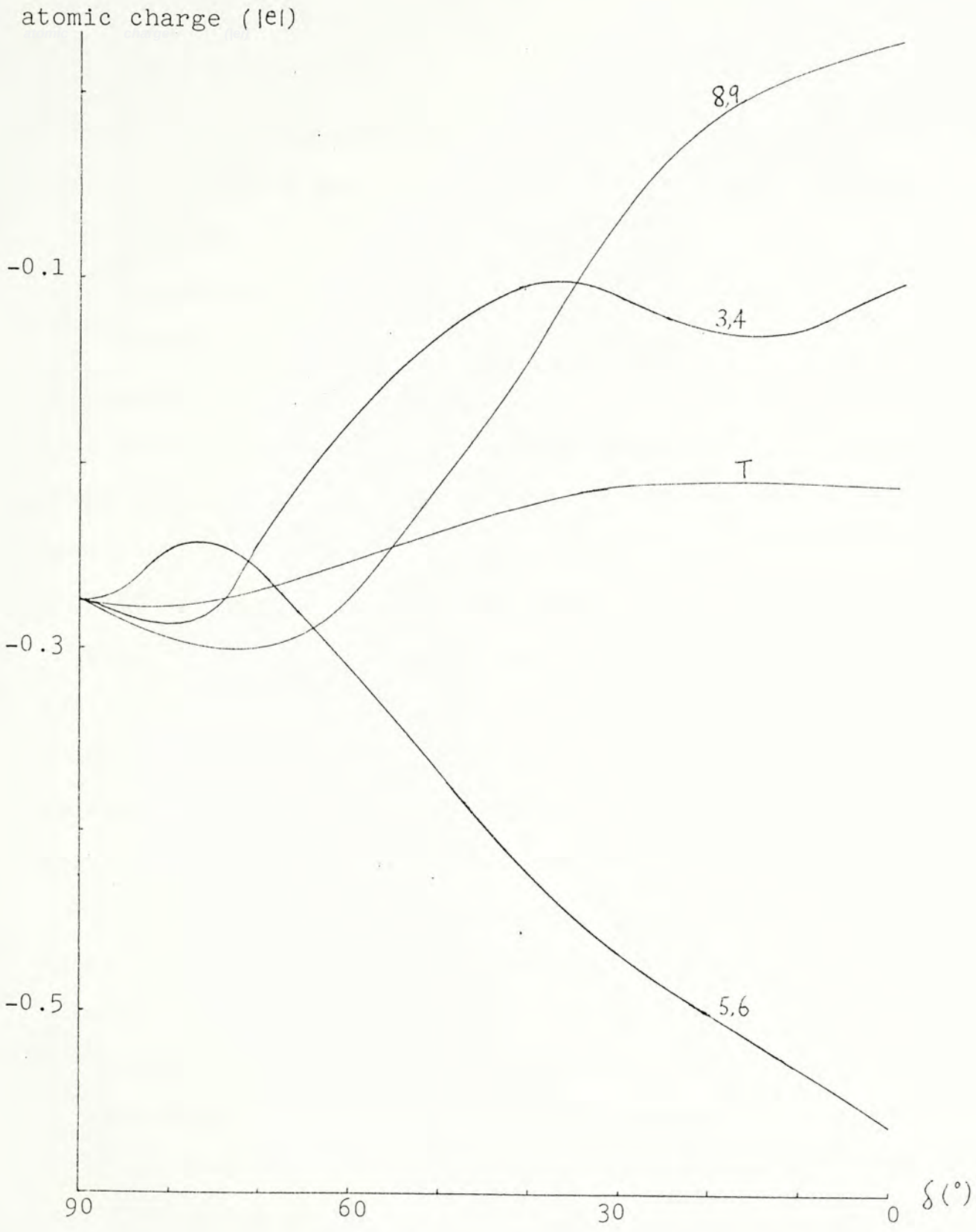

Fig. 2.12 The charge distributions on the borons along the pathway (c) for the isomerization of $B_6H_6^{2-}$. Charges on the hydrogens are neglected. The curve labelled T is the sum of the boron charges.

At $\delta = 70^{\circ}$, the interatomic separation between B_3 and B_5 is 2.05Å, showing that the cage is distorted to a considerable extent.

In the region $\delta < 37^{\circ}$, energy rises smoothly to reach the transition state, whose geometry is shown in Fig. 2.13. The energy of the transition state is 23.1 kcal/mol higher than the O_h structure. At the transition state, the structure looks like a distorted trigonal prism. It is noted that the separation between B_3 and B_8 is 2.12Å which indicates the cage is still not broken. Nevertheless, the interaction between B_3 and B_8 cannot apply significant influence to bend the planar coordination environment around B_3. The charge redistribution in this region is, as expected, such that charge accumulates on B_5 and B_6 which have the highest coordination numbers.

In the remaining region, energy drops to a shallow local minimum for the fused-ring structure. It is interesting that the stablization of this structure does not come from stronger bonds but rather from the release of bond angle strains. Comparing the geometry parameters of structures for $\delta = 37^{\circ}$(transition state) and $\delta = 20^{\circ}$ (local minimum) would verify this argument that all the B-B bonds are lengthened [In addition, the B-H separarions are also lengthened.]. The release of the strain of the

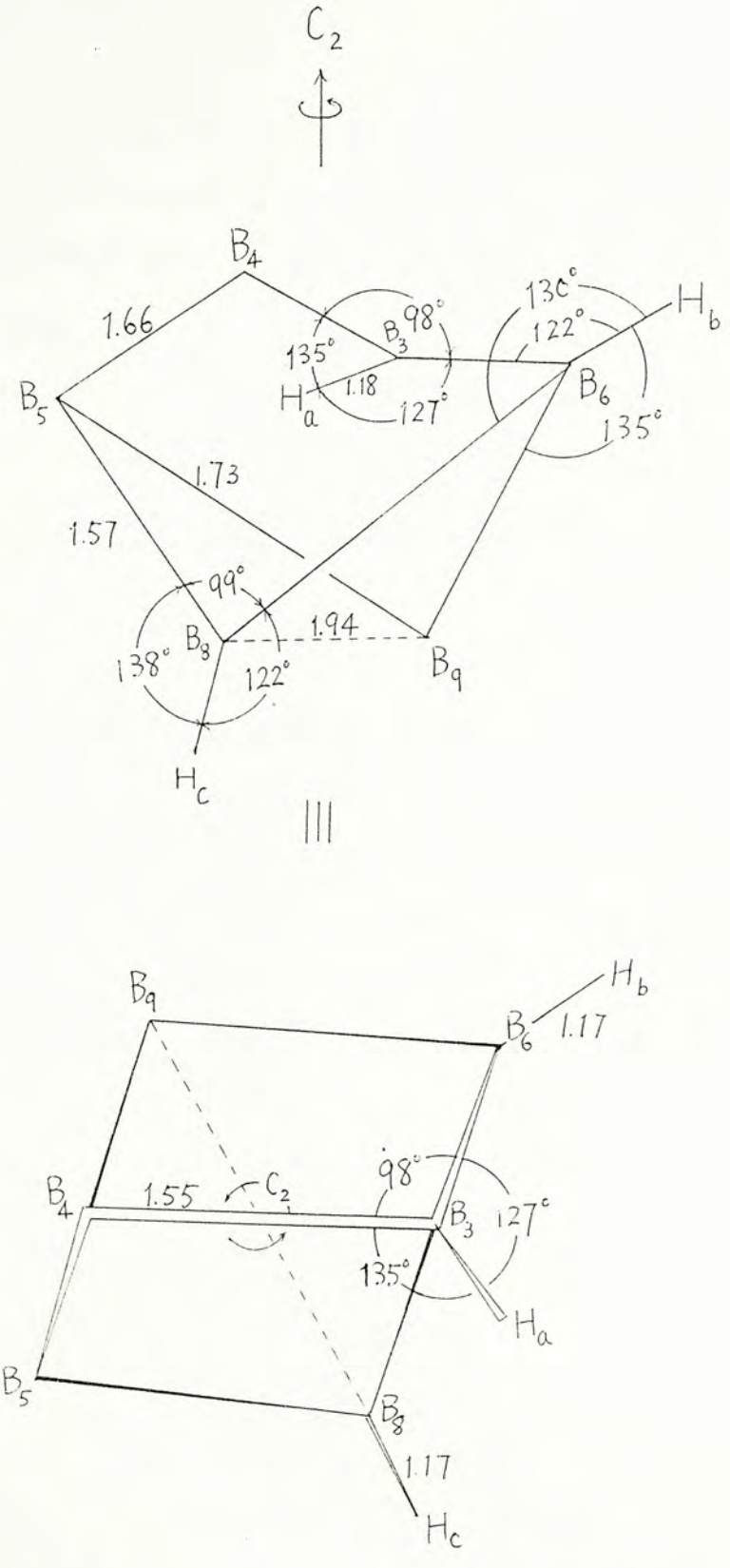

Fig. 2.13 The transition state geometry for the rearrangement pathway (c) of $B_6H_6^{2-}$. Distances are in Å.

boron bond angles can be seen by the increase of their magnitude. Since energy rises again as δ goes to zero, this indicates that the structure at the local minimum should be of the least strain.

This reaction pathway is the most facile one among the three studied. It is lower in activation energy than pathway (b) because the product of pathway (c) is still cage-like, i.e., the borons of this product have higher coordinate numbers than the borons in the D_{3d} structure. It is also easier to rearrange by pathway (c) than pahtway (a) since the latter has a much higher symmetry(D_3) and lowering the symmetry for the trigonal prism structure will give the fused-ring structure.

2.4 $B_7H_7^{2-}$

2.4.1 Introduction

This anion may have a pentagonal bipyramidal structure with D_{5h} symmetry, as suggested by its ^{11}B NMR spectrum[7] which shows two peaks with area ratio 5:2. However, such a spectrum may be arisen from a structure with lower symmetry and accidental degeneracies[8] according to the NMR time scale. This anion is less stable with reference to $B_6H_6^{2-}$ and $B_8H_8^{2-}$ in aqueous solution such that slow evolution of hydrogen commences immediately on dissolution in water.

The study of the intramolecular rearrangement of this ion is rare but is generally considered to be not facile[3,4]. This section is to investigate the degree of difficulty of the structural rearrangement.

There are three reasonable structures for this anion: square-capped trigonal prism (C_{2v} symmetry), triangular-capped trigonal prism (C_{3v}) and the pentagonal bipyramidal (D_{5h}) structure mentioned above.

The MNDO heats of formation of these three structures are 37.3 kcal/mol, 78.3 kcal/mol and 1.9 kcal/mol, respectively. In view of the high energy of the C_{3v} structure, only the pathway connecting the D_{5h} and the C_{2v} structures will be studied.

Fig. 2.14 shows the MNDO structures with D_{5h} and C_{2v} symmetries of the anion $B_7H_7^{2-}$, together with the reaction coordinate and the numbering of atoms. The reaction coordinate is taken to be the twist angle B_6-D_2-D_5-B_8, denoted as ω below. The symmetry constraint in this pathway is C_2 which passes through B_1, D_2 and D_5.

2.4.2 Results and Discussion

The energy profile of the reaction pathway is shown in Fig. 2.15. The twist angles for the D_{5h} and C_{2v} structures are 0° and 44.3°, respectively. The charge distribution throughout the rearrangement is shown in Fig. 2.16.

In the region $0^\circ < \omega < 20^\circ$, the energy rises rapidly, showing that the cage is fairly rigid toward distortion. For reference, at $\omega = 20^\circ$, the separations between B_3-B_8, B_4-B_8 and B_6-B_8 are 2.09Å, 1.74Å and 1.66Å, respectively. From Fig. 2.16, it can be seen that the charge flow in this region is small.

In the region $20^\circ < \omega < 44.3^\circ$, the C_{2v} structure is reached. The C_{2v} structure is lying 35.4 kcal/mol higher in energy than the D_{5h} structure. This structure (C_{2v}) is expected to be less stable than the D_{5h} one for the connectivities are reduced by one at the atoms B_3, B_4,

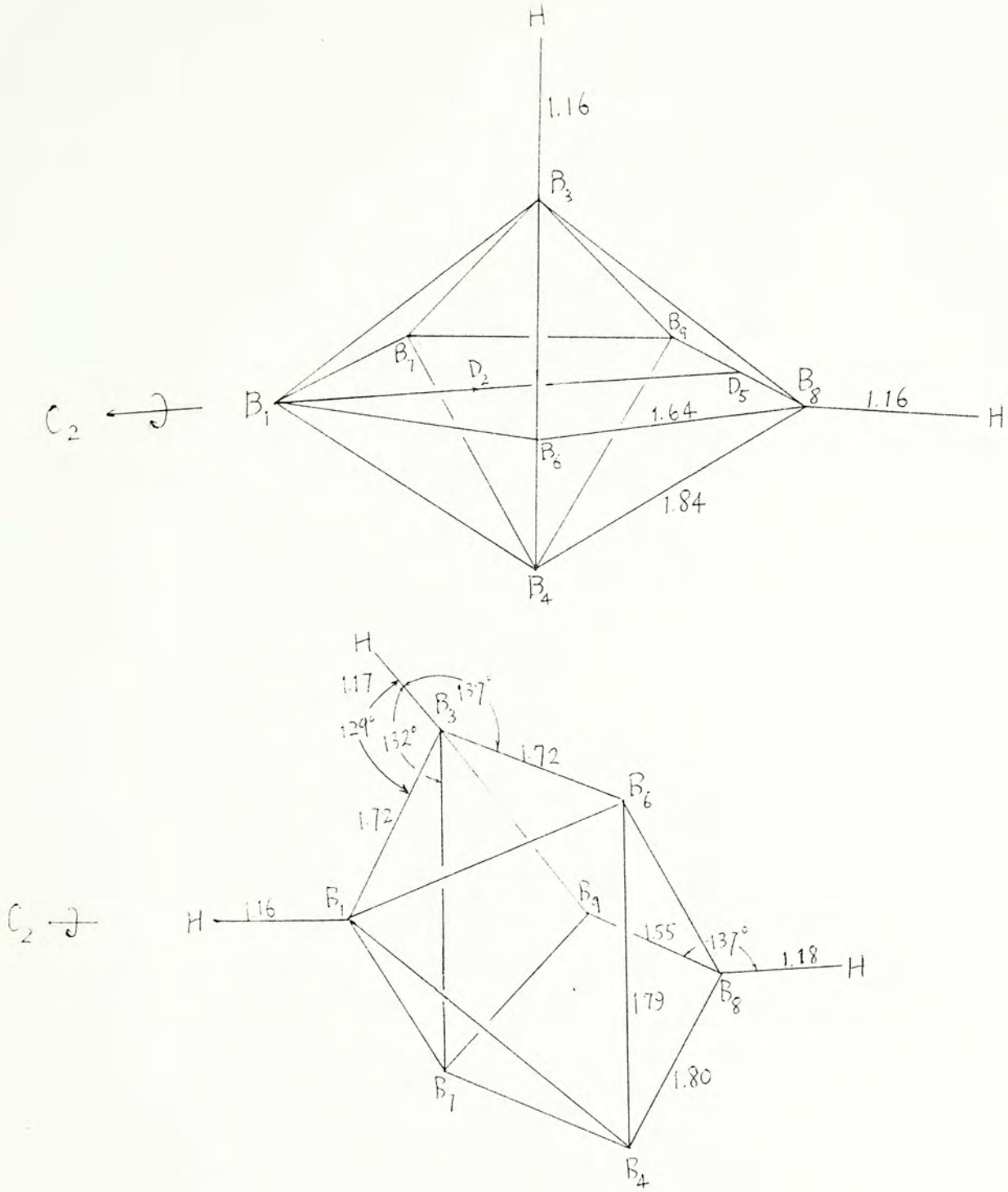

Fig. 2.14 MNDO structures of $B_7H_7^{2-}$ with D_{5h} and C_{2v} symmetries. Distances are in Å.

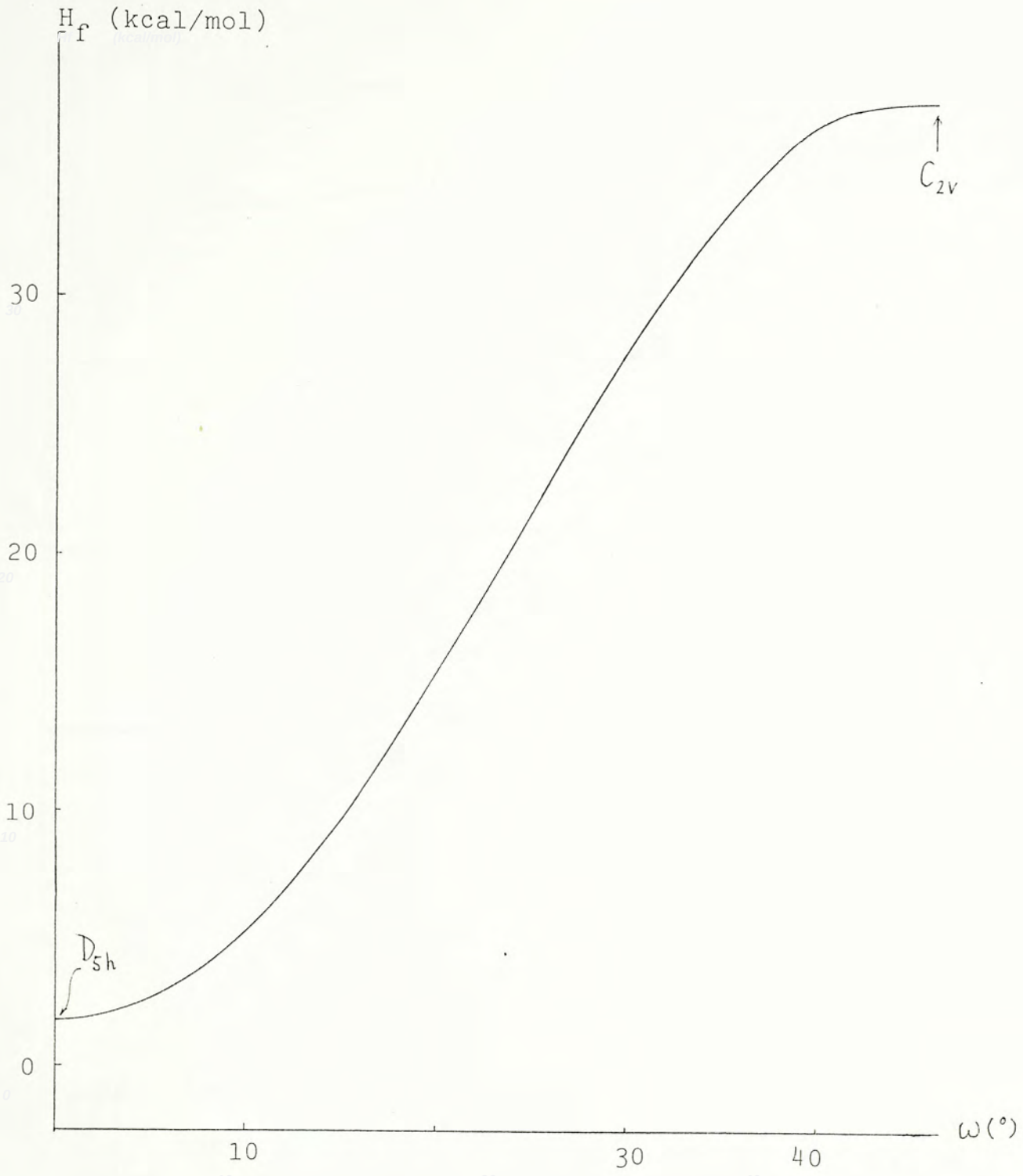

Fig. 2.15 The energy profile for the rearrangement of $B_7H_7^{2-}$.

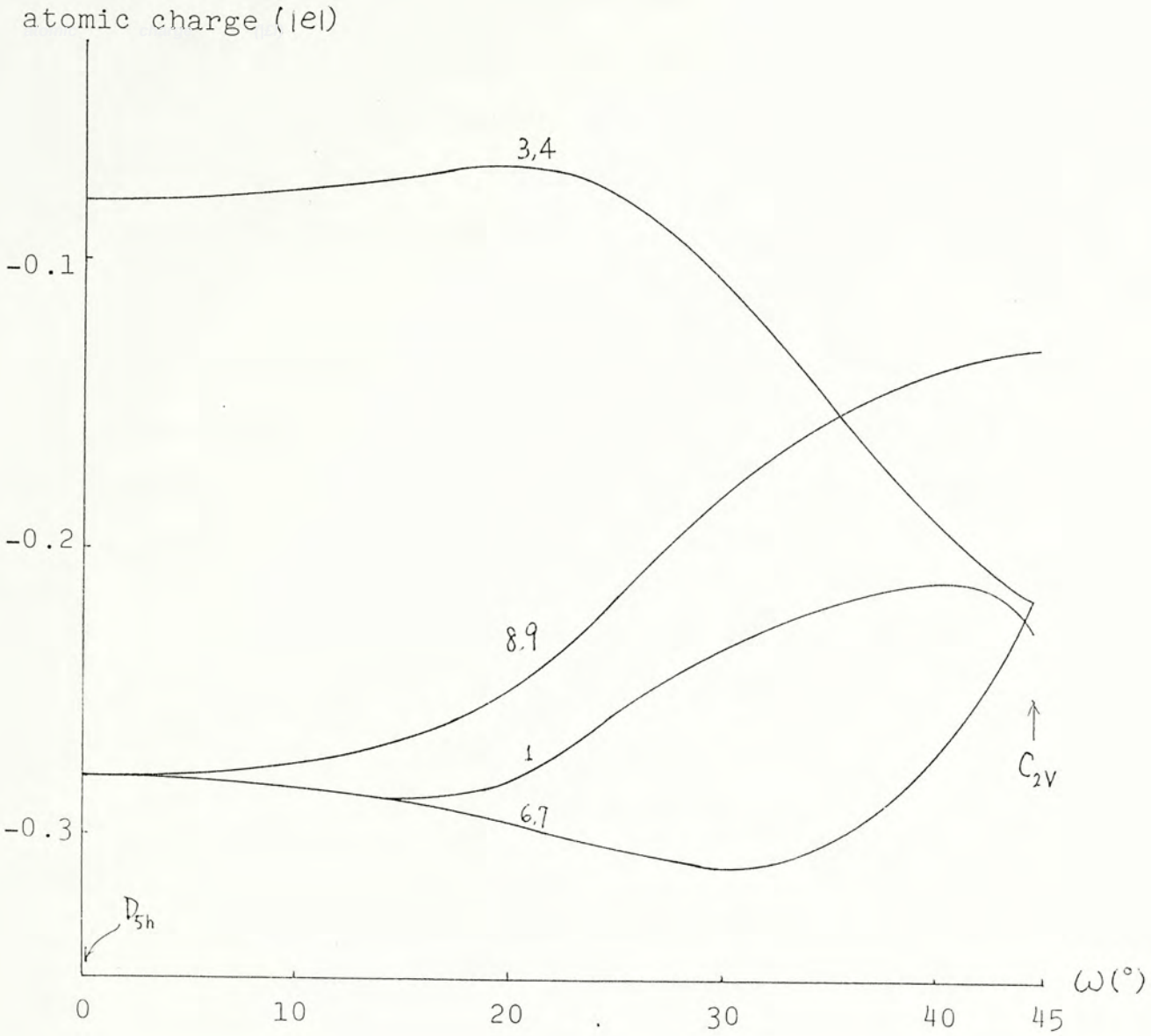

Fig. 2.16 The atomic charge distribution on the boron atoms along the rearrangement process of $B_7H_7^{2-}$.

B_8 and B_9 while the other borons has no change in their connectivities. The charge flow in this region is large, as expected. In this region, atoms B_3 and B_4 gain electronic charges and B_6 and B_7 lose electronic charge; the charges of these four atoms become equal for the C_{2v} structure.

The increase in charges on B_8 and B_9 are due to their decrease in connectivity. The MNDO approximation has a tendency to yield lower charges on atoms with high connectivity in a closo structure.

2.5 $B_8H_8^{2-}$

2.5.1 Introduction

This anion has been observed to have stereochemical nonrigidity[9,10]. It has a slightly distorted dodecahedron structure[11] in the solid state, but exists primarily in the square-antiprismatic (D_{4d} symmetry) form in protonic or highly polar media, and in the square-bicapped trigonal prismatic (C_{2v}) structure in less polar media, while the latter two forms coexist in certain nonpolar solvents[12]. Thus, the fluxional behavior of the anion in solution is suggested[13] to be a result of its interaction with the solvent. This interaction stablizes the C_{2v} and D_{4d} structures by solvation or ion pairing, with the cation locating on the anions' square face(s).

The above three structures of $B_8H_8^{2-}$ have been studied[13] by PRDDO and EH models. The PRDDO results show that the D_{2d} structure is 3.6 kcal/mol more stable than the C_{2v} structure and the C_{2v} structure is 33.2 kcal/mol more stable than the D_{4d} one. The EH model gives a reverse prediction : D_{4d} structure is more stable than the C_{2v} and the D_{2d} structures by 42.4 and 48.4 kcal/mol, respectively. The present MNDO calculations show the same trend of stability for the three structures as the PRDDO

model : the D_{2d} structure is more stable than the C_{2v} and the D_{4d} structures by 1.8 and 20.6 kcal/mol, respectively. The MNDO structures for these three species are shown in Fig. 2.17.

Two pathways have been studied to connect the above three structures. The first one [pathway (a)] concerns with the D_{2d} and the C_{2v} structures and the second one [pathway (b)] connects the D_{2d} and the D_{4d} systems.

For the first pathway, C_2 symmetry is assumed. The symmetry axis is defined by the two dummy atoms D_1 and D_2. The separation between B_3 and B_4 (d_{34}) is taken to be the reaction coordinate.

The second pathway converts the D_{2d} to the D_{4d} structure. The reaction coordinate is taken to be the angle θ, defined by B_8-D_2-D_1 such that $\theta = 75^{\circ}$ and $\theta = 90^{\circ}$ are for the D_{2d} and D_{4d} structures, respectively.

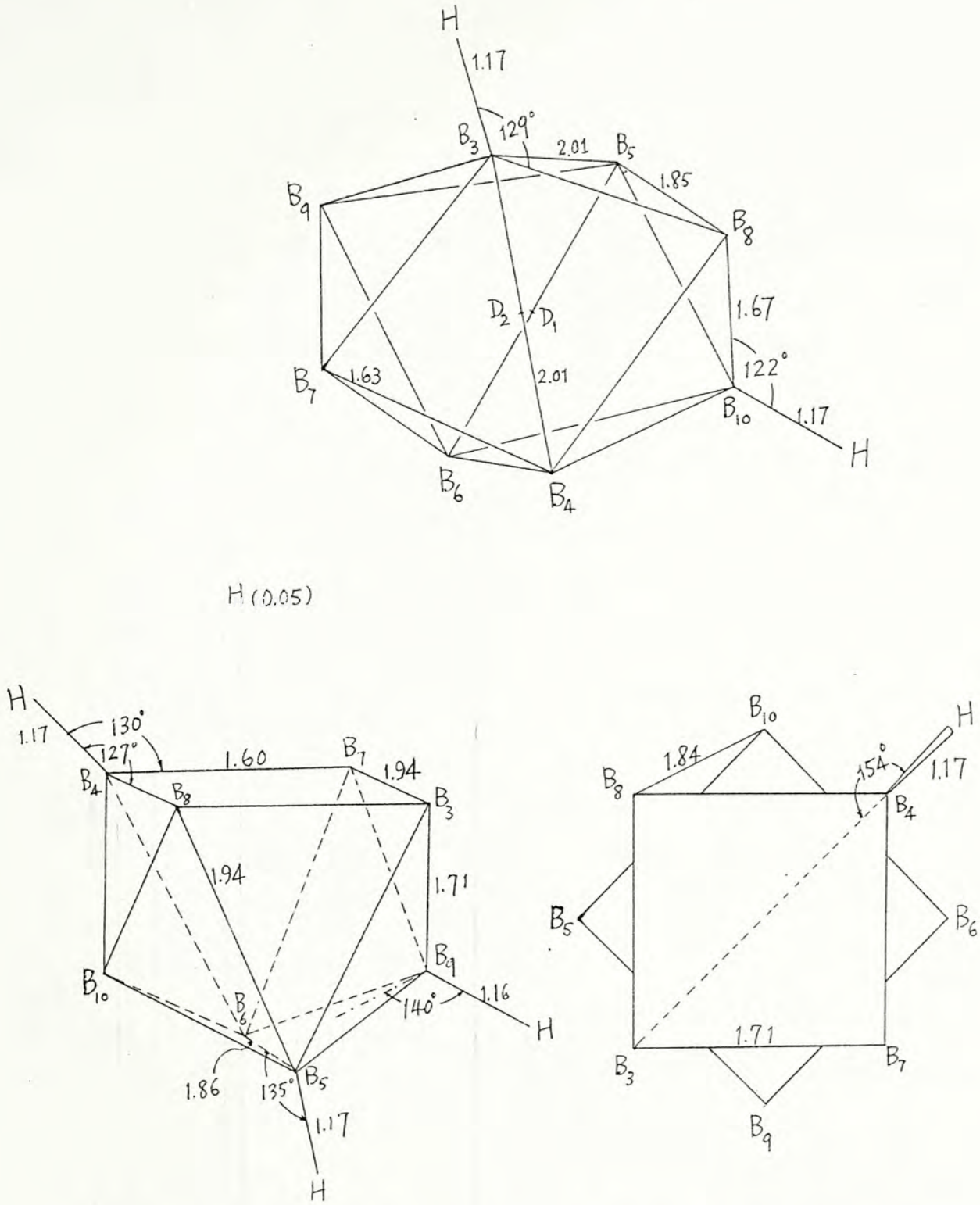

Fig. 2.17 The MNDO structures of $B_8H_8^{2-}$ with D_{2d}, C_{2v} and D_{4d} symmetries. Positive (negative) values in parenthesis indicate the distances of those atoms above (below) the paper. Bond lengths are in Å.

2.5.2 Results and Discussion

(i) Pathway (a)

The energy profile concerning the transformation of the D_{2d} structure to the C_{2v} structure is shown in Fig. 2.18. It is noted that the C_{2v} structure is attained when d_{34} is lengthened to 1.26Å. The energy required for this reaction is 1.8 kcal/mol which is low enough to allow a rapid interconvertion of the two structures. As shown in Fig. 2.19, charge flows from B_7 and B_8 to B_3 and B_4 and the charges on these atoms become equal at the C_{2v} structure. The variation in their coordination numbers may be responsible for the redistribution of charges. The atoms B_5, B_6, B_9 and B_{10} retain their charge densities in these region for their environments are practically unchanged.

As d_{34} continues to lengthen, the D_{2d} structure will be obtained again at d_{34} = 1.37Å.

Since the C_{2v} structure is only 1.8 kcal/mol higher in energy than the D_{2d} one, the former will be more stable in solution if its square face can be stablized by ion pairing. The ^{11}B NMR spectrum for the salt $[(n\text{-}C_4H_9)N]_2B_8H_8^{2-}$ in dimethoxyethane studied by Muetterties[9] gives three doublets with relative intensities of 2:4:2 at low temperature. This pattern is in agreement with the C_{2v} structure.

Fig. 2.18 The energy profile of the rearrangement pathway (a) of $B_8H_8^{2-}$.

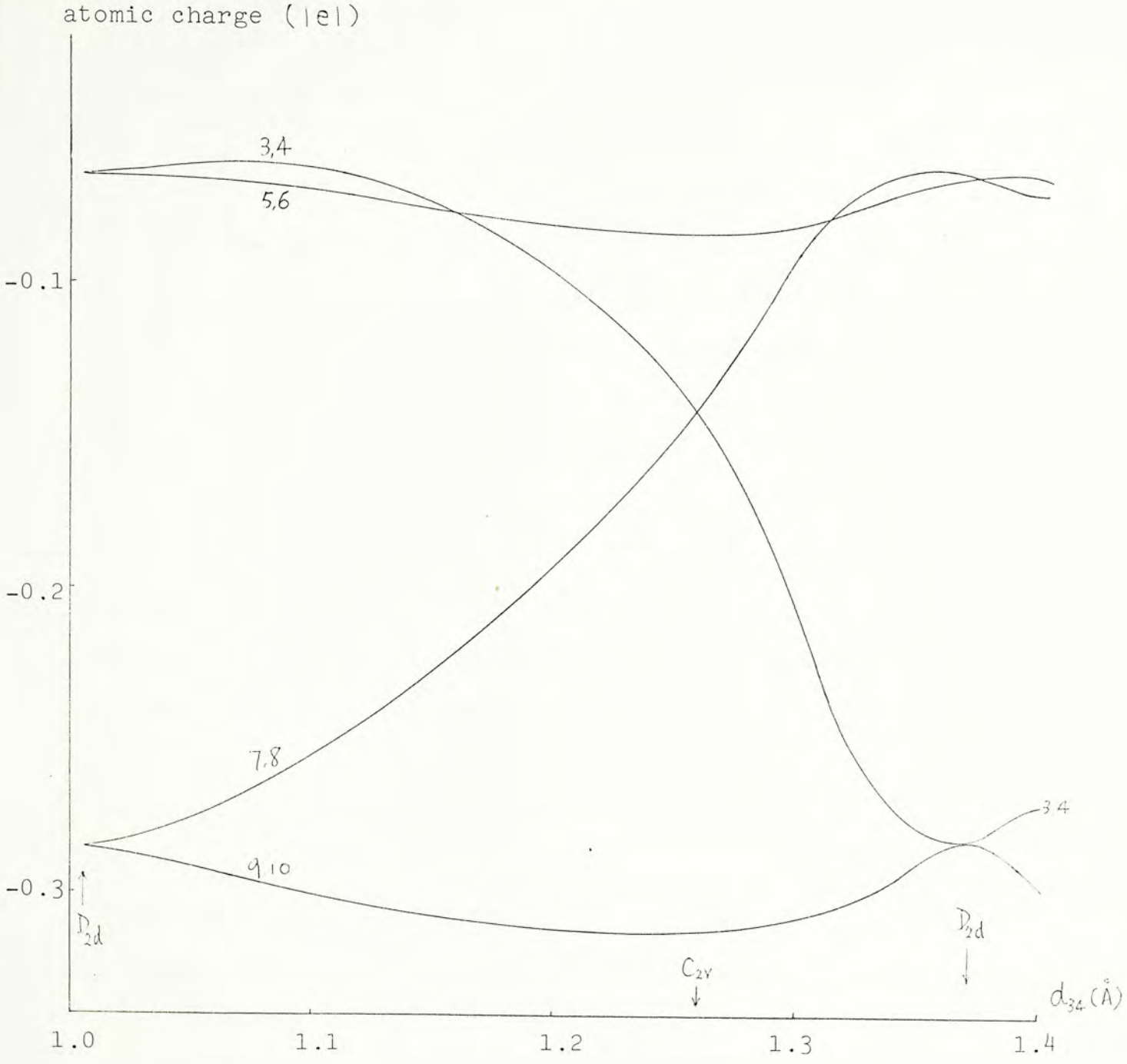

Fig. 2.19 The charge distribution of boron atoms along the reaction pathway (a) for the rearrangement of $B_8H_8^{2-}$.

(ii) Pathway (b)

The energy profile of this pathway is shown in Fig. 2.20.

For $\theta < 80^{\circ}$, the energy rises by 3.7 kcal/mol in this region. The cage is distorted very slightly such that the separation between B_4 and B_8 is 1.81Å and that between B_4 and B_7 is 1.64Å, compared to the D_{2d} values of 1.85Å and 1.63Å, respectively. Thus, it is obvious that all the atomic charge densities retain their original values, as shown in Fig. 2.21.

In the region of $80^{\circ} < \theta < 90^{\circ}$, the D_{4d} structure is reached at $\theta = 90^{\circ}$. The energy increases rather sharply to the maximum, which indicates the instability of the D_{4d} structure with respect to the D_{2d} one by 20.6 kcal/mol. The rise in energy is apparent due to the reduced connectivity of the B_3, B_4, B_9 and B_{10} from 6 to 5. Considering Fig. 2.21, it is seen that charges flow away from B_7 mainly to B_3 until their charges are equal. A small portion of the lost charge on B_7 flows to the hydrogens. The total loss of charge on the boron cage to the hydrogens between the two structures is 0.22e, which is again a normal response toward the partial opening of the cage.

The MNDO results suggest that the $B_8H_8^{2-}$ anion should have fluxional behavior among the D_{2d}, C_{2v} and D_{4d} structures, due to their small differences in energy. The

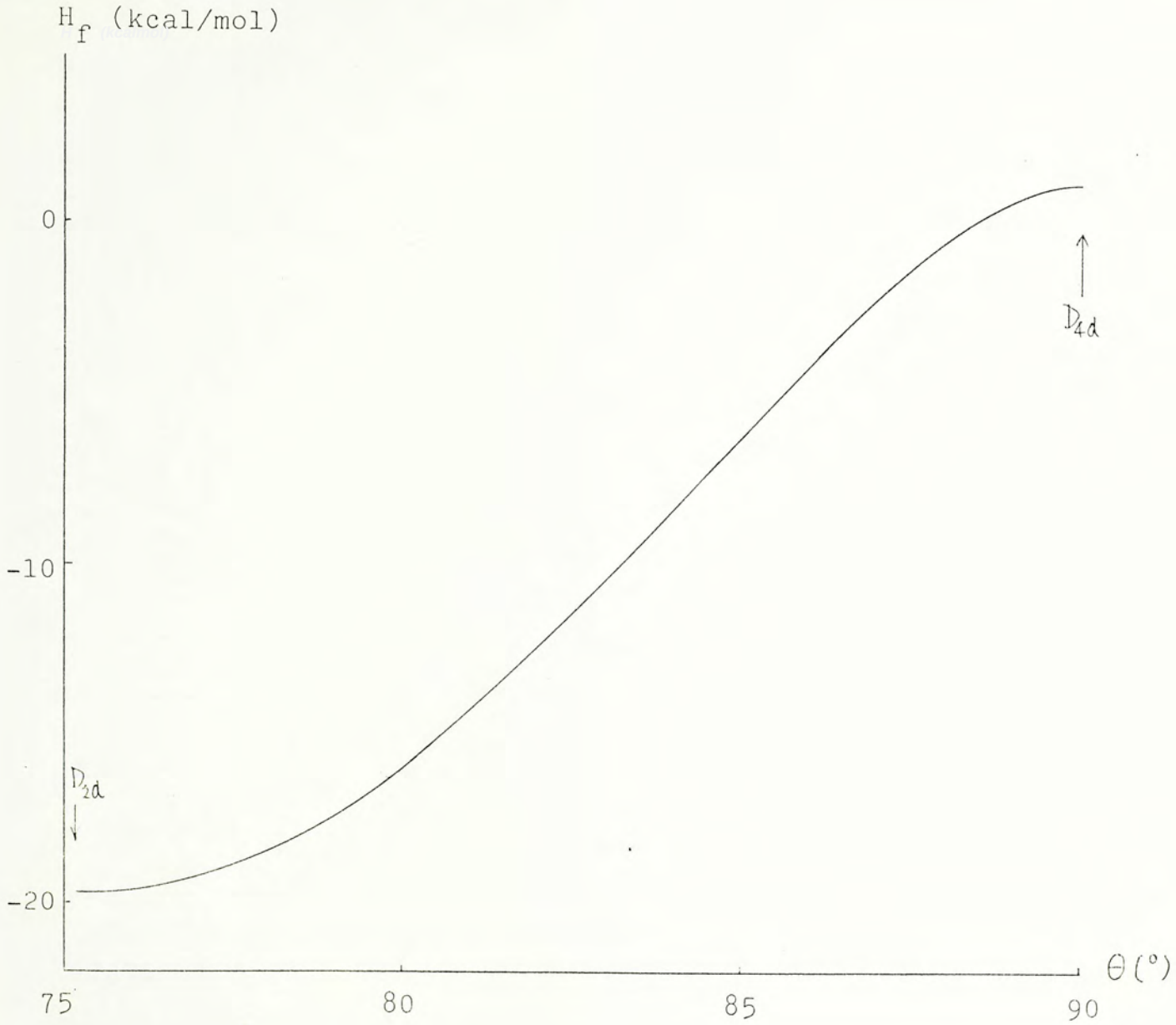

Fig. 2.20 The energy profile for the rearrangement pathway (b) connecting the D_{2d} and D_{4d} structures of $B_8H_8^{2-}$.

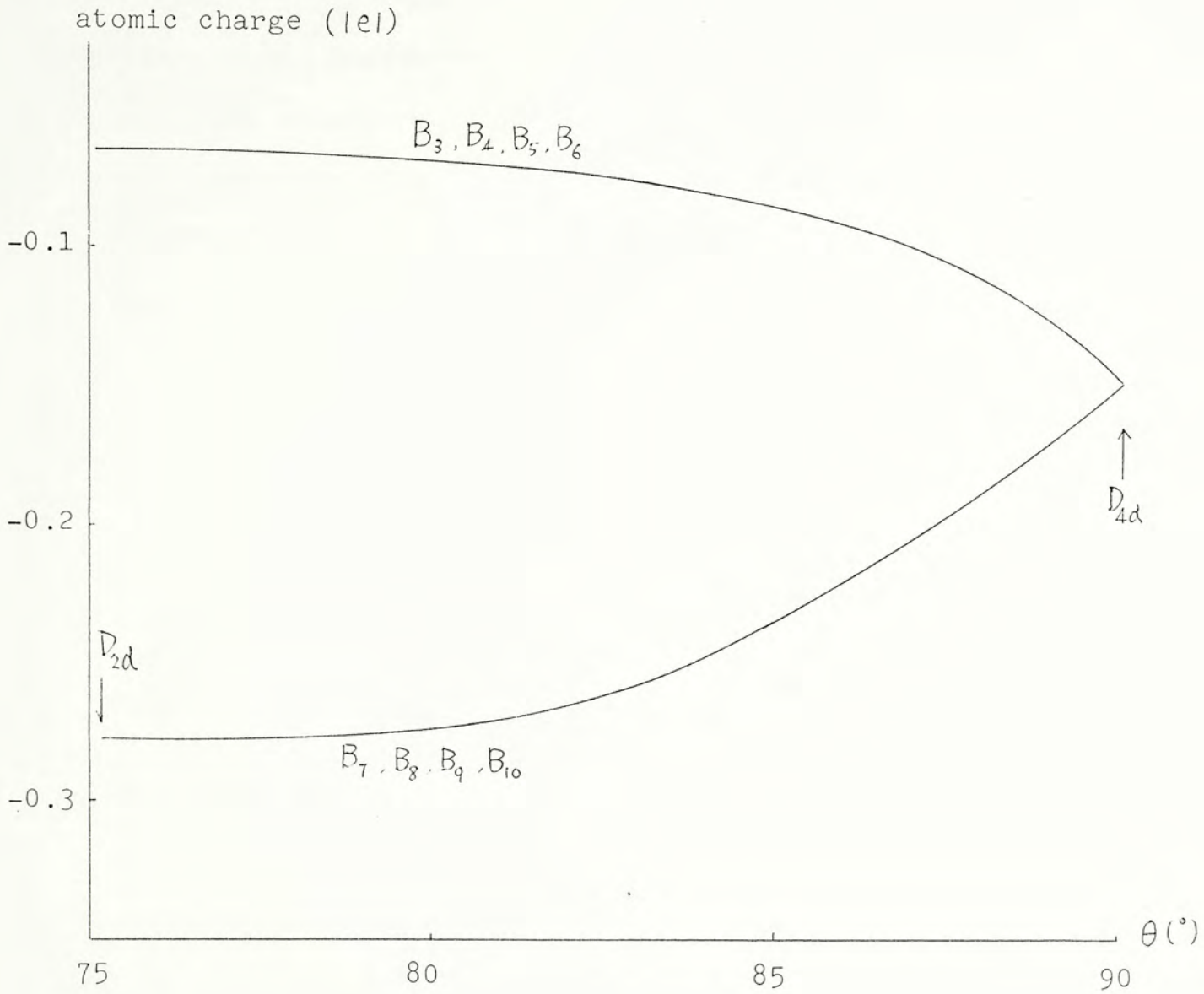

Fig. 2.21 The charge distribution on boron atoms along the reaction pathway (b) connecting the D_{2d} and D_{4d} structures of $B_8H_8^{2-}$.

pair, namely, D_{2d} and D_{4d}, having the largest difference in energy, is differred by 20.6 kcal/mol which may be reduced in solution by solvation or ion pairing. In any event, this value is in accord with Muetterties'[7] proposed barrier of about 20 kcal/mol.

2.6 Conclusion

The cage structure for the anion $B_5H_5^{2-}$ is unstable. It undergoes cage opening to a cyclopentane-like skeleton very easily. Another species having structural nonrigidity among the four anions studied is the $B_8H_8^{2-}$ anion. It interconverts among three geometries of D_{2d}, D_{4d} and C_{2v} symmetries in solution. The remaining two anions, namely, $B_6H_6^{2-}$ and $B_7H_7^{2-}$ are entities with no spontaneous intramolecular rearrangement. Moreover, the anion $B_6H_6^{2-}$ is found to have several stable structures such as chair form, closo and fused-ring structures.

Electron removal from the boron atoms to the hydrogens upon cage opening is observed for all the anions studied. The trend is also present for $B_5H_5^{2-}$,which is believed to be nonaromatic. The gain of electronic charge of the hydrogens results in the weakening of the B-H bonds. This indicates that the boron atoms of the open structures cannot accommodate the excess charges and release the charges to the anti-bonding B-H orbitals.

REFERENCES

1. W.N. Lipscomb, J. Amer. Chem. Soc., 99, 6226(1977)
2. Aihara, J. Amer. Chem. Soc., 100, 3339(1978)
3. E.L. Muetterties, Boron Hydride Chemistry, New York, Academic Press 1975.
4. E.L. Muetterties, Polyhedral Boranes, New York, Marcel Dekker 1968.
5. M.J.S. Dewar and M.L. McKee, J. Amer. Chem. Soc., 99, 5231(1977)
6. Consult referenc 4.
7. E.L. Muetterties, Tetrahedron, 30, 1595(1974)
8. E.L. Muetterties, Inorg. Chem., 6, 1271(1967)
9. E.L. Muetterties, R.J. Wiersema and M.F. Hawthrone, 95, 7520(1973)
10. E.I. Tolpin and W.N. Lipscomb, J. Amer. Chem. Soc., 95, 2384(1973)
11. L.J. Guggenberger, Inorg. Chem., 8, 2771(1969)
12. E.L. Muetterties, Inorg. Chem., 14, 951(1975)
13. W.N. Lipscomb, Inorg. Chem., 18, 1312(1979)
14. E.L. Muetterties, Inorg. Chem., 6, 1271(1967)

PART 3

MNDO STUDY OF SOME CAGE MOLECULES RELATED TO HEXAMETHYLENETETRAMINE

3.1 Introduction

Since the discovery of hexamethylenetetramine (also known by the names hexamine, methenamine, urotropine and 1,3,5,7-tetraazaadamantane, hereafter abbreviated as HMT), $(CH_2)_6N_4$ (1), by Butlerow[1] well over a century ago, an enormous number of its salts, molecular adducts, and coordination complexes have been recorded in the literature. Pertinent information on these substances, the physical and chemical properties of HMT, as well as its industrial and physiological uses are available in book form[2,3].

Although HMT is often referred to as an analog of adamantane, it was actually the first organic compound to have its molecular and crystal structure elucidated by X-ray analysis[4]. Protonation of one nitrogen atom reduces its molecular symmetry from T_d (1) to C_{3v} (2) and facilitates the occurence of various acid-catalyzed fragmentation processes. Depending on the experimental conditions, cleavage of the cage structure into two or more carbon-nitrogen subunits may result, or HMT can simply act as a source of formaldehyde and ammonia.

Thus HMT has found ever increasing use as a versatile reagent in the synthesis of heterocyclic ring systems and the introduction of amino and formyl functional groups into a wide variety of molecules[5].

The detailed dimensions of four derivatives of HMT, namely $[(CH_2)_6N_4H]^+$ (2)[19], $(CH_2)_6N_4O$ (5)[6], $(CH_2)_6N_4BH_3$ (6)[7] and $[(CH_2)_6N_4CH_3]^+$ (8)[8,9] have been determined by X-ray crystallography. In all instances, quaternization of one N atom markedly differentiates the CH_2-N single bonds in the heterocyclic cage system into three types. Moving away from the formally positive quaternary N atom, the three types of bonds vary in the order long-short-normal with respect to the standard value of 1.476(2) Å in crystalline HMT[10]. In the present work, the results of semi-empirical molecular orbital calculations which lend support to the observed deformation of the HMT cage system by quaternization are reported. We also take the opportunity to study several cage systems closely related to HMT : 3 and 4, which are isoelectronic with 2, and the pairs 6 and 7, and 8 and 9, which bear interesting inverse relationships to each other.

3.2 Method and Results

The molecular orbital method chosen for the present study is the MNDO procedure developed by Dewar and Thiel[11]. Aside from symmetry restrictions : T_d for $\underset{\sim}{1}$ and C_{3v} for the rest, all structural parameters were allowed to vary until optimized geometry was reached. The calculated molecular dimensions (in Å and degrees) and selected atomic charges are summarized in Fig. 3.1; where applicable, the experimental values for the bond lengths and valence angles are enclosed in brackets for easy comparison.

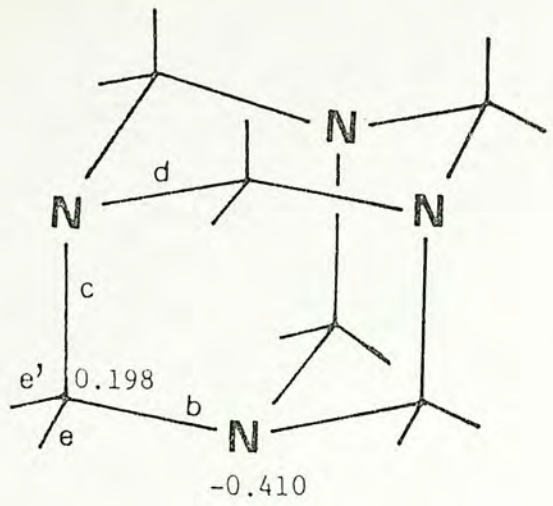

1

T_d symmetry; ΔH_f = 51.6 kcal/mol.

b = c = d = 1.49 [1.476], e = 1.12 [1.088].

bc = 109 [113.6], cd = 110 [107.2],

ee' = 106.

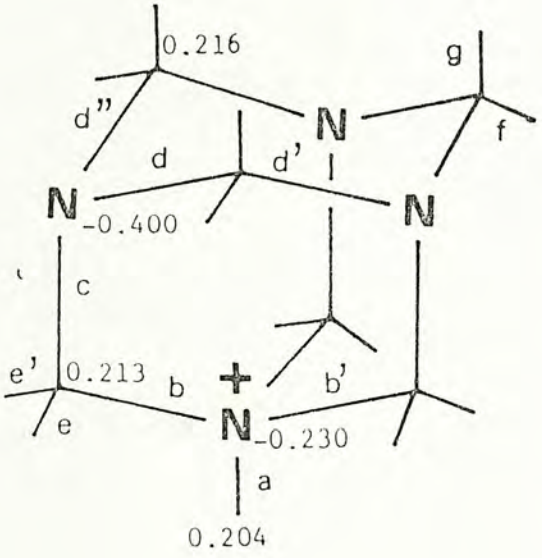

2

C_{3v} symmetry; H_f = 218.3 kcal/mol.

a = 1.02, b = 1.56 [1.512],

c = 1.46 [1.458], d = 1.50 [1.465],

e = 1.12, f = 1.12, g = 1.12.

ab = 110, bb' = 109 [109.7],

bc = 106 [108.5], cd = 112 [108.8],

dd' = 106 [112.7], dd" = 111 [108.4],

ee' = 107, fg = 106.

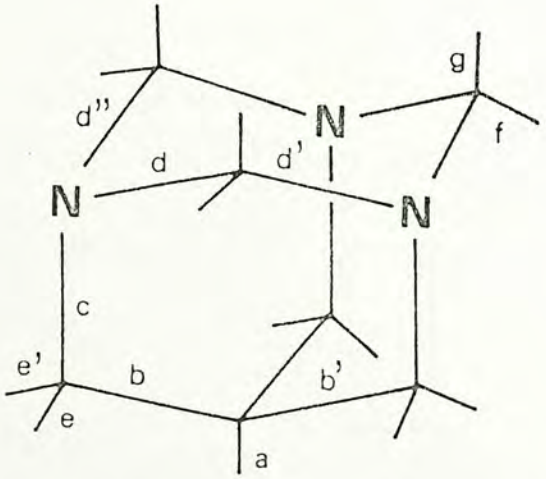

3

C_{3v} symmetry; ΔH_f = 34.5 kcal/mol.

a = 1.11, b = 1.56, c = 1.49, d = 1.49,

e = 1.11, f = 1.12, g = 1.12.

ab = 111, bb' = 108, bc = 108, cd = 110,

dd' = 109, dd" = 110, ee' = 105, fg = 106.

Fig. 3.1 MNDO structures of HMT and its related compounds.

Values in square brackets are experimental results.

-- to be continued

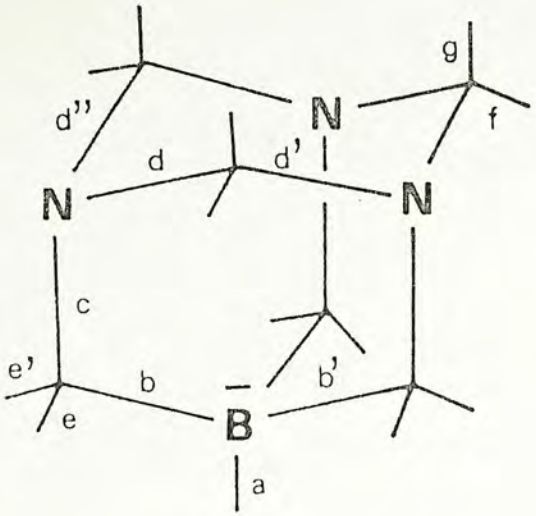

4

C_{3v} symmetry; ΔH_f = -23.7 kcal/mol.

a = 1.18, b = 1.62, c = 1.51, d = 1.49,

e = 1.12, f = 1.12, g = 1.12.

ab = 112, bb' = 107, bc = 108, cd = 110,

dd' = 112, dd'' = 109, ee' = 104, fg = 105.

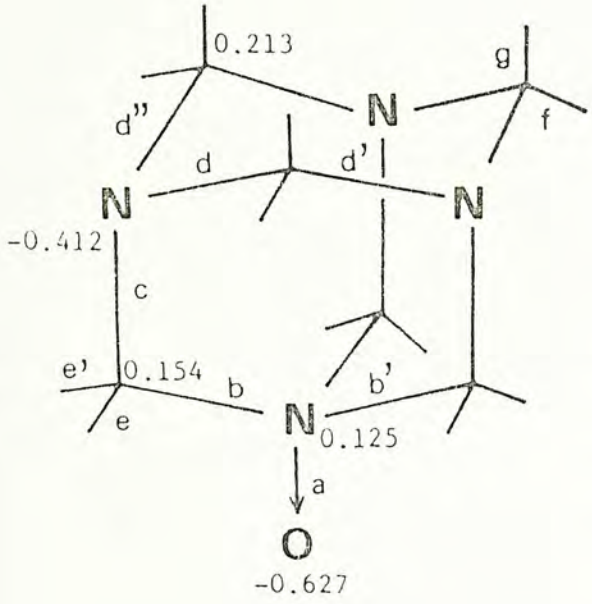

5

C_{3v} symmetry; ΔH_f = 88.2 kcal/mol.

a = 1.27 [1.363], b = 1.58 [1.514],

c = 1.48 [1.445], d = 1.49 [1.474],

e = 1.12, f = 1.12, g = 1.12.

ab = 111 [111.4], bb' = 107 [107.4],

bc = 108 [111.4], cd = 111 [109.5],

dd' = 108 [111.6], dd'' = 111 [107.2],

ee' = 107, fg = 106.

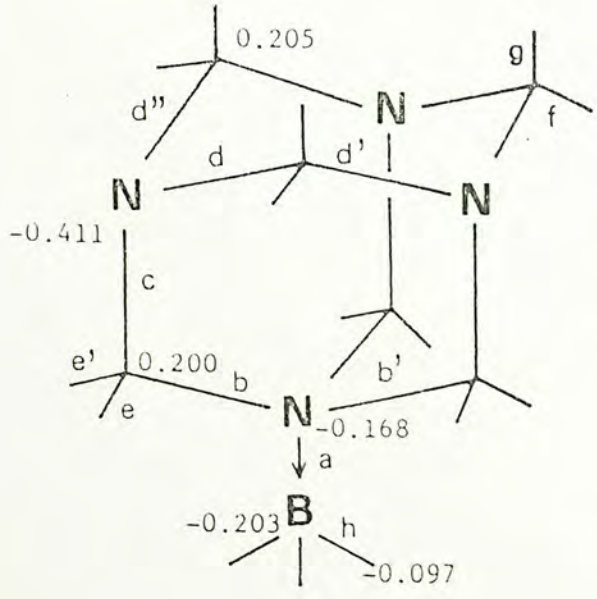

6

C_{3v} symmetry; ΔH_f = 56.4 kcal/mol.

a = 1.64 [1.661], b = 1.54 [1.527],

c = 1.48 [1.475], d = 1.49 [1.475],

e = 1.12 [1.03], f = 1.12 [1.04],

g = 1.12 [1.02], h = 1.18 [1.08].

ab = 110 [111.5], ah = 107 [117],

bb' = 108 [107.4], bc = 108 [111.4],

cd = 111 [108.2], dd' = 107 [112.7],

dd'' = 110 [108.5], ee' = 107 [110],

fg = 106 [109].

Fig. 3.1 (continued)

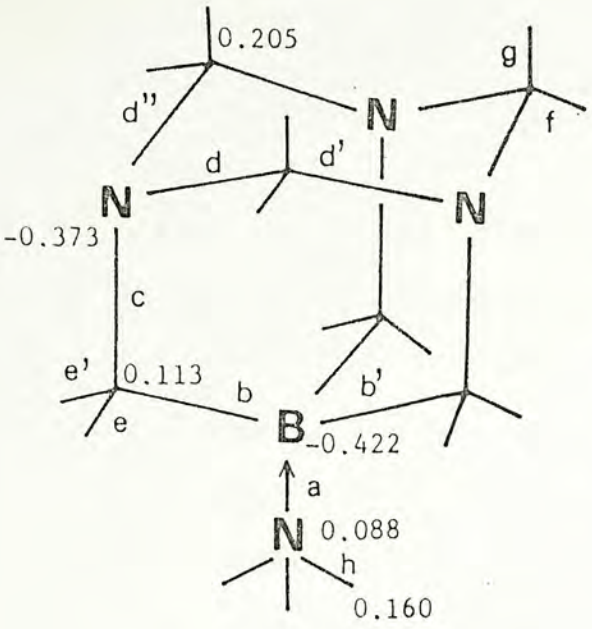

7

C_{3v} symmetry; ΔH_f = 14.4 kcal/mol.

a = 1.58, b = 1.63, c = 1.49, d = 1.49,

e = 1.12, f = 1.12, g = 1.12, h = 1.02.

ab = 111, ah = 112, bb' = 108, bc = 107,

cd = 111, dd' = 111, dd" = 110,

ee' = 104, fg = 106.

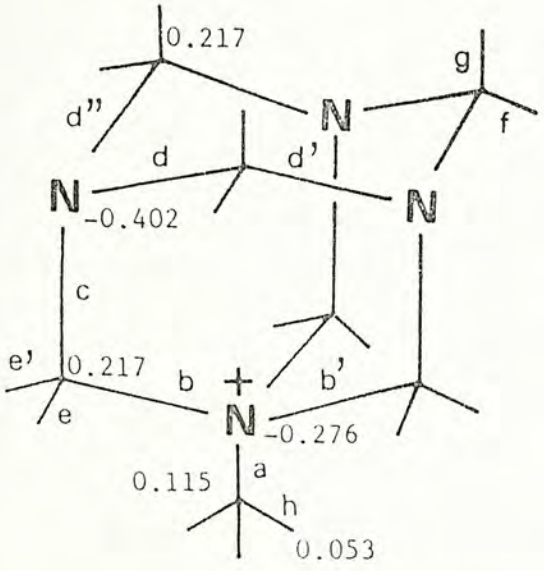

8

C_{3v} symmetry; ΔH_f = 225.6 kcal/mol.

a = 1.52 [1.47], b = 1.57 [1.53],

c = 1.46 [1.45], d = 1.49 [1.45],

e = 1.12, f = 1.12, g = 1.12, h = 1.11.

ab = 111 [111], ah = 110, bb' = 108 [107],

bc = 108 [110], cd = 112 [109],

dd' = 106 [112], dd" = 111 [109],

ee' = 108, fg = 106.

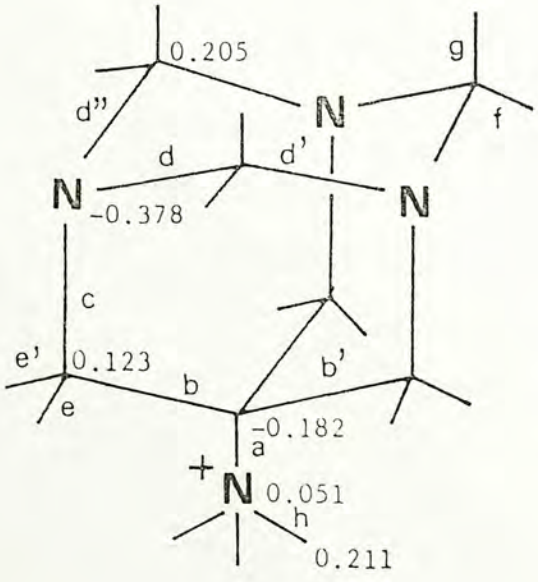

9

C_{3v} symmetry; ΔH_f = 212.2 kcal/mol.

a = 1.52, b = 1.59, c = 1.48, d = 1.49,

e = 1.12, f = 1.12, g = 1.12, h = 1.03.

ab = 111, ah = 112, bb' = 108, bc = 107,

cd = 111, dd' = 108, dd" = 111,

ee' = 106, fg = 106.

Fig. 3.1 (continued)

3.3 Discussion

Upon examining the results, the following points are noted :

(i) For 1, the MNDO bond lengths are in excellent agreement with the experimental results. However, the calculated bond angles are less satisfactory. Specificially, MNDO comes up with C-N-C angles (110^{o}) slightly greater than the ideal tetrahedral value, in contradiction with expected lone-pair repulsion effects and the experimental results. Also, the MNDO N-C-N bond angles (109^{o}) are not significantly larger than the tetrahedral angle (the experimental value is 113.6^{o}). Nevertheless, since the MNDO bond angles are off by only a few degrees, the overall agreement between theory and experiment may be termed quite satisfactory.

(ii) For 5 (HMT oxide), the MNDO model overestimates the interaction between atoms N and O. As a result, the calculated N-O bond distance (1.27 Å) is much shorter than the experimental value (1.363Å); also, the calculated length for bond b is much too long. Still, MNDO does suggest that the formally negative exocyclic oxygen behaves like a lone pair, as indicated by the bond angles around the quaternary N atom.

(iii) For $\underset{\sim}{2}$, the MNDO results are in fairly good agreement with the experimental results. It is noted that the lengthening of the bond b is exaggerated by MNDO calculations upon protonation of the parent compound $\underset{\sim}{1}$. The bond angles on the quaternary nitrogen is in good accord to the experimental results. This indicates the MNDO model tends to underestimate the bulkiness of a lone pair of electrons and the model can give reliable structures around an atom which bears no lone pair. As can be seen from this molecule, the protonation of HMT will lengthen the quaternary N-C bond significantly. Hence, acid catalysed cleavage of the cage to give formaldehyde and ammonia is probable. A plausible mechanism has been suggested by Mak and co-workers[19].

(iv) For $\underset{\sim}{6}$ ($HMT-BH_3$), the agreement between the MNDO and experimental results is excellent. The B-N bond length in this compound is comparable to those found in $(CH_3)_3N-BH_3$ (1.609 or 1.637 Å)[12] and in CH_3CN-BF_3 (1.64 Å)[13]. On the other hand, the unknown compound $\underset{\sim}{7}$, which is isoelectronic to $\underset{\sim}{6}$, is predicted to have a slightly shorter B-N bond (1.58Å). This value is comparable to those found in $(CH_3)_3N-BF_3$ (1.585 Å)[14] and $(CH_3)H_2N-BF_3$ (1.57 Å)[15].

(v) When 1 and BH_3 form an adduct (6), bond b becomes 1.527Å (MNDO value : 1.54Å), considerably lengthened from the standard N-C bond length of 1.476Å (MNDO value : 1.49Å) in 1, with the remaining N-C distances relatively unchanged. It is of interest to note that the MNDO model is able to reproduce such an effect for 6, thus lending credence to the trend observed for the other adducts in this work. For instance, in 2, (or protonated 1), bond b is lengthened from the MNDO value of 1.49Å (experimental value : 1.486Å) to 1.56Å, bond c is shortened to 1.46Å, and bond d is relatively unchanged (1.50Å). The lengthening of bond b in 2 is consistent wtih the occurrence of various patterns of acid-catalyzed fragmentation of HMT.

(vi) For 4 and 7, the B-C distances are 1.62Å and 1.63Å, respectively. As might be expected, this is much longer than the B-C bond distance of 1.564Å found in the adamantane-like molecule $(MeB)_6(CH)_4$[16], which has trigonal planar sp^2 hybridization for each B atom.

(vii) For 8, considered formally as an adduct of 1 and H_3C^+, the MNDO results can only be called fair. The lengths of bonds a and b are about 0.05Å too long. The lengthening of bond b upon adduct formation is infact overestimated in this case.

(viii) Guided by the pioneering work of Lindqvist[17], Gutmann has formulated a set of lond-length variation rules[18] applicable to a great variety of donor-acceptor intermolecular interactions :

I. The stronger the interaction (i.e., the closer the interacting sites to each other), the greater the induced lengthening of the adjacent intramolecular bonds both in the donor and acceptor components.

II. A σ bond is lengthened when, as a result of the donor-acceptor interaction, the electron shift occurs from a nucleus bearing a positive fractional charge to one bearing a negative fractional charge, whereas it is shortened when the electron shift is in the reverse direction.

III. As the coordination number increases, so do the lengths of the bonds originating from the coordination center.

Scrutiny of the results presented in Fig. 3.1 shows that these rules apply remarkably well for the cage systems studied in the present work, even though the term molecular adduct in conventional usage strictly applies only to 6 and 7.

(ix) Compound 7, as yet unknown and seemingly very difficult to synthesize, is thermodynamically more stable than its known isomer 6; likewise, the unknown species 9 is more stable than 8. It is interesting to note that both 7 and 9 involve stronger donor-acceptor interactions with NH_3 as the Lewis base and the substituted HMT as the Lewis acid. In both 6 and 8, the Lewis base is HMT. The extent of charge transfer from donor to acceptor is calculated to be 0.494, 0.568, 0.274 and 0.683 electron for 6, 7, 8 and 9, respectively.

(x) Comparison of the net charge transfer in the series of HMT adducts 5, 6, 7 and 8 leads to the following Lewis acid order : O (strongest) > BH_3 > H^+ > H_3C^+. [The relatively high negative charge for O in 5 is partly due to MNDO's overestimation of the interaction in the N-oxide group, as noted in (ii).]

REFERENCES

1. A. Butlerow, Ann., 111, 250(1859); 115, 322(1860)
2. J. Altpeter, Das Hexamethylentetremin und Seine Verwendung, Verlag von Wilhelm Knapp, Halle, 1931.
3. J. Walker, Formaldehyde, Reinhold, New York, 1944; 2nd edition, 1953; 3rd edition, 1964.
4. R.G. Dickinson and A.L. Raymond, J. Amer. Chem. Soc., 45, 22(1923)
5. N. Blaževic, D. Kolbah, B. Belin, V. Šunjic and F. Kajfež, Synthesis, 161(1979)
6. T.C.W. Mak, M.F.C.Ladd and D.C. Povey, J. Chem. Soc., Perkins Trans. II, 593(1979)
7. F. Hanic and V. Šubrtová, Acta Cryst., B25, 405(1969)
8. P.K. Hon, T.C.W. Mak and J. Trotter, Inorg. Chem., 18, 2916(1979)
9. P.K. Hon, T.C.W. Mak and J. Trotter, Z. Kristallogr., 158, 213(1982)
10. L.N. Becka and D.W.J. Cruickshank, Proc. Royal Soc., A273, 435(1963)
11. M.J.S. Dewar and W. Thiel, J. Amer. Chem. Soc., 99, 4899(1977)
12. J.R. Durig, Y.S. Li and J.D. Odom, J. Mol. Structure, 16, 443(1973)
13. J.L. Hoard, O.B. Owen, A. Buzzell, and O.N. Salmon, Acta Cryst., 3, 130(1950)

14. S. Geller and J.L. Hoard, Acta Cryst., 4, 399(1951)

15. S. Geller and J.L. Hoard, Acta Cryst., 3, 127(1950)

16. I.Payment and H.M.M. Shearer, J. Chem. Soc., Dalton Trans., 136(1977)

17. I. Lindqvist, Inorganic Adduct Molecules of Oxo-Compounds, Springer-Verlag, Berlin/Göttingen/ Heidelberg, 1963.

18. V. Gutmann, The Donor-Acceptor Approach to Molecular Interactions, Plenum, New York,1978; and references cited therein.

19. T.C.W. Mak, W.K. Li and W.H. Yip, Acta Cryst., C39, 136(1983)

PART 4

LEWIS ACID-BASE REACTION — A STUDY OF $H_3NBH_nF_{3-n}$

4.1 Introduction

The Lewis base property of NH_3 has been well established. On the other hand, the Lewis acid $BH_3(B_2H_6)$ and its trifluorinated derivative have also been proved to be very useful in organic synthesis. However, study on the remaining two fluorinated derivatives of BH_3 is rare. This section will examine the electron pair donor-acceptor reactions between ammonia and borane as well as its fluorinated derivatives.

The MNDO structures of the adducts $H_3NBH_nF_{3-n}$, n = 0 to 3, are shown in Fig. 4.1, along with their MNDO atomic charges. As a reference, the results for the five reacting molecules are shown in Fig. 4.2.

All the reacting molecules in this section are computed with the following symmetry constraints : C_{3v} for NH_3, D_{3h} for BF_3 and BH_3, C_{2v} for BHF_2 and BH_2F, while no symmetry condition has been imposed on the adducts.

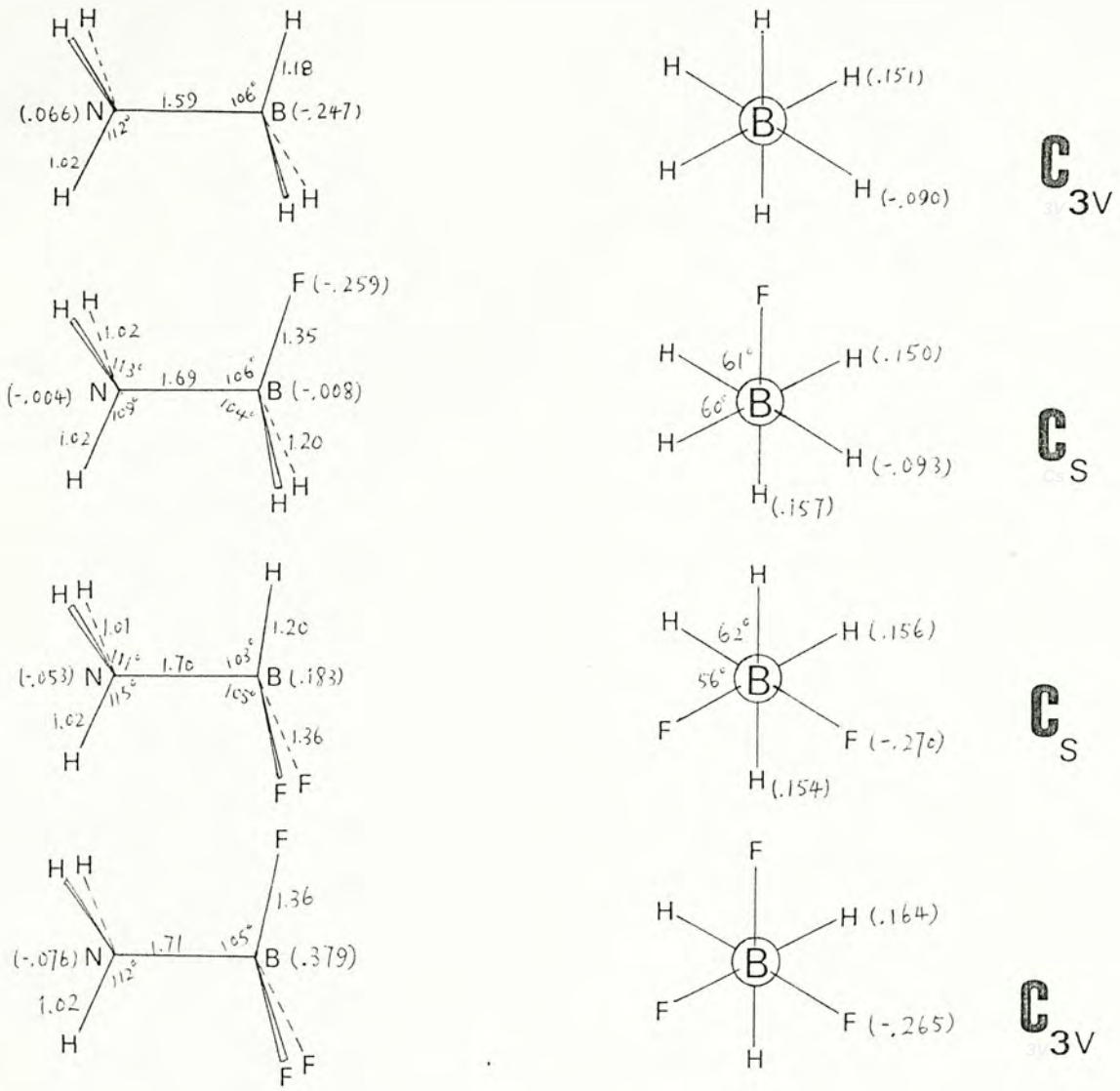

Fig. 4.1 The MNDO structures of the adducts $H_3NBH_nF_{3-n}$ for n = 0 to 3. Bond lengths are in angstrons. Bracketed values are the atomic charges.

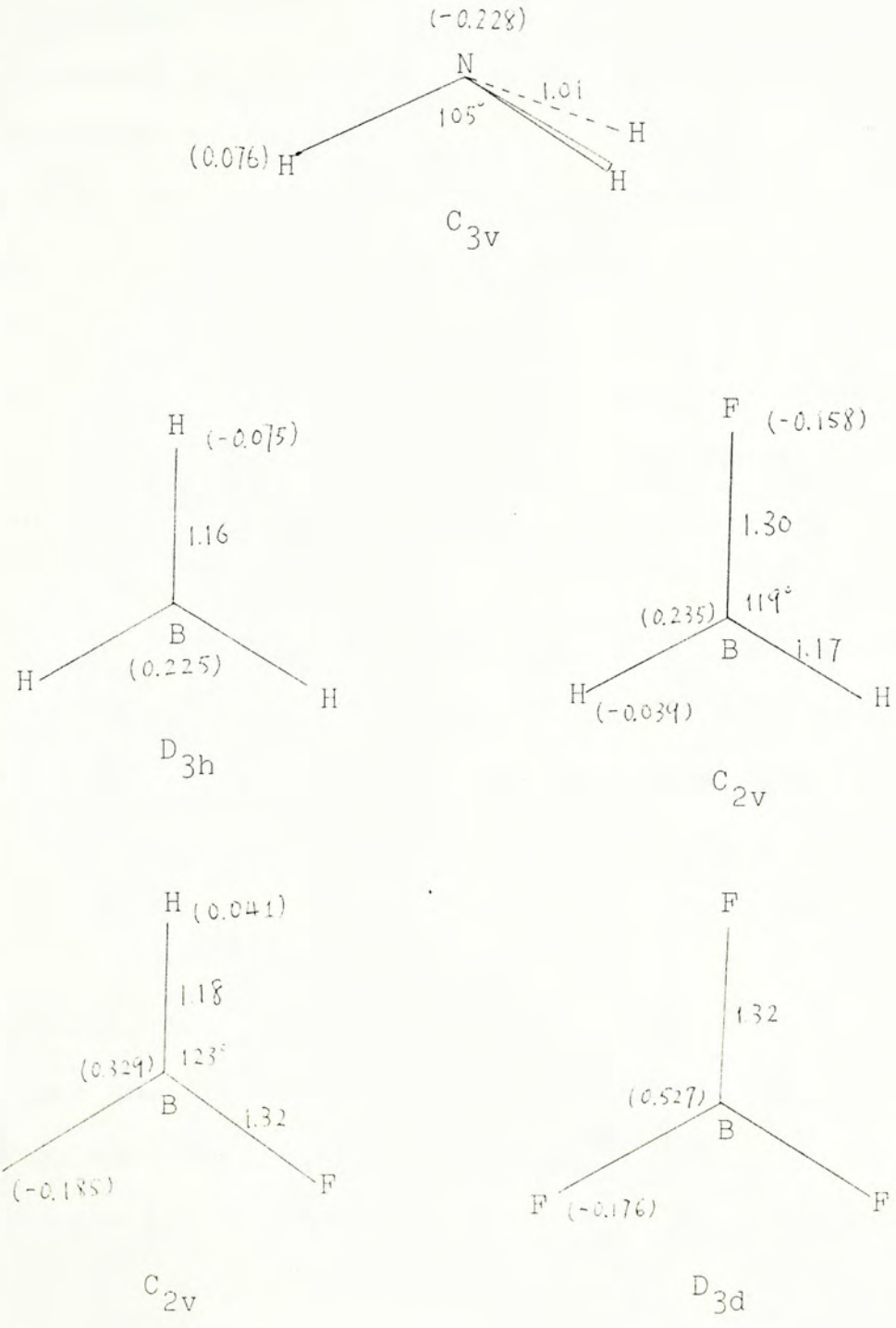

Fig. 4.2 MNDO structures of the five reacting molecules. Bond lengths are in angstroms. Values in brackets are the atomic charges.

4.2 Results and Discussion

4.2.1 Reacting Molecules

The molecule NH_3 is known to have a trigonal pyramidal shape. The experimental values for the structural parameters are : The N-H bond length is 1.011Å and each N-H bond makes an angle of 112° with the principle C_3-axis. The MNDO values for these two parameters are 1.01Å and 113°, respectively, which are in excellent agreement with the experimental values. The MNDO atomic charge distribution shows that NH_3 is a strong Lewis base, with the nitrogen atom carrying a charge of 0.23e.

Borane, BH_3 is of D_{3h} symmetry with B-H bond length of 1.16Å. The hydrogens in this compound are electron withdrawing such that the boron atom carries a positive charge of 0.23. Thus, BH_3 is a very strong Lewis acid and is ready to accept a pair of electrons from Lewis bases to form adducts.

The speices BH_2F has C_{2v} symmetry. The F-B-H bond angle is less than 120°, indicating that the H-H non-bonding repulsion is greater than the H-F repulsion. This may be due to the larger separation between H and F. As shown in Fig. 4.2, it is noted that all the atoms except boron carry negative charges. The bond length of

B-H is 1.17Å which is slightly longer than 1.16Å in BH_3. The B-F bond length is 1.30Å, considerably shortened compared to 1.40Å in BF_4^- [1]. The electron population in the out of plane p orbital is 0.20e.

The difluorinated borane, BHF_2, also has C_{2v} symmetry. The trend that the fluorides are less bulky than the hydride is also present in this case. The F-B-F bond angle is 114°, considerably less than 120°. MNDO gives satisfactory geometry for this compound compared to the analysis of high resolution IR spectra[2], which gives approximate values for the B-F bond length(1.30 ± 0.15Å) and the F-B-F bond angle ($120 \pm 5^\circ$). Also, MNDO gives a good value for the heat of formation, -177.1 kcal/mol, with reference to the experimental value[3] of -175.7 ± 1.5 kcal/mol. In this compound, the powerful electron withdrawing abilities of fluorines make the boron and the hydrogen carry positive charges. It is of interest that the fluorine atoms in this compound are more negatively charged than that in BH_2F. This may be explained by the degree of back donation. The p_π orbital on boron is populated by 0.20e and 0.32e in BH_2F and BHF_2, respectively. If there is no back donation, the fluorine in BH_2F should carry a charge of o.36e and that in BHF_2 should be 0.35e, showing the expected trend of electron withdrawing power of the fluorines in the two compounds.

Compound BF_3 has B-F bond length of 1.32Å, same as that in BHF_2. The atomic aharge on F is -0.18 and that on B is about 0.53. Based on the boron charge, BF_3 appears to be a stronger Lewis acid than BHF_2, BH_2F and BH_3. But the counter factor of the higher population on the p_π orbital of boron by back donation from the three fluorines will retard the availability of the p_π orbital of BF_3. This argument is borne out by the rather high p_π orbital population, 0.41e in BF_3. Moreover, the bending of the molecular plane for the adduct formation will require energy to compensate the loss in the bonding multiplicity between B and F. This energy will be largest for BF_3 among the fluorinated boranes.

4.2.2 Adducts

For the formation of the adduct BH_3NH_3, the heat of reaction is -28.1 kcal/mol, which is in good agreement with the ab initio values of -27.6 ± 1 kcal/mol[4] and -30.2 kcal/mol[5]. The large amount of energy released indicates the adduct is very stable. The formation process is found to be facile, with a very low energy barrier of 2.0 kcal/mol. In forming this adduct, ammonia has transferred 0.52e to the BH_3 moiety. The transferred charge mainly resides on the boron, making it negatively charged. Thus, the polarity on the nitrogen and the boron atoms are reversed. This indicates the stability of the adduct mainly comes from the charge transfer and not from the electrostatic interaction. Previous ab initio calculation[6] on this adduct gives a comparatively small value for the transferred charge, 0.25e. On the other hand, other theoretical calculation[7] has conflicting claims that the electrostatic interaction is the predominant factor for the stability of the adduct.

The next adduct to be discussed is BH_2FNH_3. The heat released for its formation is only 14.2 kcal/mol, which is smaller than the case of BH_3NH_3. The energy barrier is 2.5 kcal/mol, which is still very low. The

smaller heat release for this reaction indicates that the acidity of BH_2F is not as strong as BH_3. This result is contradicting to the expected trend by considering the inductive effect. The charge transferred from NH_3 is 0.45e, smaller than that in the case of BH_3NH_3. This shows that fluorine, by back donation, retards the charge transfer process and hence decreases the heat of reaction.

The heat released in the formation of the adduct NH_3BHF_2 is only 5.8 kcal/mol. The activation energy for the adduct formation is 4.2 kcal/mol, i.e., the barrier for the dissociation of the adduct is about 10 kcal/mol. Hence, the adduct should be of fair stability. The charge transfer is 0.41e, indicating that the back donation by the two fluorines retards the charge transfer even more. Consequently, MNDO suggests that BHF_2 does not possess a strong tendency to accept an electron pair.

The Lewis acid BF_3 and base NH_3 form a weak adduct which is only 6.7 kcal/mol more stable than the two separated halves. Radiospectroscopic measurement[8] leads to the conclusion that the vapor of this adduct is highly dissociated. On the other hand, the experimental[9] heat of reaction for the reaction $NH_{3(g)} + BF_{3(g)} \rightarrow NH_3BF_{3(s)}$ is -41.3 kcal/mol. In addition, Perkins[10] estimates the sublimation energy for the adduct is about 45 kJ/mol,

yielding a heat change of -30.5 kcal/mol for the gas phase reaction. Moreover, Perkins gives a value of -41.8 kcal/mol for the heat of reaction by ab initio calculation. These two values are quite different from the MNDO result and the radiospectroscopic measurement. Concerning the geometry, the MNDO structure is in fair agreement with the X-ray data[11]. The experimental structural parameters are : 1.60Å, 1.38Å and 1.01Å for the N-B, B-F and N-H bond lengths; the F-B-N bond angle is 107°. The charge flow from the NH_3 moiety to the other half is 0.42e, which is very close to that in the NH_3BHF_2 case. From the values of atomic charges on the nitrogen and boron atoms, the stability of the adduct comes from electrostatic interaction, a conclusion also suggested by Morokuma[7].

4.3 Conclusion

Some conclusions are discernible by studying the summarized results given in Table 4.1. They are :

(i) The heats of reaction decrease as the borane unit is fluorinated. This indicates that the acidity of BH_nF_{3-n} decreases as n decreases.

(ii) As a consequence of the weakening of the Lewis acid-base interaction by fluorination, the equilibrium B-N distances increase with the degree of fluorination. Moreover, the B-N distances in the transition states decrease as fluorination increases. This may be due to the retarded acceptor ability.

(iii) All the adducts studied are formed with very small activation energies. This is usually encountered in reactions involving empty valence orbital which will become a bonding orbital in the product.

(iv) All the bonds in the Lewis acids and NH_3 are lengthened upon adduct formation.

Adduct	Heat of reaction (kcal/mol)	Activation energy (kcal/mol)	Equilibrium B-N separation (Å)	B-N distance in the transition state (Å)
H_3NBH_3	-28.1	2.6	1.59	2.58
H_3NBH_2F	-14.2	2.5	1.65	2.47
H_3NBHF_2	- 5.8	4.2	1.70	2.36
H_3NBF_3	- 6.7	2.5	1.71	2.36

Table 4.1 Some MNDO results on the formation of the adducts $H_3NBH_nF_{3-n}$.

REFERENCES

1. Interatomic Distances in Molecules and Ions, Chem. Soc. Spec. Publ., 11, 1958
2. M. Perec and L.N. Becka, J. Chem. Phys., 43, 721(1965)
3. R.F. Porter and S.K. Wason, J. Phys. Chem., 69, 2208(1965)
4. C. Zira and R. Ahlrichs, J. Chem. Phys., 75, 4980(1981)
5. L.T. Redmon, G.D. Purvis III and R.J. Barlett, J. Amer. Chem. Soc., 101, 2856(1979)
6. Consults M.J.S. Dewar and M.L. McKee, J. Amer. Chem. Soc., 99, 5231(1977)
7. H. Umeyama and K. Morokuma, J. Amer. Chem. Soc., 98, 7208(1976)
8. A.M. Prokhorov and G.P. Shipulo, Optikikai Spektroskopiya, 8, 419(1960)
9. A.W. Laubengayer and G.F. Condike, J. Amer. Chem. Soc., 70, 2274(1948)
10. R.M. Archibald, D.R. Armstrong and P.G.Perkins, Chem. Soc., London, Faraday Trans. II, 69, 1793(1973)
11. W.N. Cashin, Acta. Cryst., 4, 396(1951)

PART 5

STUDY OF THE CYCLOPENTATHIAZENIUM CATION, $S_5N_5^+$

5.1 Introduction

Two stable geometries for the cation, $S_5N_5^+$, have been determined by Banister[1,2] using the X-ray diffraction technique. Both of these two structures are almost planar in the crystalline states. One of them has the heart-shaped structure with a sulfur atom locating at the tip of the heart. The other one is an azulene-like structure. These two structures are drawn in Fig. 5.1, together with the MNDO and experimental structural values.

Gleiter suggested that there are not two isomeric structures of this cation, based on the EHT calculation results[3]. He suggests[4] that a careful re-examination of the experimental X-ray data by Banister should clarify the discrepancy between the calculation results and the experimental data. Superposition of two azulene-like structures(Fig. 5.2) may lead to the heart-shaped structure. Moreover, Banister himself points out that, compared with the bond angles and bond lengths of other nitrogen-sulfur containing compounds[5,6], the azulene-like structure is less-strained.

However, MNDO results indicate that the two isomers are nearly the same in energy : the heats of formation

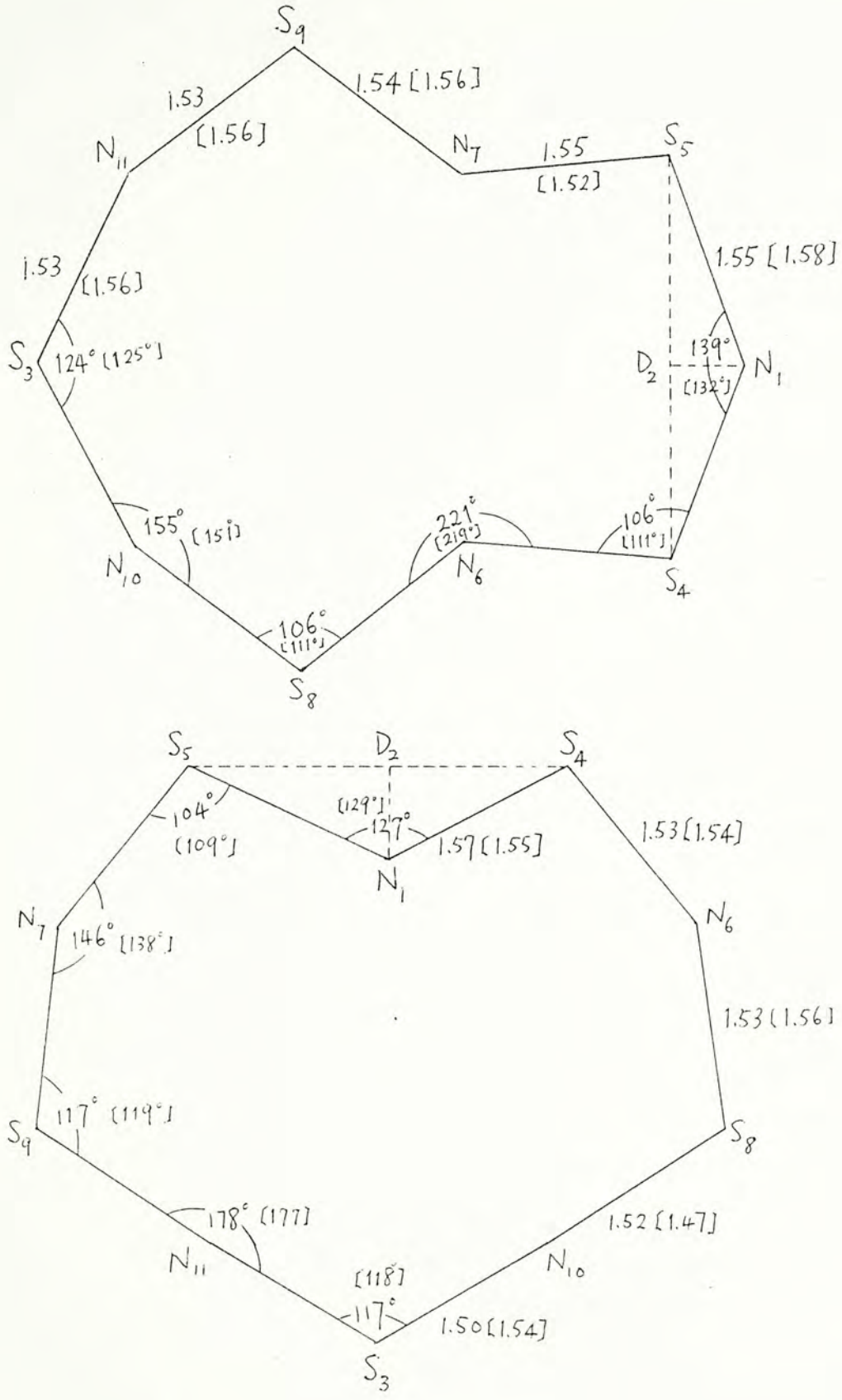

Fig. 5.1 The MNDO and experimental(in square brackets) structures for the heart-shaped and azulene-like cations of $S_5N_5^+$. Bond lengths are in Å.

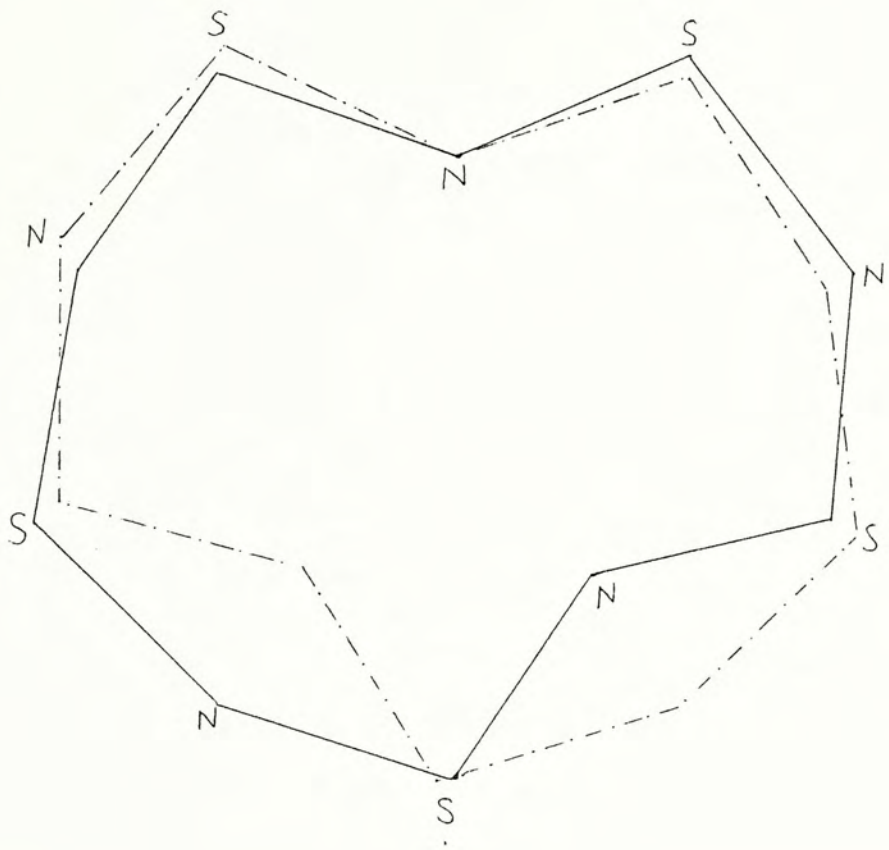

Fig. 5.2 Picture showing the superposition of two azulene-like structrues may lead to a heart-shaped one.

for the heart-shaped and the azulene-like structures are 434.3 kcal/mol and 434.7 kcal/mol, respectively. Moreover, the MNDO structural parameters are quite close to the X-ray data (Fig. 5.1).

In this section, we attempt to connect the two structures by intramolecular rearrangement. In addition, the electronic change during the rearrangement will also be discussed.

5.2 Method of Calculation

The reaction coordinate d of the rearrangement is defined by the separation between the nitrogen atom N_1 and the dummy atom D_2, as shown in Fig. 5.1. Throughout this reaction pathway, C_s symmetry is assumed such that the symmetry plane contains only atoms N_1, D_2 and S_3. The separation is taken to be positive when N_1 and S_3 are on the opposite sides and is negative when N_1 and S_3 are on the same side. Thus, with reference to Fig.5.1, the reaction coordinate equals 0.54Å and -0.70Å for the azulene-like and heart-shaped structures, respectively.

5.3 Results and Discussion

The energy profile of the transformation between the two structures are shown in Fig. 5.3. It is found that C_{2v} symmetry is preserved throughout the reaction path, even though only C_s symmetry is imposed. The change in electronic distribution throughout the pathway is shown in Fig. 5.4.

In the region $0.08\text{Å} < d < 0.54\text{Å}$, energy rises rapidly to reach the transition state with energy 443.0 kcal/mol, yielding an activation energy of about 8 kcal/mol. With reference to the transtition state geometry(Fig. 5.5), it is obvious that as d decreases, atoms N_6 and N_7 moves away from the center of the ring and finally a structure with D_{5h} symmetry results. It is noted that, at the transition state, all the bonds are shortened to 1.51Å, which can be regarded as "typical" S=N bonds[7]. However, it is difficult to come up with a reasonable valence structure for the transition state. Nevertheless, the high energy state for the D_{5h} structure may be due to the strain around the N-S-N bond angles[5,6]. The charge flow in this reagion has a general trend that considerable electronic charge passes from sulfurs to the nitrogens. Totally, 0.94e is transferred to the nitrogen atoms. As a consequence, the shortening of the bonds can be explained

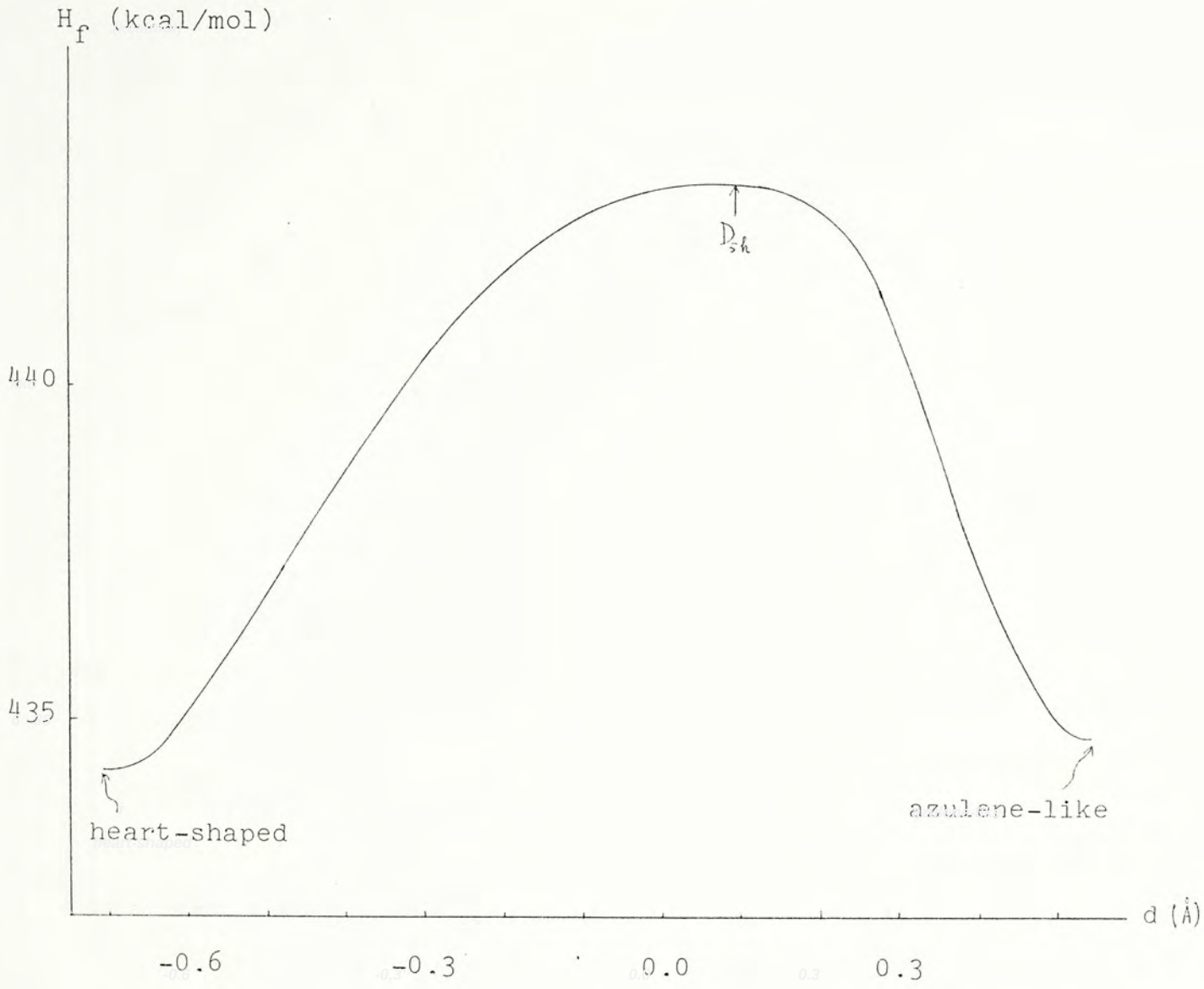

Fig. 5.3 The energy profile for the rearrangement of $S_5N_5^+$ connecting the heart-shaped and azulene-like structures.

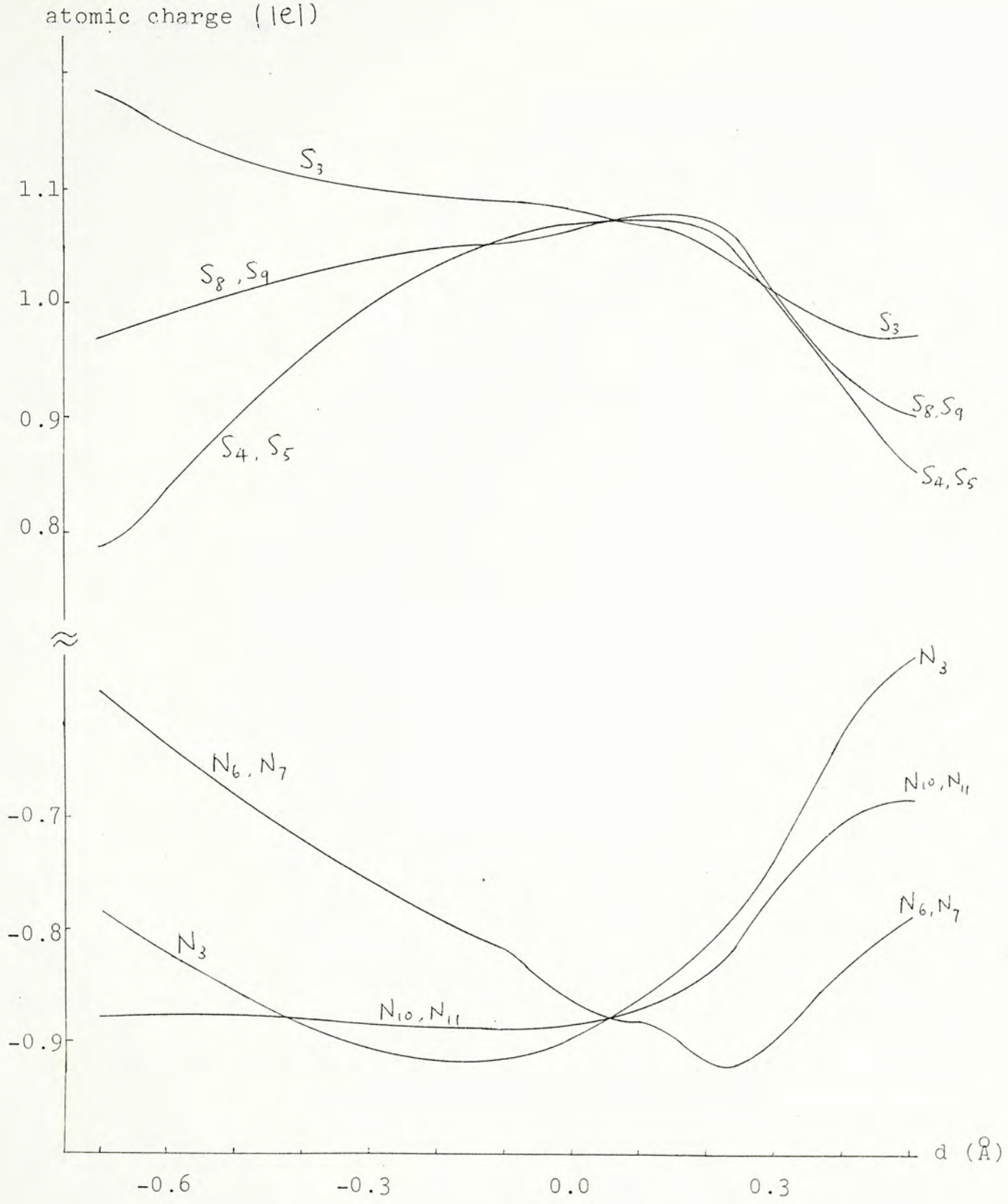

Fig. 5.4 The atomic charge distribution along the rearrangement pathway of $S_5N_5^+$.

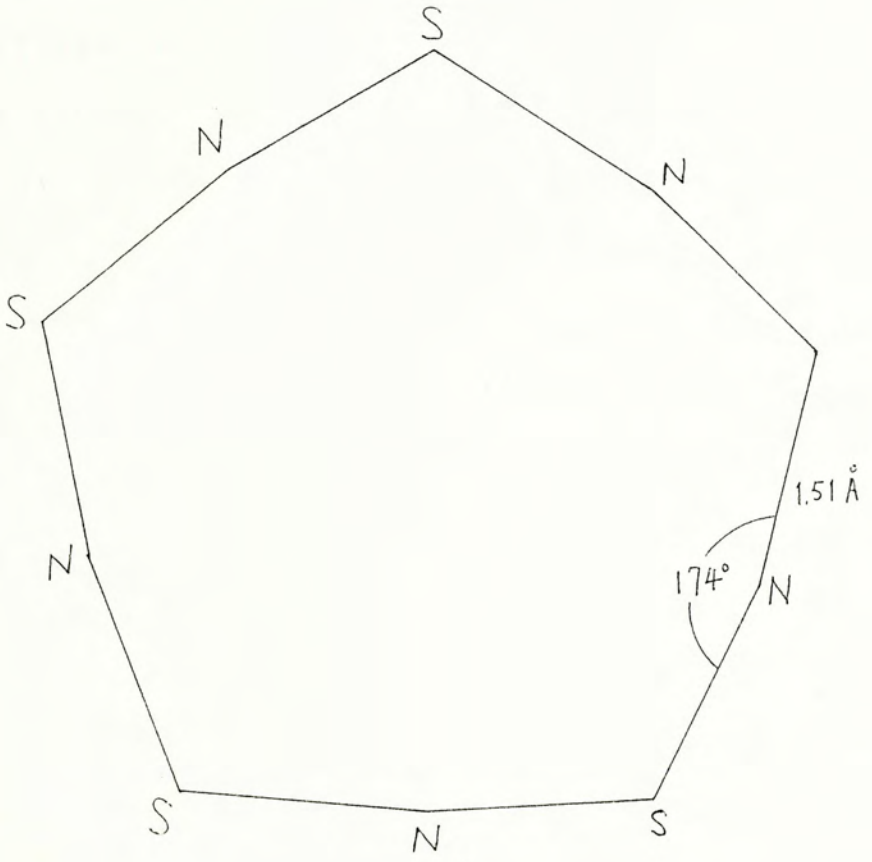

Fig. 5.5 The transition state geometry for the rearrangement pathway of $S_5N_5^+$. Its symmetry is D_{5h}.

by the increase in bond polarities rather than multiple-bond formation.

For the region between the transition state and the heart-shaped structure, energy drops sharply to a minimum of 434.3 kcal/mol for the product. Most of the bond lengths increase in this region except the bond between S_3 and N_{10}. The bond between N_1 and S_4 has the greatest increase. This may be due to the greatest decrease in bond strength which in turn is a result of the decrease in bond polarity, as suggested by their atomic charges. This is also applicable to the shortening of the S_3-N_{10} bond since the bond polarity is enhanced, as seen in Fig.5.4. The charge flow compared to the region before the transition state is in opposite direction. This may be a response to the release of bond strains formerly established. It is noted that the charges on N_{10} and S_6 are rather abnormal to the others. The loss in electronic charge on S_6 may be due to the two attached " sp hybridized " nitrogens, N_{10} and N_{11}. The fact that N_{10} and N_{11} centers retain their charges in this region may be due to their unchanged environments.

As a conclusion, with the low energy barrier found for the transformation between the two structures, it is not surprising for them to coexist. Crystal forces may be responsible to determine which structure is predominant.

Finally, it is noted that Gleiter[8] mistook the D_{5h} structure to be a local minimum, while, actually, it is only a stationary point.

REFERENCES

1. A.J. Banister and H.G. Clarke, J. Chem. Soc., Dalton Trans., 2661(1972)
2. A.J. Banister, J.A. Durant, I. Rayment and H.M.M. Shearer, J. Chem. Soc., Dalton Trans., 928(1976)
3. R. Bartetzko and R. Gleiter, Inorg. Chem., 17(4), 995(1978)
4. R. Gleiter, Angew. Chem. Int. Ed. Engl. 20, 444(1981)
5. A.J. Banister and J.A. Durrant, J. Chem. Research(S), 150(1978)
6. A.J. Banister and J.A. Durrant, J. Chem. Research(S), 152(1978)
7. N.C. Nyburg, J. Cryst. Mol. Struct., 3, 331(1973)
8. R. Gleiter and R. Bartetzko, Z. Naturforsch. 36b, 956(1981)